

1-1-2007

# Generation and evaluation of dynamic compact thermal model of electronic packages

Mohsen Marami  
*Ryerson University*

Follow this and additional works at: <http://digitalcommons.ryerson.ca/dissertations>

 Part of the [Electrical and Computer Engineering Commons](#)

---

## Recommended Citation

Marami, Mohsen, "Generation and evaluation of dynamic compact thermal model of electronic packages" (2007). *Theses and dissertations*. Paper 147.

GENERATION AND EVALUATION OF DYNAMIC  
COMPACT THERMAL MODEL OF  
ELECTRONIC PACKAGES

TTC  
10/10/1K  
1M37  
2/10/97

by

Mohsen Marami

BASc. K.N.Toosi University of Technology

Tehran, Iran

September 1996

A thesis  
presented to Ryerson University  
in partial fulfillment of the  
requirement for the degrees of  
Master of Applied Science  
in the program of  
Electrical and Computer Engineering.

Toronto, Ontario, Canada 2007

© Mohsen Marami 2007

## **Author's Declaration**

I hereby declare that I am the sole author of this thesis.

I authorize Ryerson University to lend this thesis to other institutions or individuals for the purpose of scholarly research.

Signature

I further authorize Ryerson University to reproduce this thesis by photocopy or by other means, in total or in part, at the request of other institutions or individuals for the purpose of scholarly research.

Signature

## **Instruction on Borrowers**

Ryerson University requires the signatures of all persons using or photocopying this thesis. Please sign below, and give address and date.

# Abstract

Mohsen Marami

## Generation and Evaluation of Dynamic Compact Thermal Model of Electronic Packages

Master of Applied Science, electrical and Computer Engineering  
Ryerson University, Toronto, 2007

The goal of this research is to develop a *Dynamic Compact Thermal Model (DCTM)* of electronic packages. The general objectives of thermal modeling are to increase the accuracy of electrical analysis by taking the effect of temperature variation into consideration, predicting the reliability of the product, and acquiring the information which is necessary to design the cooling system in order to enhance the performance of the electronic systems. The project is focused on generating the dynamic compact thermal model of electronic packages so that the transient thermal behaviors of the package could be predicted fast and accurately. The approach proposed by DELPHI consortium (a collaborative European project) for static compact thermal model generation is extended in this work to generate the dynamic compact model of a BGA package represented by a RC network or admittance matrix.

Two steps performed as the methodology of dynamic compact model generation in this work are: 1- A static compact thermal model of BGA package is generated and validated from the static thermal simulation and 2- A RC network is proposed as the contribution of this work and calculated by optimization as the dynamic compact thermal model of the package using the data of transient simulation. The size of the proposed RC network then is optimized by eliminating some capacitors from the original RC network and validated by comparing its output to the output of finite element simulation.

COMSOL®, a Finite element analysis tool is used for thermal simulation and detailed steady state and transient model generation. The optimization algorithm implemented for both static and dynamic compact model generation is Nelder-Mead multidimensional optimization which is realized by MATLAB® programming. The obtained results from the compact models for both static and dynamic analysis of the BGA package are in agreement with the detailed thermal model results and with the available results in literature.

## **Acknowledgment**

First of all I would like to thank Dr. Farah Mohammadi my supervisor for not only accepting me as her MAsc. student at Ryerson University, but also for the advices, instructions, and information aimed at resolving the problems I faced during my study and research. Without these great supports it would be impossible for me to finish my research. I would like to appreciate her again for this opportunity and congratulate Ryerson University for having her as a member of Electrical Engineering faculty.

I would also like to appreciate Dr. Kamran Raahemifar for the advices and information he gave me generously during the admission period and introducing me to Dr Mohammadi. Thank him again and Dr. Xavier Fernando my committee members.

I would like appreciate Ryerson University and Department of Electrical Engineering faculty and staffs for giving me the opportunity to study in such a high reputable institute and also for the research facilities and financial assistance.

Finally thank my parents, brother, and sister as well as my friends Mr. Mahmoud Taheri and his lovely family, and Mr Farhad Azar for their support and every thing else.

## Table of Contents

List of Figures.....	ix
List of Tables.....	xii
1. Introduction.....	1
1.1 Motivation .....	1
1.1.1 Component Level of Thermal Analysis.....	1
1.1.2 Package Level of Thermal Analysis .....	2
1.1.3 System Level of Thermal Analysis.....	2
1.2 Detailed Thermal Modeling .....	3
1.3 Compact Thermal Modeling (CTM) .....	3
1.4 Thesis Objectives .....	4
1.6 Thesis Outline.....	5
2. Governing Heat Transfer Equations and Finite Element Analysis.....	8
2.1 Introduction.....	6
2.2 Different Methods of Heat Transfer .....	6
2.2.1 Conduction.....	6
2.2.2 Convection.....	7
2.2.3 Radiation.....	7
2.3 Heat Transfer Equation by Conduction .....	8
2.4 Boundary and Initial Conditions.....	12
2.5 Numerical Methods and Finite Element Analysis.....	13
2.5.1 Finite Element Method.....	14
2.6 Summary.....	18

3. Electronic Packages and the Detail Thermal Analysis of a BGA Electronic Package.....	19
3.1 Introduction.....	19
3.2 Electronic Packaging and BGA Packages .....	19
3.3 BGA packaging technology .....	24
3.4 Detailed Finite Element Thermal Model of BGA Package .....	25
3.5 Summary.....	33
4. Linear Steady State Compact Thermal Model .....	34
4.1 Introduction.....	34
4.2 DELPHI compact thermal model .....	34
4.3 Static compact model definition .....	35
4.4 Compact model generation.....	36
4.4.1 Network topology .....	37
4.4.2 Resistors' value .....	38
4.4.3 Nelder-Mead Simplex optimization method.....	39
4.5 Validation .....	43
4.6 Summary.....	48
5. Dynamic Compact Thermal Model .....	49
5.1 Introduction.....	49
5.2 Thermal Capacity .....	50
5.3 Other Methods of Dynamic Compact Modeling.....	51
5.4 Definition of a RC Dynamic Compact Thermal Model .....	52
5.5 Detailed Thermal Model .....	54
5.6 Compact Model Generation .....	61
5.7 Validation .....	65
5.7.1 Case Study 1: Boundary condition no. 6.....	69
5.7.2 Case Study 2: Boundary condition no. 20.....	74
5.7.3 Case Study 3: Boundary Condition no. 43.....	78

5.8 Summary.....	82
6. Conclusion and Future works.....	83
References .....	85
Publications .....	90
Appendix A - NID and AWE methods of Dynamic Compact Modeling ..	A-1
A.1 Network Identification by Deconvolution (NID).....	A-1
A.2 Asymptotic Waveform Evaluation (AWE).....	A-3
Appendix B - Dynamic CTM Case studies.....	B-1
B.1 Case study 4 BC no. 12 Free Convection Boundary Condition. ...	B-2
B.2 Case study 5: BC no. 23 Forced Convection Boundary Condition.	B-5
B.3 Case study 6: BC no. 35 Heat Sink and Free Convection Boundary Condition. ....	B-8
B.4 Case study 7: BC no. 40 Heat Sink and Forced Convection Boundary Condition. ....	B-11
B.5 Case study 8: BC no. 46 Cold Plate Convection Boundary Condition. .....	B-14
B.6 Case study 9: BC no. 52 Fluid Bath Boundary Condition. ....	114

## List of Figures

Figure 2.1: Typical isolated system consisting of a solid and its surrounding space and energy elements existed in the system.....	8
Figure 2.2: Small solid object and heat energy elements affecting its thermal balance.....	9
Figure 2.3: Some typical generic elements for 1D, 2D and 3D mesh geometries. ....	14
Figure 2.4: Thermal system consisting of a thin rod and, isolations and surrounding fluid	16
Figure 2.5: Thin rod divided into finite elements.....	17
Figure 3.1: Typical 18 pins plastic DIP package .....	20
Figure 3.2: Typical 16 pins SOIC package.....	21
Figure 3.3: SOIC package with 32 pins.....	21
Figure 3.4: (a) gull wing lead (b) J-type lead.....	21
Figure 3.5: PLCC44 package.....	22
Figure 3.6: PQFP package .....	23
Figure 3.7 Pentium 4 PGA package .....	23
Figure 3.8: Three types of BGA package. (a) PBGA. (b) PBGA-H, (c) TBGA.....	25
Figure 3.9: BGA package used in the research (a) Cross section view (b) Bottom view ..	26
Figure 3.10: Quarter Symmetry cross section of BGA .....	27
Figure 3.11: Final geometry of BGA package.....	28
Figure 3.12: 3D view of the meshed BGA geometry .....	29
Figure 3.13: Heat flux distribution on the top surface of BGA package for 2 different boundary conditions applied to the top surface.....	30
Figure 3.14: (a) TOP1, TOP2, and SIDE, (b) LEAD1, LEAD2, and BOTTOM areas .....	30
Figure 3.15: Graphical illustration of thermal simulation .....	32
Figure 4.1: (a) TOP1, TOP2, and SIDE areas, (b) LEAD1, LEAD2, and BOTTOM areas	37
Figure 4.2: Resistor network static compact model of BGA package .....	38
Figure 4.3: Five steps of Nelder-Mead algorithm .....	41
Figure 4.4: Junction temperature relative errors .....	44
Figure 4.5: Relative errors of top1 surface. ....	45
Figure 4.6: Relative errors of top2 surface. ....	45
Figure 4.7: Relative errors of lead1.....	46
Figure 4.8: Relative errors of lead 2.....	46
Figure 4.9: Relative errors of side walls.....	47
Figure 4.10: Relative errors of bottom walls. ....	47
Figure 5.1: RC chain.....	52
Figure 5.2: Proposed Dynamic Compact topology for BGA package .....	53
Figure 5.3: Quarter symmetric Geometry of BGA Package.....	55

Figure 5.4: Finite element model of the BGA package .....	56
Figure 5.5: Frequency responses of junction temperatures for BC no. 20 and 45 .....	57
Figure 5.6: Graphical representation of temperature variation during transitions period ...	60
Figure 5.6: Detailed model simulation results: Junction temperature of BGA package for boundary condition no. 20 .....	60
Figure 5.7: Different steps of generating dynamic compact model .....	62
Figure 5.8: RC network of dynamic compact model.....	63
Figure 5.9: Reduced RC network of dynamic compact model.....	64
Figure 5.10: Compact model prediction results: Junction temperature of BGA package for boundary condition no. 20 .....	65
Figure 5.11: Compact model when boundary conditions are applied .....	65
Figure 5.12: (a) TOP1, TOP2, and SIDE areas, (b) LEAD1, LEAD2, and BOTTOM areas of the BGA package. ....	68
Figure 5.13: (a) Detailed and Compact model junction temperature for boundary condition no. 6, (b) Their relative error percentage.....	69
Figure 5.13: (c) Junction temperature of BGA for the first 2 seconds of transition period.	70
Figure 5.14: Relative error percentages of outward heat fluxes from Top1, Top2, Lead1, Lead2, Side, and bottom of BGA package for boundary condition no. 6. ....	73
Figure 5.15: (a) Detailed and Compact model junction temperature for boundary condition no. 20, (b) Their relative error percentage.....	75
Figure 5.16: Relative error percentages of outward heat fluxes from Top1, Top2, Lead1, Lead2, Side, and bottom of BGA package for boundary condition no. 20. ....	77
Figure 5.17: (a) Detailed and Compact model junction temperature for boundary condition no. 45, (b) Their relative error percentage.....	78
Figure 5.18: Relative error percentages of outward heat fluxes from Top1, Top2, Lead1, Lead2, Side, and bottom of BGA package for boundary condition no. 43. ....	81
Figure A.1.1: Single time constant system. ....	A-1
Figure A.1.2: Foster RC network .....	A-2
Figure A.1.3: Cauer RC network.....	A-3
Figure B.1: (a) TOP1, TOP2, and SIDE areas, (b) LEAD1, LEAD2, and BOTTOM areas of the BGA package. ....	B-1
Figure B.1.1: Detailed and Compact model junction temperature for BC no. 12.....	B-2
Figure B.1.2: Junction temperature relative error for BC no. 12 .....	B-2
Figure B.1.3: Top1 heat flux relative error for BC no. 12.....	B-3
Figure B.1.4: Top2 heat flux relative error for BC no. 12.....	B-3
Figure B.1.5: Lead1 heat flux relative error for BC no. 12 .....	B-3
Figure B.1.6: Lead2 heat flux relative error for BC no. 12 .....	B-4
Figure B.1.7: Sidewalls heat flux relative error for BC no. 12 .....	B-4
Figure B.1.8: Bottom heat flux relative error for BC no. 12 .....	B-4
Figure B.2.1: Detailed and Compact model junction temperature for BC no. 23.....	B-5
Figure B.2.2: Junction temperature relative error for BC no. 23 .....	B-5

Figure B.2.3: Top1 heat flux relative error for BC no. 23 .....	B-6
Figure B.2.4: Top2 heat flux relative error for BC no. 23 .....	B-6
Figure B.2.5: Lead1 heat flux relative error for BC no. 23 .....	B-6
Figure B.2.6: Lead2 heat flux relative error for BC no. 23 .....	B-7
Figure B.2.7: Sidewalls heat flux relative error for BC no. 23 .....	B-7
Figure B.2.8: Bottom heat flux relative error for BC no. 23 .....	B-7
Figure B.3.1: Detailed and Compact model junction temperature for BC no. 35.....	B-8
Figure B.3.2: Junction temperature relative error for BC no. 35 .....	b-8
Figure B.3.3: Top1 heat flux relative error for BC no. 35 .....	B-9
Figure B.3.4: Top2 heat flux relative error for BC no. 35 .....	B-9
Figure B.3.5: Lead1 heat flux relative error for BC no. 35 .....	B-9
Figure B.3.6: Lead2 heat flux relative error for BC no. 35 .....	B-10
Figure B.3.7: Sidewalls heat flux relative error for BC no. 35 .....	B-10
Figure B.3.8: Bottom heat flux relative error for BC no. 35 .....	B-10
Figure B.4.1: Detailed and Compact model junction temperature for BC no. 40.....	B-11
Figure B.4.2: Junction temperature relative error for BC no. 40 .....	B-11
Figure B.4.3: Top1 heat flux relative error for BC no. 40.....	B-12
Figure B.4.4: Top2 heat flux relative error for BC no. 40.....	B-12
Figure B.4.5: Lead1 heat flux relative error for BC no. 40 .....	B-12
Figure B.4.6: Lead2 heat flux relative error for BC no. 40 .....	B-13
Figure B.4.7: Sidewalls heat flux relative error for BC no. 40.....	B-13
Figure B.4.8: Bottom heat flux relative error for BC no. 40 .....	B-13
Figure B.5.1: Detailed and Compact model junction temperature for BC no. 46.....	B-14
Figure B.5.2: Junction temperature relative error for BC no. 46 .....	B-14
Figure B.5.3: Top1 heat flux relative error for BC no. 46.....	B-15
Figure B.5.4: Top2 heat flux relative error for BC no. 46.....	B-15
Figure B.5.5: Lead1 heat flux relative error for BC no. 46 .....	B-15
Figure B.5.6: Lead2 heat flux relative error for BC no. 46 .....	B-16
Figure B.5.7: Sidewalls heat flux relative error for BC no. 46.....	B-16
Figure B.5.8: Bottom heat flux relative error for BC no. 46 .....	B-16
Figure B.6.1: Detailed and Compact model junction temperature for BC no. 52.....	B-17
Figure B.6.2: Junction temperature relative error for BC no. 52 .....	B-17
Figure B.6.3: Top1 heat flux relative error for BC no. 52.....	B-18
Figure B.6.4: Top2 heat flux relative error for BC no. 52.....	B-18
Figure B.6.5: Lead1 heat flux relative error for BC no. 52 .....	B-18
Figure B.6.6: Lead2 heat flux relative error for BC no. 52 .....	B-19
Figure B.6.7: Sidewalls heat flux relative error for BC no. 52.....	B-19
Figure B.6.8: Bottom heat flux relative error for BC no. 52 .....	B-19

## List of Tables

Table 3.1: BGA package size and physical properties .....	27
Table 3.2: Mesh parameters of detailed model .....	29
Table 3.3: Area and volume of CTM nodes .....	31
Table 3.4: Boundary Conditions .....	31
Table 4.1: Optimized resistor values of CTM.....	48
Table 5.1: Free Mesh parameters .....	61
Table 5.2: Mesh statistics.....	62
Table 5.3: Boundary Conditions .....	58
Table 5.4: Resistors' value of Dynamic Compact Thermal Model .....	61
Table 5.5: Capacitors' value of Dynamic Compact Thermal Model .....	64
Table B.1: Boundary Conditions.....	B-1

# Chapter 1

## Introduction

### 1.1 Motivation

Due to the continuous increase of component density and speed of VLSI circuits, it's possible to design high performance, small and fast electronic circuits. This achievement comes however with the price of power dissipation increase. The amount of dissipated power by the chip has direct relation with its temperature which is a crucial parameter in electrical behavior of electronic components, circuit performance, and reliability of the electronic system [1]. Thermal analysis is an important part of modern electronic design thus that enables the designer to calculate the critical thermal variables as key factors in electrical analysis and accurate performance estimation.

There are three levels of macroscopic thermal analysis and depending on the level of the design an electronic designer is engaged, one of these analyzing levels must be chosen that gives out only the sufficient and not unnecessary information about the thermal behavior of the subject of the thermal analysis. These levels are as following:

#### 1.1.1 Component Level of Thermal Analysis

In component level a single component or some specific components of the electronic circuit are the subjects of thermal analysis. It's desirable for the designer to study the effect of thermal behavior of components on their own electrical behaviors and the mutual effects of the thermal behaviors of components on the electrical behaviors and operating points of their adjacent components. This level of analysis is usually used in electro-thermal analysis of the electronic circuit [2, 3]. When there are some components which play key rules in the circuit and it's very important for the designer to predict their electrical and thermal operating points in order to design a stable, predictable, and reliable circuit, electro-thermal analysis of the circuit is necessary. Unlike ordinary electrical analysis by which the electrical operating point of the circuit is calculated for a fixed and predetermined temperature (usually room temperature), electro-thermal analysis performs both electrical and thermal analyses concurrently. It has well known

that electrical current flowing through the materials causes heat dissipation and temperature elevation. This phenomenon is called Joule heating and in most cases changes the electrical operating point of the component and the circuit in which it is operating. Electrical analysis with fixed temperature thus is not sufficient for an accurate analysis and electro-thermal analysis should be performed so the mutual effects of temperature variation and electrical operating point variation are taken into the consideration.

### **1.1.2 Package Level of Thermal Analysis**

This level of thermal analysis is useful when the electronic designer needs to calculate the temperature profile and inward/outward heat fluxes of an electronic package working as a part of an electronic system. A package can be analyzed thermally using a simulation software or by its compact thermal model as explained later in this chapter and the rest of this work. Detailed analysis of package is expensive in terms of money and simulation time but it gives a relatively accurate temperature profile for every location inside or on the surface of package. Compact thermal model of package on the other hand is fast, almost free, and easy to use but it calculates the average temperature and heat flows for predetermined volumes inside or areas on the surface of the package with acceptable accuracy. The subject of this project is thermal analysis in package level and in future chapters detail and compact modeling of electronic packages will be explained thoroughly.

### **1.1.3 System Level of Thermal Analysis**

Accurate thermal analysis of a complex electronic system including several packages, discrete elements, printed circuit boards, connectors and mechanical parts, heat sinks and cooling mechanism, and covering case is almost impossible with currently available thermal simulation softwares, because of its complexity and the large number of thermal characteristics affecting the thermal behavior of the system and the output of the analysis includes large amount of unnecessary information. The alternative solution is to generate the compact model of packages, boards, and other parts of the system separately and use them as the building blocks of the thermal model of the system. This system level model then generates the thermal variables of the desired locations within the system.

## **1.2 Detailed Thermal Modeling**

The temperature profile (temperature at any desirable location of a solid object) and inward/outward heat flux from the surfaces of the solid object obey the heat transfer equation by conduction (This will be explained in chapter 2 in more detail). However, if an object with a complex geometry such as a modern electronic package with several layers of materials is the subject of the thermal analysis problem, it's impossible to find an analytical solution for this equation.

The very first alternative to overcome this problem is employing numerical methods developed for solving the heat transfer equation with specified boundary and initial conditions and obtain the temperature profile and outward/inward heat fluxes. Some of the most well known and highly developed numerical methods are Boundary Elements Method (BEM), Finite Difference Method (FDM), and Finite Elements Method (FEM). Detail discussion and explanation on these methods are available in [7, 8] and other numerical analysis and heat transfer text books. The first issue rises immediately is the cost of analysis in terms of tools and time. Unless the object has a very simple geometry, a high price software package such as ANSYS© or COMSOL© Multiphysics specially designed for numerical calculation of partial differential equations is needed to be installed and available on a powerful machine and the computation time is also considerably long. This makes the use of numerical method expensive and inefficient for the customer of the electronic package, the second issue is the confidentiality of the electronic packages. In order to perform the detail thermal analysis of an electronic package, exact information about the internal structure the package, dimensions and physical properties such as thermal conductivities, thermal capacities, and densities of the different layers of the package is necessary. Package producers however usually consider these specifications as classified information and don't publish theme to public domain. This makes the detail thermal analysis impossible for the package customer. The solution to overcome this situation is Compact Thermal Modeling (CTM) of packages.

## **1.3 Compact Thermal Modeling (CTM)**

In many cases of thermal analysis most of the information provided as the detailed model is unnecessary for the consumer because it includes the thermal characteristics of undesired locations. A smaller model that is capable of calculating only the hot spots, the

temperatures and heat fluxes at some desired locations can help the designer to perform the thermal analysis much more easily and quickly with the required accuracy. Such model is called Compact Thermal Model (CTM). CTM can be generated from the detailed model. However, the detailed model must be boundary condition independent (BCI) because the package may be used in different boundary conditions.

There are two types of CTM: static and dynamic. Static models are capable to calculate the thermal behavior and operating point under steady state conditions [9, 10]. Dynamic models on the other hand are more complex and capable to calculate the temperature profile and heat flows during transition times in which the temperature has not reached to its final value yet or the electrical and environmental conditions are not stable [11, 12].

## 1.4 Thesis Objectives

The goal of this research is to develop a capability for the *dynamic compact thermal modeling* of packages. The objective of the dynamic compact thermal modeling process is to create a simplified model that represents the thermal behavior of the package to perform a quick transient thermal analysis with the required accuracy in system design process. This research project aims to create methodology to enable rapid assessment of thermal behaviour of package in electronic equipment. This methodology is applied then to predict the transient thermal behavior of the Ball Grid Array (BGA) package.

Boundary condition independent *static compact thermal model* generation methodology based on the resistor network for a typical BGA package is discussed. This model is generated and optimized by MATLAB© [33] for various boundary conditions. The results obtained from this model is validated and compared to the finite element detailed model.

We also present a methodology to create boundary condition independent *dynamic compact thermal model* by which, compact models of electronic packages based on transient detailed finite element analysis results are generated. This methodology is applied to calculate a proposed RC network compact model of the BGA package. The proposed model is optimized so that the cost function representing the distance between the detailed and compact model is minimized. The performance of compact model is

investigated for various boundary conditions such as free convection, forced convection, heat sink free convection, heat sink forced convection, cold plate, and fluid bath types of boundary conditions.

## **1.5 Thesis Outline**

In this research we attempt to provide coverage of important subjects required for generation and validation of boundary condition independent static and dynamic compact thermal modeling of packages.

The first two chapters are designed to present the fundamental building blocks in generation of a compact thermal model. Chapter 2 discusses a general introduction to heat transfer and the governing equations for electronic components. The available methodologies to solve the heat transfer governing equations are also elaborated in this chapter.

In chapter 3, some of the currently popular electronic packages are introduced briefly. The emphasis is given to the BGA technology and packages because this type of package is selected to be thermally modeled in this project. In addition a detailed finite element model of BGA package generated using COMSOL© [31] is discussed in detail. Moreover, the desired temperatures and heat fluxes are obtained for various boundary conditions.

Chapter 4 concentrates on the presentation and validation of a boundary condition independent static compact thermal model based on the resistor network for a typical BGA package

Chapter 5 addresses a methodology to create boundary condition independent dynamic compact thermal model. This method is applied to predict the transient thermal behavior of the BGA package. The optimization of the dynamic model is also described. Finally, the conclusions and suggested future works are summarized in chapter 6.

## Chapter 2

# Governing Heat Transfer Equations and Finite Element Method of Analysis

### 2.1 Introduction

In this chapter we briefly review the theory of heat transfer and mathematical background needed to understand the rest of thesis and the work done in this project. First different methods of heat transfer are explained. Then accepting the energy conservation law or the first thermodynamics law as assumption, the heat transfer equation which is the governing equation of thermal analysis will be formulated. Note that the heat transfers equation is also called diffusion equation in some text books or papers. Final section of this chapter is a brief explanation of Finite Element Analysis as a numerical method to solve the derived heat transfer equation. This method will be used in next chapters by the COMSOL finite element software for thermal simulation of a typical Ball Grid Array (BGA) package.

### 2.2 Different Methods of Heat Transfer

There are three methods of heat energy transfer: conduction, convection, and radiation.

#### 2.2.1 Conduction

Thermal conductivity is a thermodynamic property of materials and in this method of energy transfer the heat energy transports through materials without any macroscopic mass motion. In source point or region heat energy causes the increase of atoms vibration. This vibration transfers to the neighbor atoms and heat energy is transferred. The rate of energy transfer is described by the following equation:

$$q = -kA \frac{\partial T}{\partial x} \quad (2.1)$$

where:

$q = \frac{\partial Q}{\partial t}$  (W) is the rate of heat energy transporting in  $\bar{x}$  direction by conduction,

$k$  (W/m.K) is the thermal conductivity of medium material,

$A$  ( $m^2$ ) is the area through which heat energy flows and is normal to the transfer direction  $\bar{x}$ ,

$T$  (K) is the temperature of material at location  $x$ , and

$x$  (m) is the location variable.

Equation (2.1) is also called Fourier rate equation.

### 2.2.2 Convection

Heat transfer by convection is the method of energy transportation happens in fluid materials including gases and liquids. Because of very high mobility of molecules in fluid materials these molecules start moving because of the heat energy applied to them. When a fluid is in contact with a solid the energy transfer rate between solid and fluid by convection is calculated by the following equation:

$$q = hA(T_w - T_\infty) \quad (2.2)$$

where:

$q = \frac{\partial Q}{\partial t}$  (W) is the rate of heat transfer by convection method,

$h$  (W/m<sup>2</sup>K) is the heat transfer coefficient,

$A$  ( $m^2$ ) is the surface area through which heat energy transfer from solid to fluid,

$T_\infty$  (K) is the ambient or room temperature, and

$T_w$  (K) is the wall temperature or temperature of solid at its boundary surface.

The reader is referred to [13, 14] for more detailed discussion on heat transfer mechanism.

### 2.2.3 Radiation

In this method the heat energy is transferred by electromagnetic radiations. The energy transfer rate from a solid to infinite is calculated by the following equation:

$$q = \sigma \varepsilon A (T_w^4 - T_\infty^4) \quad (2-3)$$

where:

$q = \frac{\partial Q}{\partial t}$  (W) is the rate of heat transfer from solid material to space by radiation,

$\sigma = 5.6686 \times 10^{-6}$  (W/m<sup>2</sup>K<sup>4</sup>) is Stefan-Boltzmann constant,

$\varepsilon$  is the emissivity of the surface,

$A$  (m<sup>2</sup>) is the surface area through which heat energy transmitted,

$T_w$  (K) is the absolute surface temperature, and

$T_\infty$  (K) is the absolute ambient temperature.

### 2.3 Heat Transfer Equation by Conduction

The process of deriving the heat transfer equation starts from energy conservation law or the first thermodynamics law which states the total amount of energy within a system perfectly isolated from other systems is constant but may change from one form to another form. For a typical system consist of a solid material and its surrounding space shown in figure 2.1 this law can be expressed as following:

*Transferred heat energy from surrounding space into the solid + Heat energy generated inside the solid = Transferred heat energy from solid into the surrounding space + Heat energy stored inside the solid*

$$Q_{in} + Q_g = Q_{out} + Q_s \quad (2.4)$$

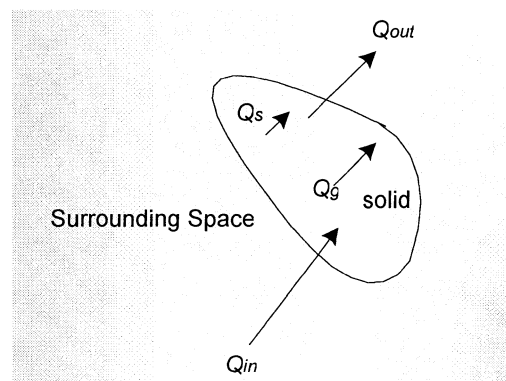


Figure 2.1: Typical isolated system consisting of a solid and its surrounding space and energy elements existed in the system.

deriving equation (2.4) with respect to time:

$$\frac{dQ_{in}}{dt} + \frac{dQ_g}{dt} = \frac{dQ_{out}}{dt} + \frac{dQ_s}{dt} \quad (2.5)$$

Equations (2.4) and (2.5) are also called energy balance and show the energy balance in a thermal system and are always valid. Assuming conduction is the only method of heat transfer inside solid materials, the energy balance equation (2.5) for a small piece of the object shown in figure (2.2) is rewritten as following:

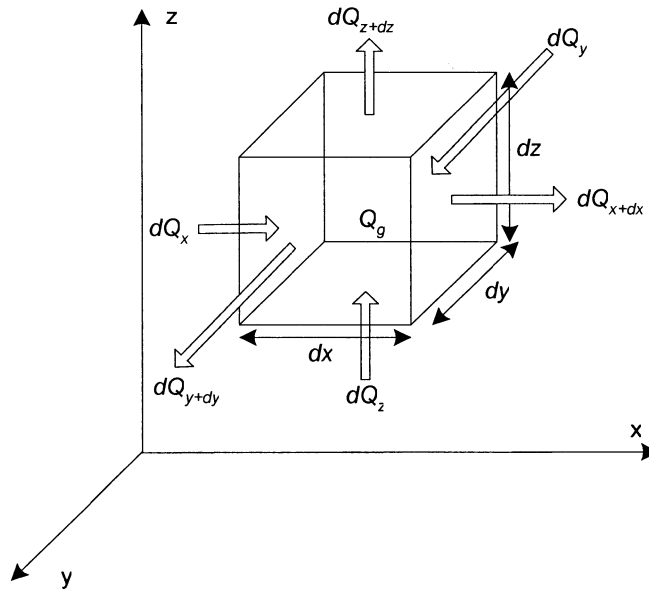


Figure 2.2: Small piece of a solid object and heat energy elements affecting its thermal balance.

$$\left( \frac{dQ_x}{dt} + \frac{dQ_y}{dt} + \frac{dQ_z}{dt} \right) + \frac{dQ_g}{dt} = \left( \frac{dQ_{x+dx}}{dt} + \frac{dQ_{y+dy}}{dt} + \frac{dQ_{z+dz}}{dt} \right) + \frac{dQ_s}{dt} \quad (2.6)$$

A solid material is **non-isotropic** if its thermal conductivity depends on the direction in which it is measured:

$$k_x \neq k_y \neq k_z$$

and **non-homogeneous** if its thermal conductivity depends on the location:

$$k_j = k_j(x, y, z)$$

and **non-linear** if its thermal conductivity depends on the temperature:

$$k_j = k_j(T)$$

Applying equation 2-1 (Fourier law) to figure 2.2:

$$dQ_x = -(dy \cdot dz) \cdot \left( k_x \cdot \frac{\partial T_x}{\partial x} \right) \cdot dt \quad (2.7)$$

Equation (2.7) is the amount of heat energy going into the cell by conduction. According to Taylor Series [15]:

$$f(x + dx, T) \approx f(x, T) + \frac{\partial f(x, T)}{\partial x} \cdot dx$$

and applying it to equation (2.7):

$$dQ_{x+dx} = -(dy \cdot dz) \cdot \left[ k_x \cdot \frac{\partial T_x}{\partial x} + \frac{\partial}{\partial x} \left( k_x \cdot \frac{\partial T}{\partial x} \right) \cdot dx \right] \cdot dt \quad (2.8)$$

Equation (2.8) is the amount of heat energy going out of the cell at  $x+dx$  by conduction. The net heat flux in the  $x$  direction thus is calculated by subtracting equation 2-8 from equation (2.7).

$$dQ_x - dQ_{x+dx} = \frac{\partial}{\partial x} \left( k_x \cdot \frac{\partial T}{\partial x} \right) \cdot dx \cdot dy \cdot dz \cdot dt \quad (2.9)$$

and for two other directions:

$$dQ_y - dQ_{y+dy} = \frac{\partial}{\partial y} \left( k_y \cdot \frac{\partial T}{\partial y} \right) \cdot dx \cdot dy \cdot dz \cdot dt \quad (2.10)$$

$$dQ_z - dQ_{z+dz} = \frac{\partial}{\partial z} \left( k_z \cdot \frac{\partial T}{\partial z} \right) \cdot dx \cdot dy \cdot dz \cdot dt \quad (2.11)$$

The stored heat energy can be expressed as:

$$Q_s = m \cdot C \cdot dT = \rho \cdot dx \cdot dy \cdot dz \cdot C \cdot dT$$

and the heat storage rate is:

$$dQ_s = \rho \cdot dx \cdot dy \cdot dz \cdot C \cdot \frac{dT}{dt} \quad (2.12)$$

where:

$C$  (J/K) is the specific heat capacity of solid material, and

$\rho$  (Kg/m<sup>3</sup>) is the density of material.

Replacing equations (2.9), (2.10), (2.11), and (2.12) in equation (2.6):

$$\frac{\partial Q_g}{\partial t} + \frac{\partial}{\partial x} \left( k_x \frac{\partial T}{\partial x} \right) + \frac{\partial}{\partial y} \left( k_y \frac{\partial T}{\partial y} \right) + \frac{\partial}{\partial z} \left( k_z \frac{\partial T}{\partial z} \right) = \rho \cdot C \cdot \frac{\partial T}{\partial t} \quad (2.13)$$

Equation (2.13) is the general form of heat transfer equation by conduction or diffusion equation. The more compact form of this equation is:

$$q_g + \nabla \cdot (k \nabla T) = \rho \cdot C \cdot \frac{\partial T}{\partial t} \quad (2.14)$$

where:

$\nabla = \frac{\partial}{\partial x} \vec{i} + \frac{\partial}{\partial y} \vec{j} + \frac{\partial}{\partial z} \vec{k}$  is the vector of divergence operator.

For most electronic component, heat conduction is the most important heat transfer phenomenon; therefore most researchers consider a component that has thermal conduction as its only mode of internal heat transfer. Therefore, heat conduction equation described by equation 2-14 will be used for thermal modeling of electronic component in this research work.

For a homogeneous and isotropic solid material where thermal conductivity is a scalar parameter independent of direction and location, equation 2-13 is simplified to the following equation:

$$\frac{\partial^2 T}{\partial x^2} + \frac{\partial^2 T}{\partial y^2} + \frac{\partial^2 T}{\partial z^2} + \frac{q_g}{k} = \frac{1}{\alpha} \frac{\partial T}{\partial t} \quad (2.15)$$

where:

$\alpha = \frac{k}{C \cdot \rho}$  is the thermal diffusivity of the solid material.

If there is no heat generation within the solid object, Equation 2-15 is simplified to:

$$\frac{\partial^2 T}{\partial x^2} + \frac{\partial^2 T}{\partial y^2} + \frac{\partial^2 T}{\partial z^2} = \frac{1}{\alpha} \frac{\partial T}{\partial t} \quad (2.16)$$

Equation (2.16) is called Fourier partial differential equation.

In steady state condition equation (2.15) is rewritten as following:

$$\frac{\partial^2 T}{\partial x^2} + \frac{\partial^2 T}{\partial y^2} + \frac{\partial^2 T}{\partial z^2} + \frac{q_g}{k} = 0 \quad (2.17)$$

Equation (2.17) is called Poisson partial differential equation.

If there is no heat generation, steady state thermal equation is:

$$\frac{\partial^2 T}{\partial x^2} + \frac{\partial^2 T}{\partial y^2} + \frac{\partial^2 T}{\partial z^2} = 0 \quad (2.18)$$

Equation (2.18) is called Laplace partial differential equation.

## 2.4 Boundary and Initial Conditions

Equation (2.14) describes the spatial and time domain behavior of temperature variable within a solid object specified by a computational domain  $\Omega$  limited by  $\partial\Omega$  which represents the boundaries of object. Like any other differential equations in order to solve equation (2.14) boundary and initial conditions are necessary. The temperature profile at  $t=0$  for every point of object is called the initial condition.

$$\forall r \in \Omega, \quad t = 0 \quad T(r, t) = T_0(r) \quad (2.19)$$

where  $r$  is the arbitrary position vector in the computational domain  $\Omega$ .

The temperature profile of  $\partial\Omega$  for the total desired period of time is called the boundary condition. There are different types of boundary conditions for a partial differential equation. If boundary temperature is assumed to be a constant value, the boundary condition is called **Dirichlet boundary condition** and described as following:

$$\forall r \in \partial\Omega, \quad T(r) = T_{\partial\Omega}(t) \quad (2.20)$$

If the boundary condition determines the normal inward/outward heat flux through the boundary of object, it is called **Neumann boundary condition** and expressed as following:

$$\forall r \in \partial\Omega, \quad q_{\perp}(r) = q_{\partial\Omega}(t) \quad (2.21)$$

The normal heat flux mentioned in equation (2.21) may be calculated by equation (2.2) or equation (2.3) if the method of heat transfer from solid object to surrounding space is convection or radiation respectively. More explanation on these boundary conditions and other types of boundary conditions such as **Robin** and **Cauchy** can be found in [16] or other advanced engineering mathematics text books.

## 2.5 Numerical Methods and Finite Element Analysis

Solving heat conduction equation (2.14) is very difficult and in fact there is no analytical solution for most real cases of thermal analysis problems, unless for the object that has a simple geometry,. Numerical methods thus are necessary to solve the heat transfer equation.

There are different methods to solve heat conduction equations such as, Fourier series, Finite element method (FEM), Finite difference method (FDM), Boundary element method (BEM), and Extraction approximation approaches. However, two best known numerical methods which are well developed to be realized by computer programming are Finite Differences Method and Finite Elements Method. The FDM tries to solve the partial differential equation by approximating the derivatives by fractions of differences. The subject of analysis (solid object) thus must be divided into small square shape cells in 2Dimensional problems and cubic shape cells in 3Dimensional problems. FEM on the other hand tries to convert the differential equation into an integral and solve the Integral by means of numerical approximation. The main advantage of FEM to FDM is that to solve the problem by FEM we are not limited to square and cubic cells but using triangular cells in 2Dimensional problems and **tetrahedron cells in 3D problems** are also possible which can discretize the object with higher accuracy specially when the object has a complex geometry. Figure 2.3 illustrates some typical generic elements for 1Dimensional, 2Dimensional, and 3Dimensional geometries.

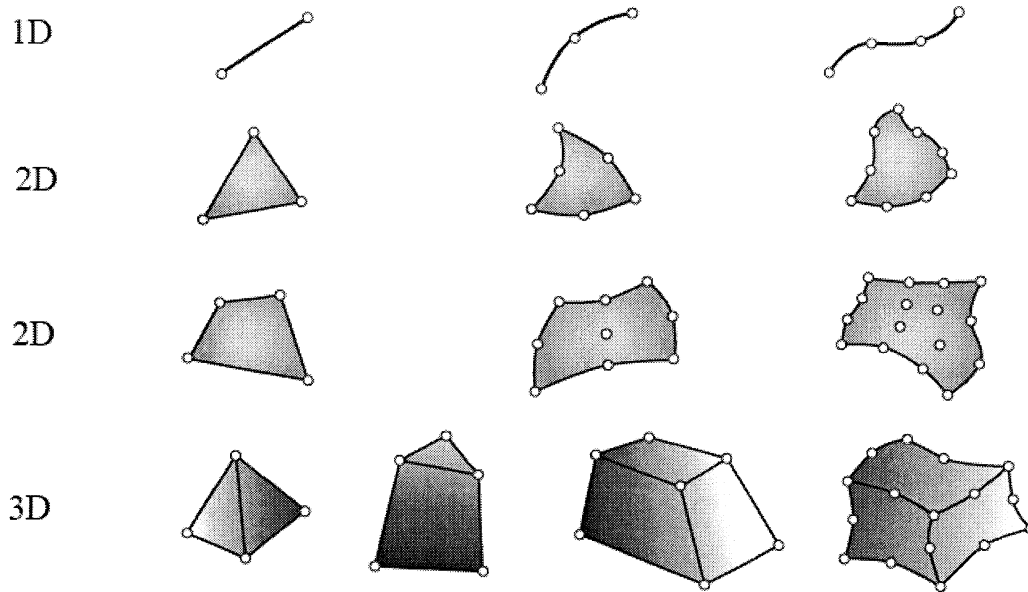


Figure 2.3: Some typical generic elements for 1Dimensional, 2Dimensional, and 3Dimensional geometries.

For a detail explanation on Finite Differences Method, Finite Elements Methods, and their advantages and disadvantages reader is referred to [8].

Finite element method is chosen in this research as the numerical thermal simulation method. This is one of the most popular numerical methods used by design engineers in today's product design process in industry. A brief description of this method is presented in the next section. For more detail, reader may refer to [17]

### 2.5.1 Finite Element Method

Finite element method was first developed for problems in stress analysis of solids and structural systems. However, its power and wide applicability can be fully recognized when it is applied on nonstructural problems such as heat transfer and fluid flow [17]. Following is a brief description of the theory behind this powerful method.

The calculus of variations provides a method of transforming a differential equation into an integral. According to the variational calculus, it can be proved that the integral  $I$  expressed by equation (2.22):

$$I = \int_{x=0}^L F\left(x, u(x), \frac{\partial u(x)}{\partial x}\right) dx \quad (2.22)$$

where:

$x \in \mathbb{R}$  and  $x \in [0, L]$  is an independent variable,

$u$  is an arbitrary function of  $x$ , and

$F$  is an arbitrary function of  $x$ ,  $u$ , and derivative of  $u$  with respect to  $x$ .

will be minimized if the function  $u(x)$  satisfies equation 2.23.

$$\frac{\partial F}{\partial u} - \frac{d}{dx} \left( \frac{\partial F}{\partial u'} \right) = 0 \quad (2.23)$$

where  $u' = \frac{\partial u(x)}{\partial x}$

Equation (2.23) is called Euler-Lagrange equation. Detail explanations about variation calculus may be found in [18]. If we can rewrite the differential equation (to be solved) in a form that is similar to equation 2.23, instead of solving the differential equation directly we can find the function  $F$  by minimizing the integral  $I$  (equation 2.22) with respect to  $u(x)$ .

**Example:** Figure 2.4 shows a thin rod with the length equal to  $2L$ , perimeter equal to  $P$ , and cross section area equal to  $A$ . The two ends of the rod are thermally isolated and their temperatures are equal to  $T_0$ . The ambient temperature is  $T_{amb}$ . The steady state heat transfer equation for this system is:

$$\frac{d}{dx} \left( kA \frac{dT}{dx} \right) - hP(T - T_{amb}) = 0 \quad (2.24)$$

$$T(0) = T_0 \quad \text{and} \quad \left. \frac{dT}{dx} \right|_{x=L} = 0$$

where:

$k$  is the thermal conductivity of thin rod, and

$h$  is the thermal coefficient of surrounding fluid.

Equation (2.24) can be easily extracted from equation (2.14) or directly calculated by writing the energy balance equation.

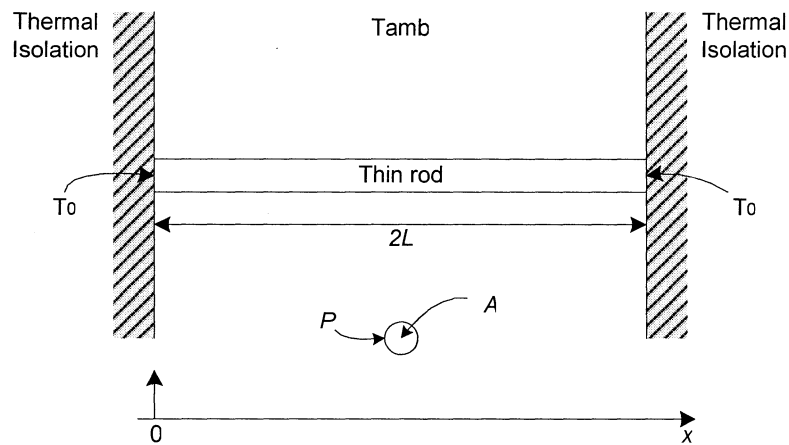


Figure 2.4: Thermal system consisting of a thin rod and, isolations and surrounding fluid.

We can rewrite the equation (2.24) as following:

$$\frac{\partial F}{\partial T} - \frac{d}{dx} \left( \frac{\partial F}{\partial T'} \right) = 0 \quad (2.25)$$

where:

$$F = \frac{1}{2} \left[ hP(T - T_{amb})^2 + kA \left( \frac{dT}{dx} \right)^2 \right] \quad (2.26)$$

Equation (2.25) is similar to equation (2.23). An equivalent solution of this equation is minimizing the following integral as explained earlier.

$$I = \frac{1}{2} \int_{=0}^L \left[ hP(T - T_{amb})^2 + kA \left( \frac{dT}{dx} \right)^2 \right] \cdot dx \quad (2.27)$$

In order to minimize equation (2.27) its derivative with respect to  $T(x)$  must be set equal to zero:

$$\frac{d}{dT} I = \frac{d}{dT} \left[ \frac{1}{2} \int_{=0}^L \left[ hP(T - T_{amb})^2 + kA \left( \frac{dT}{dx} \right)^2 \right] \cdot dx \right] = 0 \quad (2.28)$$

To make sure the solution of equation (2.28) gives the minimum (and not the maximum) of  $I$ , second derivative of integral should be calculated. If it has a positive value, equation (2.28) calculates the minimum.

The concept of finite element analysis is based on solving Equation (2.28) numerically. The numerical approximation of the integral inside the bracket is performed by breaking the domain of the integration into several sub domains and approximating the integral of each sub domain by calculating the area under the function curve. This has been illustrated in figure 2.5.

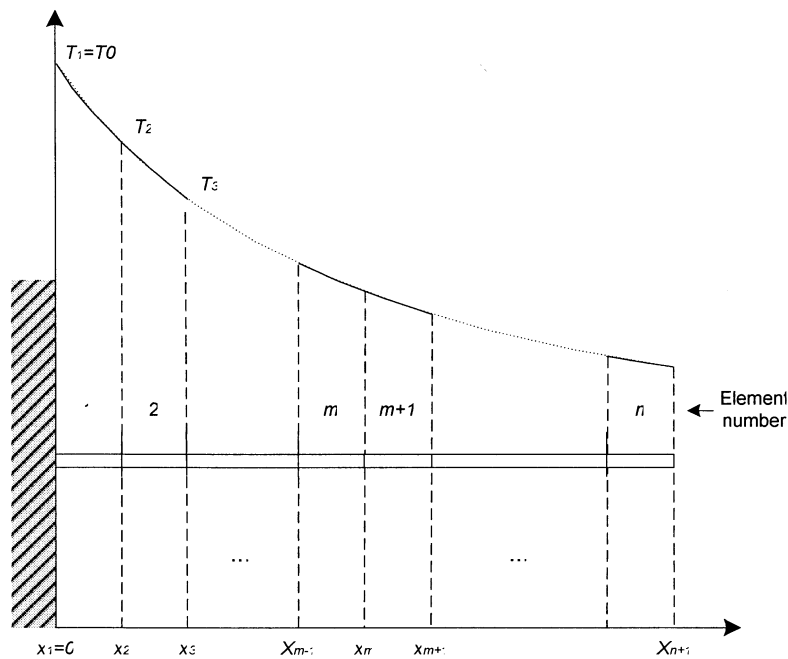


Figure 2.5: Thin rod divided into finite elements.

According to figure 2.5 the integral  $I$  can be rewritten as following:

$$I = I_1 + I_2 + \dots + I_n \quad (2.29)$$

and equation (2.28) becomes the following set of equations:

$$\frac{\partial I}{\partial T_m} = \frac{\partial I^{(m)}}{\partial T_m} + \frac{\partial I^{(m+1)}}{\partial T_m} \quad m = 1 \dots n + 1 \quad (2.30)$$

After solving the set of  $n+1$  equations and calculating the nodal temperatures, the temperature inside each elements will be calculated by the following equation:

$$T^{(m)} = \frac{1}{x_m - x_{m-1}} [(x_m T_{m-1} - x_{m-1} T_m) + (T_m - T_{m-1})x] \quad (2.31)$$

Equation (2.31) is the result of the following assumption:

$$T^{(m)} = a_m + b_m x \quad (2.32)$$

According to equation (2.32), the temperature inside each element has been approximated by a linear function. FEM software tools however have the capability of providing higher degrees of polynomials for approximation. A thorough discussion on the Finite Elements Method for 2D and 3D problems may be found in [17, 19]. This method will be used in next chapters by the COMSOL finite element software for thermal simulation of a typical Ball Grid Array (BGA) package.

## 2.6 Summary

Heat transfer mechanisms (Conduction, Convection, and Radiation) and governing equations are discussed. For most electronic component, heat conduction is the most important heat transfer phenomenon; therefore most researchers consider a component that has thermal conduction as its *only* mode of internal heat transfer. The thermal boundary conditions and the initial temperature condition are described.

Numerical methods such as finite element method and finite difference method can be applied to various kinds of heat conduction problems (e.g. isotropic, non-isotropic, linear, non-linear, homogeneous, and non-homogeneous) for thermal analysis of electronic system.

Finite element method is selected in this research work as the numerical thermal simulation tool. This is one of the most popular numerical methods used by design engineers in today's product design process in industry.

## Chapter 3

# Electronic Packages and the Detail Thermal Analysis of a BGA Electronic Package

### 3.1 Introduction

This chapter is dedicated to the presentation of a three-dimensional model developed to study the thermal properties of a Ball Grid Array (BGA) electronic package. Different types of currently popular electronic packages are introduced and briefly described. A more detailed and thorough discussion on the BGA package is then presented. The process of finite element (FE) model generation including, BGA geometry, the physical properties, boundary conditions, and initial conditions has been discussed. Using the developed FE model, numerical simulation was performed. The FE simulation results in terms of temperature distribution and heat flux are presented.

### 3.2 Electronic Packaging and BGA Packages

Packaging is one the final steps of Integrated Circuits and semiconductor devices fabrication. In this step the electronic die is mounted inside a package that provides physical protection and electrical access to the die. The process of packaging includes 3 major steps: Attaching, Bonding, and encapsulation. Attaching is the process of mounting and attaching the die inside the package. Bonding is the process of connecting the electronic circuit to the electrical pins of package. And encapsulation is the process of covering the top of the die and encapsulating it by plastic, ceramic, or other materials to make the physical protection. A detailed discussion on the area of electronic packaging may be found in [20]. For more information about the materials being used in the packaging process [21] is suggested.

There are many types of electronic packages which are divided into several categories based on the material used for fabrication, the method they are mounted on the PCB, pin arrangements, and other characteristics. For example materials used in packages can be plastic, ceramic, or epoxy. The mounting methods include insertion, surface, chip carrier, socket, and ball grid array (BGA). Before a thorough explanation about BGA packaging

technology some of the other types of packages which are popular and produced by manufacturers are introduced in the following section.

**Dual Inline Parallel (DIP) package** which is also called DIL is a rectangular shape package with two parallel rows of electrical connecting pins coming out of the two sides of the package. Material used in this type of packages is either plastic or ceramic. The method of connecting DIP package to the PCB is insertion. It means the metal pins of DIP are inserted from one side of the PCB to the holes already drilled in the board and soldered on the other side of the board. Some of the characteristics of DIP are as following:

- Lead Pitch (Pin spacing): 2.54 mm or 0.1" and 1.778 mm (0.07").
- Row spacing (the distance between the rows): 7.62 mm (0.3") and 15.24 mm (0.6").
- Pin counts (number of electrical pins): 8, 14, 16, 18, 20, 22, 24, and 28 for 0.3" row spacing and 24, 28, 32, 36, 40, 48, and 52 for 0.6" row spacing.

A typical 18 pins, 0.3" row spacing plastic DIP package [22] is shown in Figure 3.1.

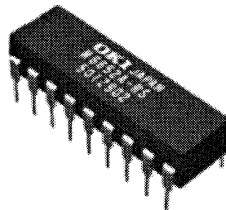


Figure 3.1: Typical 18 pins plastic DIP package

**Small Outline Integrated Circuit (SOIC)** has also two parallel rows of electrical pins which are gull wing leads. Small out line package is made from plastic and mounted on the surface of the PCB using surface mounting technology (SMT). Some of the characteristics of SOIC package are:

- Lead Pitch: 1.27 mm (0.05").
- Row spacing: 3.81 mm or 0.15" (narrow body) and 7.62 mm or 0.3" (wide body).
- Pin counts: 8, 14 and 16, 20, 28, 44.

A typical 16 pins, 0.15" row spacing SOIC package [23] is shown in Figure 3.2.

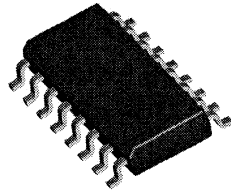


Figure 3.2: Typical 16 pins SOIC package

**J-Leaded Small Outline (SOJ)** like two previous types has two parallel rows of electrical pins which are J-type leads. SOJ package is made from plastic and mounted on the board using a chip carrier. Some of the characteristics of SOJ package are:

- Lead Pitch: 1.27 mm (0.5").
- Row spacing: 7.62 mm (0.3") and 10 mm.
- Pin counts: 20, 26, 28, 32, 40, and 42.

A typical 32 pins, 10 mm row spacing SOJ package [24] is shown in Figure 3.3.

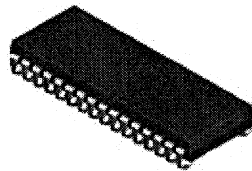


Figure 3.3: SOJ package with 32 pins

The gull wing lead and J-type lead is shown in Figure 3.4.

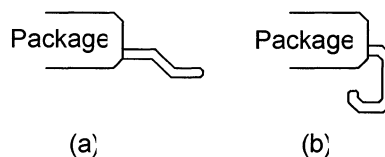


Figure 3.4: (a) gull wing lead (b) J-type lead

**Plastic Leaded Chip Carrier (PLCC)** is a square or rectangular shape package made from plastic and has J-type electrical pins coming out from all four sides of the package. PLCC packages also need chip carriers to be mounted on the PCB. Some of the pin and body characteristics of PLCC are as following:

- Lead Pitch: 1.27 mm (0.5").
- Row spacing: 8.8 mm, 11.4 mm, 16.5 mm, 19.0 mm, 24.1 mm, 29.2 mm, and 11.4×13 mm (rectangular body).
- Pin counts: 20, 28, 32, 44, 52, 68, 84.

A typical PLCC44 package is illustrated in Figure 3.5 [25].

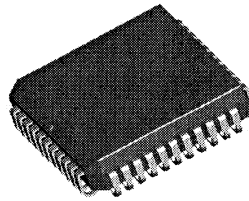


Figure 3.5: PLCC44 package

**Quad Flat Pack (QFP)** is another square shape electronic package that has electrical pins extending from its 4 sides. This type of package is a surface mounted device (SMD) and must be mounted directly on the surface of PCB and connections from pins to tracks of PCB are made at the same side that package is mounted. There are several variants of QFP package as following:

Fine Pitch Quad Flat Package (FQFP),

Heat sinked Quad Flat Package (HQFP),

Low Profile Quad Flat Package (LQFP),

Ceramic Quad Flat Package (CQFP),

Plastic Quad Flat Package (PQFP),

Metric Quad Flat Package (MQFP),

Small Quad Flat Packag (SQFP),

Very small Quad Flat Package (VQFP),

Thin Quad Flat Package ( TQFP),

Very Thin Quad Flat Package (VTQFP),

Bumpered Quad Flat Package (BQFP),

Bumpered Quad Flat Package with Heat spreader (BQFPH),

and some of the characteristics of QFP package are:

- Lead Pitch: 0.4mm to 1 mm.
- Row spacing: 10×10 mm to 40×40 mm square shape.
- Pin counts: 32 to 304.

A typical 100 pins PQFP package is illustrated in Figure 3.6 [26].

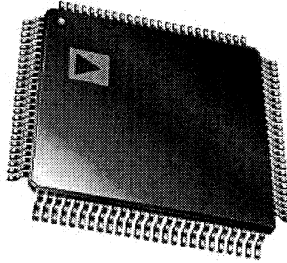


Figure 3.6: PQFP package

**Pin Grid Array (PGA)** is a square shape ceramic package that its electrical pins are extended from the bottom side of the package and must be mounted either directly on the PCB or by the means of a zero insertion force (ZIF) socket. Most of the modern Desktop CPUs are built by this technology. Some variants of PGA package are:

Plastic Pin Grid Array (PPGA),

Flip-Chip Pin Grid Array (FCPGA) and FC-PGA2

Ceramic Pin Grid Array (CPGA),

Organic Pin Grid Array (OPGA),

The most famous PGA packages with 478 pins [27] are shown in Figure 3.7.

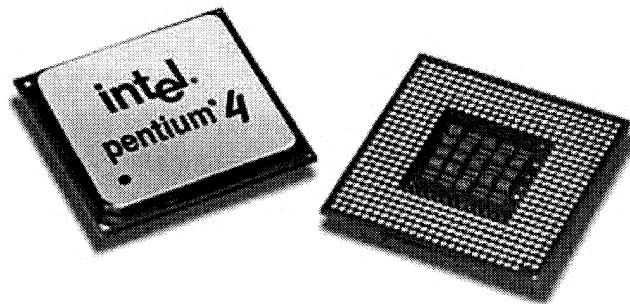


Figure 3.7 Pentium 4 PGA package

### **3.3 BGA packaging technology**

The Ball Grid Array or BGA is an advanced packaging technology descended from PGA. Like PGA package one side of BGA is fully or partially covered by electrical pins and the other side is exposed to the free or forced convection or in contact with heat sink. Unlike other types of packages in BGA technology electrical connections between the chip and PCB are established via solder balls instead of metal pins. The process of mounting the BGA package on the PCB has three steps:

- 1- BGA is precisely placed and align on top of the PCB so the balls are in contact with PCB pads.
- 2- The contact location is then heated usually by infrared heater so the solder balls start melting.
- 3- The last step is cooling down so the solder starts to solidify.

This process of mounting is considerably more complex than what is needed for other types of package. There are however some key advantages that make this technology desirable for microelectronic designers. These advantages are:

- 1- High connection density: in order to connect other types of package to the PCB, pins must be soldered. This will restrict the proximity of the pins so the danger of unwanted bridging between two adjacent pins is reduced. BGA however does not have this problem so the number of pins can be increased up to 1152 leads when the lead pitch is 1.0 mm.
- 2- Increased Heat conduction: the thermal resistance between the BGA package and PCB is lower than other packages. The operating temperature thus is lower.
- 3- Low Inductance of connections: the small size of leads in BGA technology comparing to the metal pins reduces the electrical inductance and switching noise and other distortions.
- 4- Higher reliability: the short length of balls comparing to the pins reduces the danger of failures caused by mechanical tensions and vibrations.

There are several variants of BGA packages and some of them are as following:

Fine Ball Grid Array (FBGA)  
Ceramic Ball Grid Array (CBGA)  
Plastic Ball Grid Array (PBGA)  
Plastic Ball Grid Array - Heat Spreader (PBGA-H)  
Plastic Ball Grid Array – Multi Die (PBGA-MD)  
Enhanced Ball Grid Array (EBGA)  
Tape Ball Grid Array Package (TBGA)

Figure 3.8 illustrates three BGA packages [28]. More information on the technology, material properties, and specification of BGA packages may be found in [29].

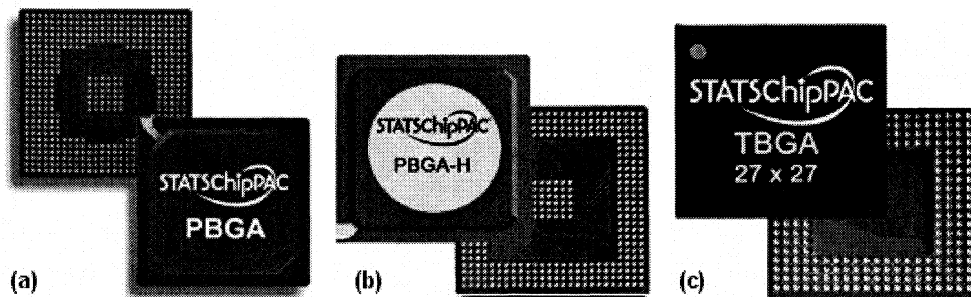


Figure 3.8: Three types of BGA package. (a) PBGA. (b) PBGA-H, (c) TBGA

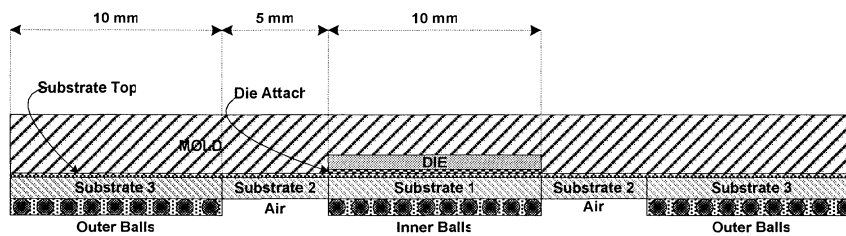
### 3.4 Detailed Finite Element Thermal Model of BGA Package

In this work the single chip BGA package proposed in [30] has been selected as a case study of Compact Thermal Model (CTM) generation process. This package has several layers as following:

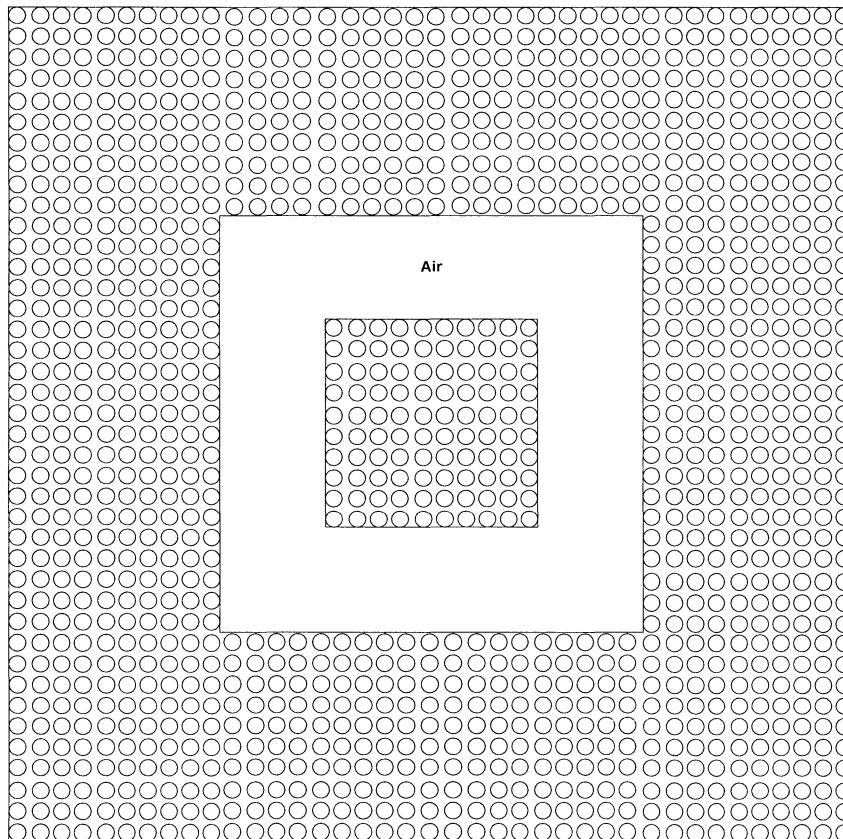
- Leads or balls that establish the electrical connections between the PCB and the electronic circuit inside the package. This layer includes inner balls which will be called LEAD1 later in this work and outer balls which will be LEAD2.
- Air is the empty space between inner and outer balls.
- Substrate 1 which is located on top of the inner balls.
- Substrate 2 which is located on top of the air layer.
- Substrate 3 which is located on top of the outer layer.
- Substrate top layer which is located on top of the substrate 1, 2, and 3 layers.

- Die attach is located on top of the substrate top layer and align with the substrate 1 and inner balls layers.
- Die which is the silicon chip where the electronic circuit is built on and located on top of the die attach layer.
- Mold which is the covering material located on top and around the die and encapsulate it for protection.

These layers have been illustrated in figure 3.9 (a) which is a cross section view of the BGA package. Figure 3.9 (b) illustrate the bottom view of the package.



(a)



(b)

Figure 3.9: BGA package used in this research (a) Cross section view (b) Bottom view

Looking at figure 3.9 it is clear that the BGA package has is quarter symmetric. We can thus enjoy this characteristic and model only a quarter of the package. This will considerably decrease the computation cost when we will simulate the package by the finite elements thermal simulator. Figure 3.10 shows the quarter symmetry cross section of package and Table 3.1 contains the one quarter sizing and material properties [30].

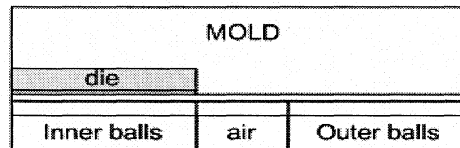


Figure 3.10: Quarter symmetry cross section of BGA

Layer	Thickness (mm)	Top View Dimensions (mm)	Thermal Conductivity (W/mK)	Thermal Capacity (J/m <sup>3</sup> K)
Mould (above die)	0.7	20×20	0.6	2.0e+6
Die	0.3	5×5	100	1.5e+6
Die Attach	0.02	5×5	1	2.0e+6
Substrate Top	0.03	20×20	200	3.0e+6
Substrate 1	0.6	5×5	kx=20 ky=20 kz=8	2.0e+6
Substrate 2	0.6	5×10	kx=5 ky=5 kz=2	2.0e+6
Substrate 3	0.6	10×20	kx=10 ky=10 kz=4	2.0e+6
Air	0.5	5×10	0.03	1.0e+3
Inner Balls	0.5	5×5	kx=0.05 ky=0.05 kz=25	1.0e+6
Outer Balls	0.5	10×20	kx=0.05 ky=0.05 kz=25	1.0e+6
Power Dissipation: 0.25 W				

The first step of generating a compact thermal model of package is simulating the thermal behavior of the package by thermal simulation software. The BGA package size and physical properties are listed in Table 3.1. A detailed thermal model of the package was built by the thermal simulation software. This model was able to simulate the thermal behavior at any point within or on the surfaces of the package. In the following chapters the simulation results will be used to generate the compact thermal model by optimization and also to validate the performance of the compact model by comparing its results to the results of detailed model.

Although different approaches for thermal analysis and simulation are available, finite element analysis, which is based on accurate constitutive models, provide the most detailed information on the spatial and temporal distribution of temperature. The

objective of the present section is to simulate the steady state thermal analysis of BGA package, using COMSOL© [31] which is a powerful finite element software package designed to solve partial differential equations using finite element method. COMSOL is widely used by the industry in many fields of engineering such as structural mechanics, MEMS, electromagnetic, acoustics, fluid dynamics, geography, quantum mechanics, semiconductor devices, and chemical reactions.

Figure 3.11 illustrate the simplified geometry of BGA package generated by the CAD tools of COMSOL.

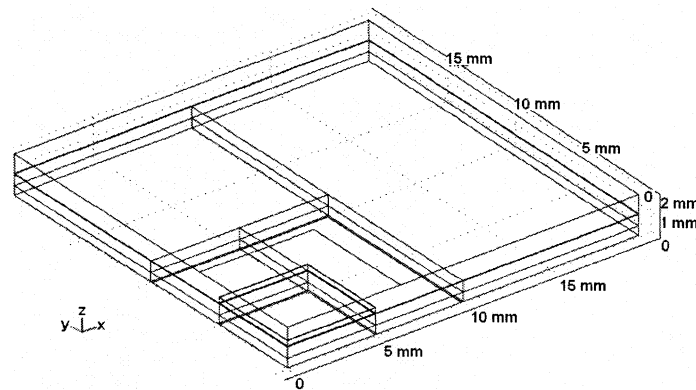


Figure 3.11: Final geometry of BGA package

COMSOL has a powerful meshing tool by which the domain of the analysis can be divided into elements with desired size and shape. Therefore, this geometry has been divided into several small cells called elements during the meshing process. These elements are the same as explained in previous chapter and are used to simulate the package by finite element analysis. Note that while the accuracy of detailed model can be enhanced by increasing the number of elements, it takes much longer time for computer to solve the model. It means the minimum number of elements is desirable by which an acceptable accuracy is achievable. The accuracy criterion here is the difference between the ideal and the detailed model calculated values of outward normal heat flux from the package. Ideally total outward heat flux from package walls is equal to the total heat generated by the junction (Inward heat flux from ambient environment is considered to be zero) because of energy conservation law. But the total outward heat flux calculated by detailed model shows a small difference from ideal because of discretization error. It was tried to find the minimum number of elements by which this error is less than half a percent.

Figure 3.12 illustrates the 3D view of the meshed BGA geometry. The meshing parameters used for the BGA geometry are listed in Table 3.2.

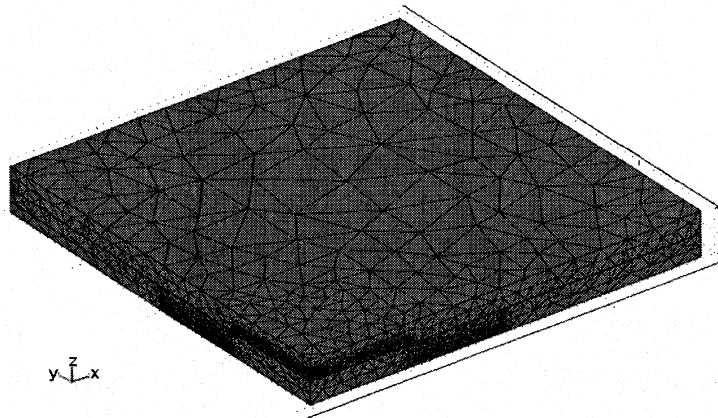


Figure 3.12: 3D view of the meshed BGA geometry

<b>Table 3.2: Mesh parameters of detailed model</b>	
Number of degrees of freedom	312717
Number of elements	224959
Number of boundary elements	52082
Number of edge elements	2005

The material properties of sub-domains such as thermal conductivity, density, thermal capacity, initial temperature, and heat generated inside the sub-domain are listed in Table 3.1. These properties have been used during the simulation efforts.

In this work the top area has been divided into 2 areas. Inner top is a square with the length equal to 6.4 mm and represented by the node Top1. The rest of top surface is modeled by the node Top2. Figure 3.13 shows the heat flux distribution profile of the top surface of the BGA package for 2 different boundary conditions applied to that surface. This distribution has a peak above the die area where  $x$  and  $y$  are smaller than 5 mm. It's clear that this heat flux distribution can not be represented linearly by just one resistor that models the heat transfer by convection from the top surface to surrounding environment because it's always assumed that within a linear electrical resistor the distribution of current flow is uniform. Using electromagnetic theory and 2D Fourier expansion of the heat flux distribution function of the top surface, it can be proved that if the surface is divided into several smaller sub surfaces in which the heat flux distribution

can be approximated uniform, modeling by linear resistors are possible with higher accuracy. More discussion and mathematical calculations can be found in [32].

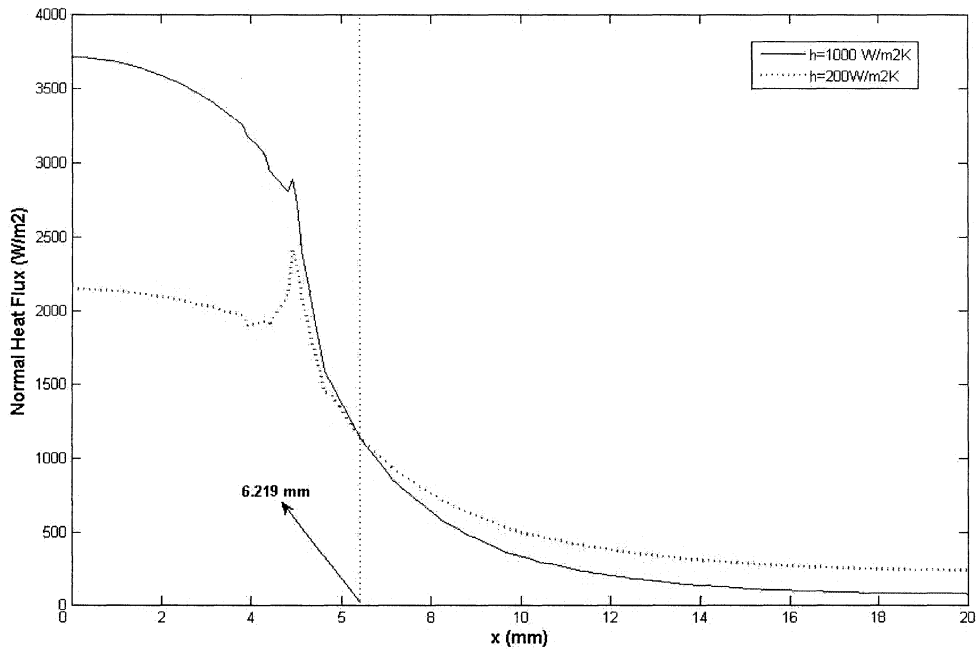


Figure 3.13: Heat flux distribution on the top surface of BGA package for 2 different boundary conditions applied to the top surface

Other surfaces of package are inner balls or LEAD1, outer balls or LEAD2, SIDE wall, and Air between inner and outer balls or BOTTOM. These surfaces have been illustrated in figure 3.14 (a) and (b). JUNCTION in which heat is generated is also the upper region of die with a thickness of 0.01 mm within the package. Table 3.3 contains the area and volume of these nodes.

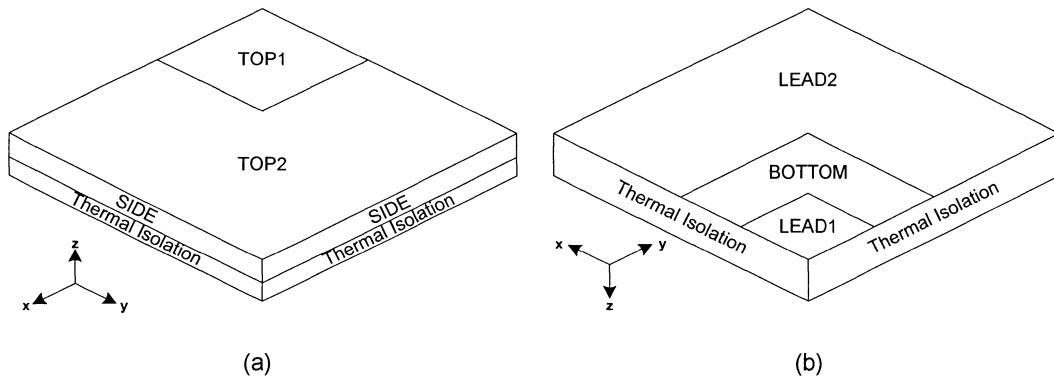


Figure 3.14: (a) TOP1, TOP2, and SIDE areas, (b) LEAD1, LEAD2, and BOTTOM areas.

Node		Area m <sup>2</sup>
Top 1 (inner top)	T1	4.12036E-5
Top 2 (outer top)	T2	3.58796E-4
Lead 1 (inner leads)	L1	2.5E-5
Lead 2 (outer leads)	L2	3E-4
Bottom	B	7.5E-5
Side	S	6.6E-5
Junction J (Volume)		5E-10 m <sup>3</sup>

Table 3.4 contains the 58 different boundary condition sets [30] which are applied to the package one by one and each time the simulation is performed. The COMSOL solver has been adjusted for the steady state simulation in each study case. Steady state simulation takes several seconds depending on the processing power and problem conditions such as linearity, number of elements, etc. Transient simulation will be explained in chapter 5.

No	h <sub>TOP</sub>	h <sub>BOT</sub>	h <sub>SIDE</sub>	h <sub>LEADS</sub>
1	5	1	5	1
2	5	10	5	10
3	5	25	5	50
4	5	50	5	50
5	5	50	5	100
6	5	100	5	200
7	15	1	15	1
8	15	10	15	10
9	15	25	15	50
10	15	50	15	50
11	15	50	15	100
12	15	100	15	20
13	30	5	30	5
14	30	30	30	30
15	30	50	30	50
16	30	200	30	200
17	80	5	80	5
18	80	30	80	30
19	80	50	80	50
20	80	200	80	200
21	200	5	200	5
22	200	30	200	30
23	200	50	200	50
24	200	200	200	200
25	25	1	5	1
26	25	10	5	10
27	25	25	5	50
28	25	50	5	50

29	25	50	5	100
30	25	100	5	200
31	75	1	15	1
32	75	10	15	10
33	75	25	15	50
34	75	50	15	50
35	75	50	15	100
36	75	100	15	200
37	150	5	30	5
38	150	30	30	30
39	150	50	30	50
40	150	200	30	200
41	500	5	200	5
21	500	30	200	30
43	500	50	200	50
44	500	200	200	200
45	10	50	10	1000
46	10	1000	10	10000
47	1000	5	10	50
48	10000	50	10	500
49	10000	10000	10000	10000
50	5000	5000	5000	5000
51	1000	1000	1000	1000
52	500	500	500	500
53	10 <sup>9</sup>	10 <sup>9</sup>	10 <sup>9</sup>	10 <sup>9</sup>
54	50000	50000	50000	50000
55	10000	10000	1	1
56	10	10000	1	1
57	10000	10	1	1
58	1	1	1	10000

Figure 3.15 shows the 3D view, cross section view, and bottom view of temperature profile of package solved for the BC no. 1. The hottest region is in the center of package where the junction (region where heat is generated) located and shown by red color. Outer regions of package shown by blue color are cooler than junction.

The average temperature and outward heat flux of desired regions within or on the surface of the geometry has been obtained using the COMSOL's postprocessor.

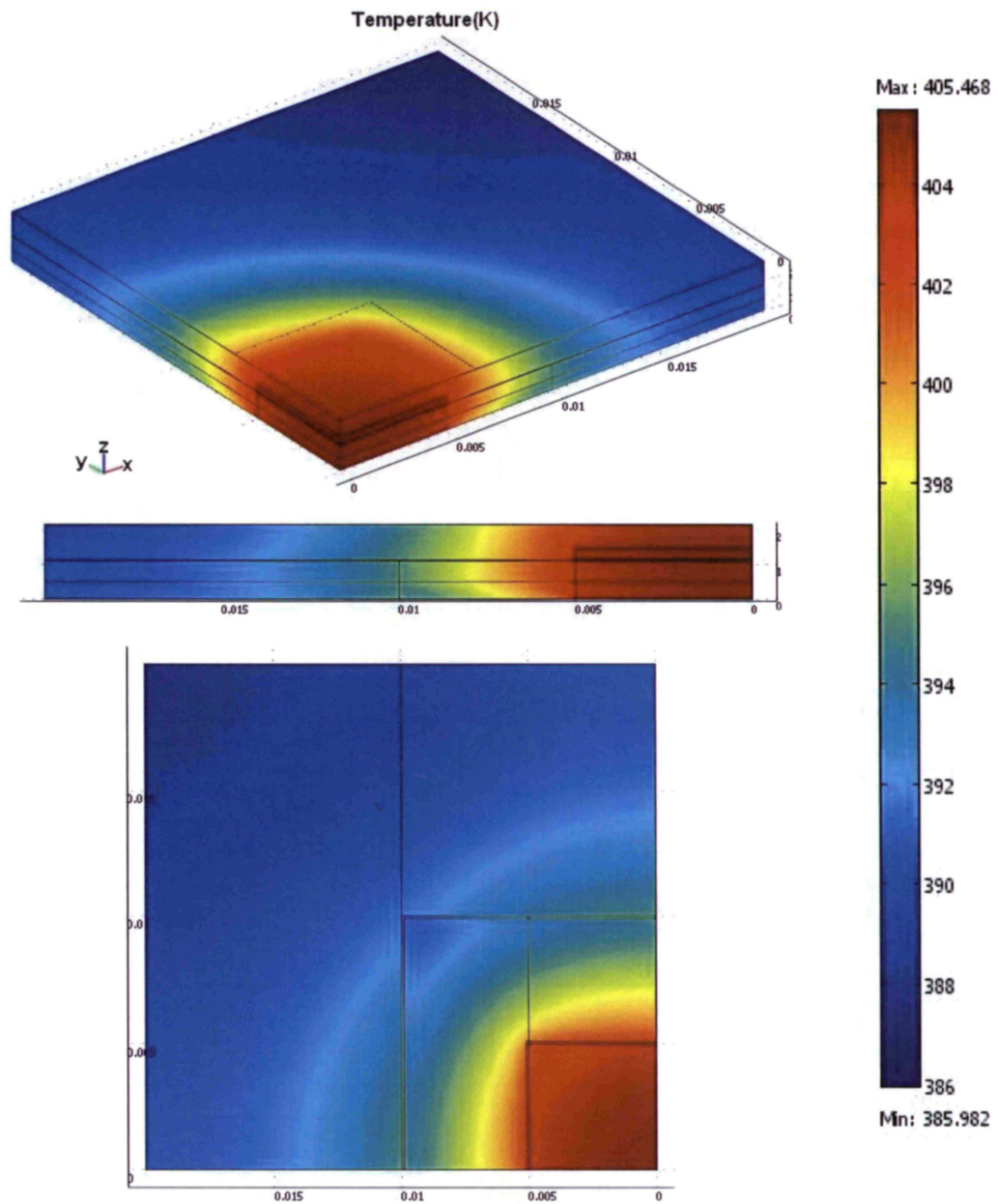


Figure 3.15: Graphical illustration of thermal simulation

Note that for all 58 boundary conditions of Table 3.3, finite element simulation have been performed and the obtained results in terms of temperature and heat flux distribution at all locations were recorded for future steps of this project (i.e. generation of compact thermal model).

### **3.5 Summary**

In this chapter some of the currently popular electronic packages were introduced briefly. The emphasis was given o the BGA technology and packages because this type of package was selected to be thermally modeled in this project. Several types of BGA packages were introduced and the process of simulating a typical BGA package by the thermal analysis software COMSOL is explained in detail. Finally the desired temperatures and heat fluxes were obtained for all boundary conditions. The obtained results will be served in next chapter to generate the steady state compact thermal model of a BGA package.

## Chapter 4

### Linear Steady State Compact Thermal Model

#### 4.1 Introduction

In chapter 2, it was mentioned that numerical methods of solving the heat transfer equation by conduction (detailed model simulation) needs expensive software and can be very time consuming specially for system level simulation where a complex electronic system including several packages, discrete elements, boards, cooling system, and case is the subject of analysis. A compact thermal model by which one can calculate the average temperature and heat flux of only desired locations within and on the surfaces of the package with sufficient accuracy hence is a necessity to simplify the system level thermal analysis. These models enable the package and system level designer to predict the temperature and heat flux of critical components with the accuracy required for reliability and performance prediction. There are several methods of compact model generation, however for steady state compact modeling purpose there is one dominant approach proposed by DELPHI consortium (a collaborative European project) which is based on resistor network and will be explained and examined thoroughly in this chapter. This method employs the similarity of thermal and electrical behaviors of solid materials and models heat fluxes by electrical currents, temperatures by electrical voltages, heat generation by current source, and thermal resistances by electrical resistances. The well known electrical formulas and simulation softwares can be used then to calculate the temperatures and heat fluxes.

#### 4.2 DELPHI compact thermal model

The main goal of this project which involved six end-user electronic equipment companies from five European states was to propose a methodology to generate Boundary Condition Independent Compact Thermal Models (BCI-CTM) for electronic packages [1]. The DELPHI consortium members were Thomson CSF, Philips CFT, Alcatel Bell, Alcatel Space, Flomerics, and the National Microelectronics Research Center in Ireland. The first four companies which were the industrial partners of project

are well known producers of electronic equipment in the area of civil and military radar, lighting and consumer electronics, telecommunications equipments, and satellite electronics. The fifth partner of project Flomerics is a developer of a thermal CAD tool used in the electronic industry [2].

The DELPHI procedure of generating static (steady state) compact thermal model has several steps as following:

- 1- A detailed thermal model of the package is generated by a thermal CAD tool.
- 2- Using the thermal CAD tool, thermal simulations are performed on package for a set of boundary conditions proposed by DELPHI consortium and average temperatures and heat fluxes of desired locations (thermal nodes that correspond to the volumes and areas inside or on the surfaces of package) are obtained.
- 3- A network is postulated. This network consists of several resistors that connect the thermal nodes to each other.
- 4- The values of resistors are then calculated using the detailed model results.

Boundary Condition Independence (BCI) is an important issue that must be addressed during the procedure of compact model generation. The rationale behind this issue is that the package producers that propose the compact models do not know in what environmental conditions their products will be used by consumers. Therefore, the compact model must be capable to predict the desired temperatures and heat fluxes accurately regardless of what boundary conditions applied to the package.

### **4.3 Static compact model definition**

Following the DELPHI methodology, the thermal characteristics of the package can be modeled by a resistor network as mentioned earlier. Using node analysis method, the general formula relating the voltages (temperatures) and currents (heat fluxes) of the electric network can be expressed as:

$$q_i = \sum_{k=0}^N Y_{ik} T_k \quad (4.1)$$

where:

$Y$  is the conductance matrix,

$N$  is the number of nodes,

$q_i$  (Amp) is the electrical current leaving the node  $i$ , and

$T_i$  (Volt) is the voltage of node  $i$ .

If the package is considered a linear thermal system (i.e. the thermal conductance and other physical properties of the package are temperature independent), it can be modeled by a linear system such as eq (4.1) and matrix  $Y$ . This can represent the static compact thermal model of the package. The higher value of  $N$ , the higher accuracy will be achieved by this modeling. Note that each node in equation (4.1) represents a specified area or volume within or on the surfaces of the package such as junction region, side walls, top surface, leads... Node voltages calculated by the equation (4.1) are equal thus to the average temperature of their corresponding volume or area. Leaving currents from nodes are also equal to the total outward heat flux from their corresponding volume or area. Equations (4.2) and (4.3) calculate the average temperature and total outward heat flux of the represented by node  $i$ :

$$T_i = \frac{1}{S_i} \int_{S_i} T(x) d^2x \quad \text{or} \quad T_i = \frac{1}{V_i} \int_{V_i} T(x) d^3x \quad (4.2)$$

$$q_i = - \int_{S_i} \lambda(x) \frac{\partial T(x)}{\partial n} \Big|_{S_i} d^2x \quad (4.3)$$

where  $S_i$  ( $m^2$ ) and  $V_i$  ( $m^3$ ) are the area and volume of any specified region within or on the surfaces of the package represented by node  $i$ .

#### 4.4 Compact model generation

Now that the compact model is defined we are ready to generate the static compact thermal model of BGA package from the detailed model generated in chapter 3. We have performed several detailed model simulations under various boundary conditions (see chapter 3) and computed average temperature and heat flows. The process of compact model generation will continue by specifying the resistor network topology, calculating the resistors' value, and validating the compact model.

#### 4.4.1 Network topology

. In previous chapter it was mentioned that the desired locations of the package that their average temperatures and outward heat fluxes must be calculated by the compact model are Junction, TOP1, TOP2, LEAD1, LEAD2, SIDE, and BOTTOM as illustrated in figure 4.1

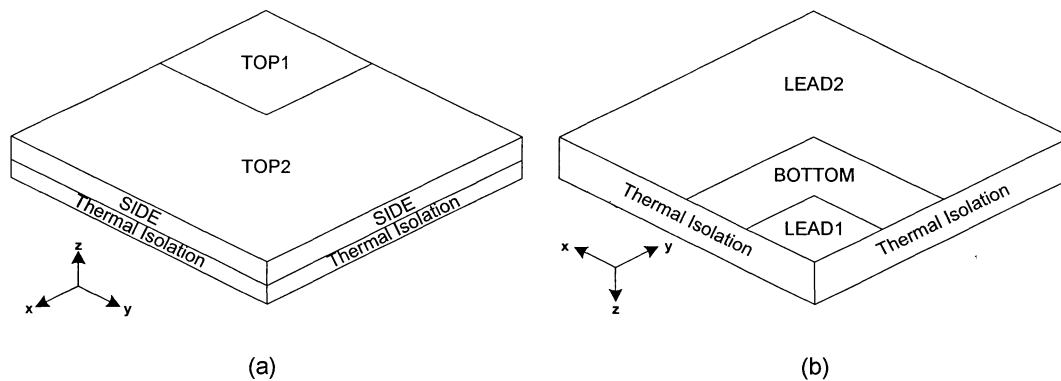


Figure 4.1: (a) TOP1, TOP2, and SIDE areas, (b) LEAD1, LEAD2, and BOTTOM areas.

The resistor network must have seven nodes thus that represent these regions. These nodes can be fully connected to each other via 21 thermal resistors. It is desirable however to eliminate as many of these resistors as possible to find the most compact network that can model the package with acceptable accuracy. It is actually possible to find the optimum topology from the fully connected network depending on the number of thermal nodes engaged in the thermal analysis and the importance of thermal variables associated to each node in the analysis. First the fully connected network (in which every node is connected to all other nodes by resistors) is calculated and the then largest resistors will be eliminated one by one. Once the network starts showing the relative errors higher than the predetermined criterion the elimination process must be stopped and the last elimination must be cancelled [3]. In this work we decided to choose the topology proposed in [4] and calculate the compact from the detailed model results from the thermal simulation we performed in chapter 3 using COMSOL© and the optimization algorithm we developed by MATLAB© programming. This model then will be used as a base for dynamic compact model generating in the next chapter. Figure 4.2 illustrate the static compact model resistor network.

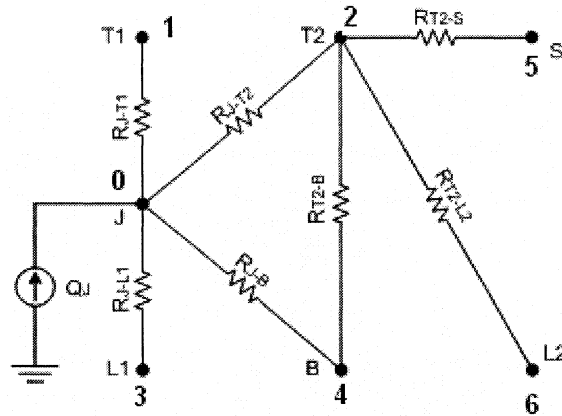


Figure 4.2: Resistor network static compact model of BGA package

Note that heat generated by the circuit on the die is equal to  $Q_j=0.25$  W as mentioned in table 3.1 and modeled by a current source. TOP1, TOP2, LEAD1, LEAD2, SIDE, and BOTTOM of the package are represented by nodes 1 to 6 respectively in both figure 4.2 and equation (4.1). Junction is also represented by node 0. Finally it must be mentioned that  $R_{mn}$  in the figure 4.2 is equal to  $1/y_{mn}$  where  $y_{mn}$  is the thermal conductance between nodes  $m$  and  $n$  and an element of the conductance matrix of equation (4.1).

#### 4.4.2 Resistors' value

Equations (4.2) and (4.3) calculate the average temperatures and total outward heat fluxes of the Networks nodes. In chapter 3 we obtained the same variables from the detailed finite element model for the specified regions of the BGA package. Therefore, the obtained results from detailed model can be used to calculate the matrix  $Y$  of equation (4.1). From figure 4.2, it is clear that we can not calculate  $Y$  by writing the node analysis equations solve them using the numbers we have saved from detailed model because we have only 6 independent equations for 7 unknown resistors. An alternative approach is trying to guess some values for the resistors, calculate output of the network and comparing it with the detailed model output. To use this solution we need to define a cost function that calculates the difference between the compact and detailed models and try to fit some resistors' value that minimize this cost function. In other words compact model calculation is an optimization process. The cost function used to represent this deviation is:

$$COST = \frac{1}{BC} \sum_{k=1}^{BC} \left( \frac{T_J^c(k) - T_J^d(k)}{T_J^d(k) - T_{amb}} \right)^2 \quad (4.4)$$

where:

$BC$  is the total number of boundary conditions which is equal to 58 different cases,

$k$  is the number that specifies the boundary condition,

$T_J^c(k)$  (Kelvin) is the junction temperature calculated by the compact model for the  $k$ th boundary condition,

$T_J^d(k)$  (Kelvin) is the junction temperature obtained from the compact model for the  $k$ th boundary condition, and

$T_{amb}$  (Kelvin) is the room temperature.

According to equation (4.4) the difference between the detailed and compact model is determine only by the junction temperatures acquired from these models. It can however be modified so other thermal variables will be effective in this process. For example [4] has proposed the following cost function

$$\frac{1}{BC} \sum_{k=1}^{BC} \left[ V \left( \frac{T_J^c(k) - T_J^d(k)}{T_J^d(k) - T_{amb}} \right)^2 + \frac{W}{N} \sum_{i=1}^N \left( \frac{q_i^c(k) - q_i^d(k)}{q_J} \right)^2 \right] \quad (4.4)$$

where:

$N$  is the number of nodes except the junction,

$W$  and  $V$  are weighting factors specifying the importance of thermal variables in the optimization process,

$q_i^c(k)$  (W) is the total heat flux leaving the node  $i$  calculated by compact model, and

$q_i^d(k)$  (W) is the total heat flux leaving the node  $i$  obtained from detailed model,

#### 4.4.3 Nelder-Mead Simplex optimization method

Nelder-Mead or Simplex method which is also called downhill method was proposed by J. A. Nelder and R. Mead 1965 [34]. This is one of the most popular and widely used methods of multi-variable our multi-dimensional optimization belongs to the class of

direct search optimization methods because it doesn't use derivatives of variables. In order to understand this method the following terms and expressions should be explained:

*Multi-variable* or *Multi-dimensional* optimization algorithm is an algorithm which is able to minimize a function of  $n$  variables.  $n$  is greater than 1, function is linear or non-linear and its variables are real or complex. Nelder-Mead method minimizes a linear function of real variables.

A *Direct search optimization method* is an optimization methods that its algorithm doesn't need derivatives of (to be optimized) variables. The detail of the concept of direct search method has been explained in [35, 36] and many other advanced optimization books.

A *Polytope* is the generalization of polygon which is a two dimensional geometric object and polyhedron which is a three dimensional geometric object to geometric spaces with higher dimensions.

A *Simplex* is a polytope with  $n+1$  vertices or angular points in a  $n$  dimensional space. In a one dimensional space ( $n=1$ ) which is a line, a line segment which has two ( $n+1=2$ ) vertices is a simplex, in a two ( $n=2$ ) dimensional space which is a plane a triangle which has three ( $n+1=3$ ) vertices is a simplex, and in a three dimensional space ( $n=3$ ) a tetrahedron which has four ( $n+1=4$ ) is a simplex.

The Nelder-Mead algorithm starts by accepting an initial point or vector of  $n$  initial variables.  $n+1$  other points are also chosen as the vertices of initial simplex which the initial point is inside it. After initialization step the algorithm starts the loop of searching the optimum point. Any iteration of this loop has 5 different steps which have been shown in figure 4.3.

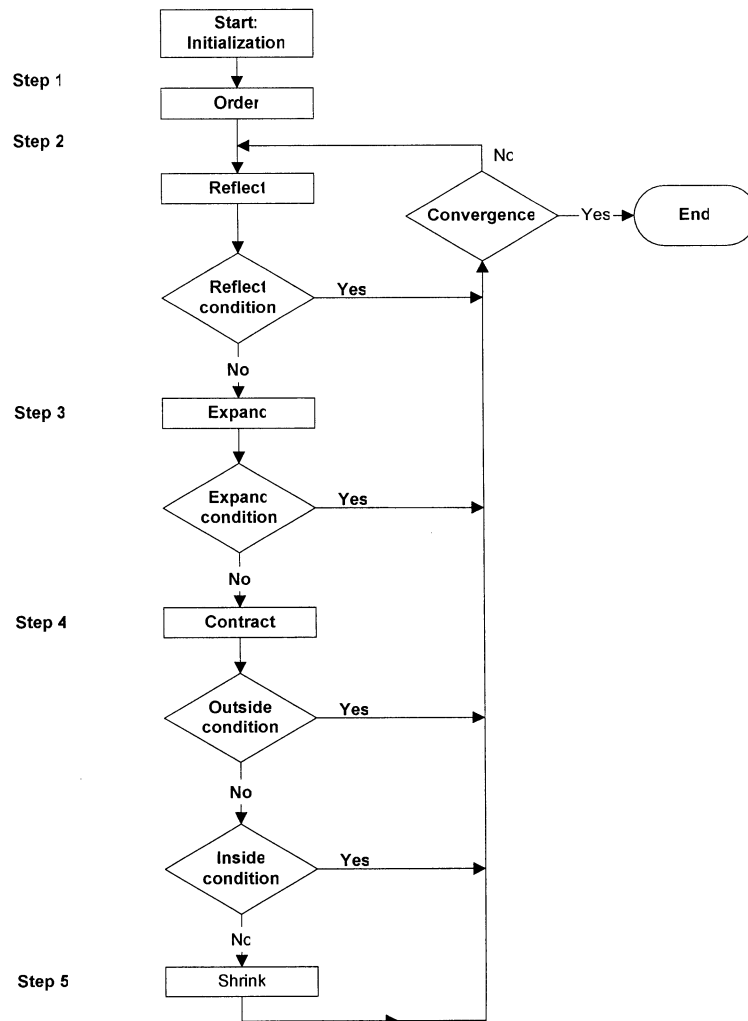


Figure 4.3: Five steps of Nelder-Mead algorithm

**Step 1- Order:** in this step the  $n+1$  vertices of simplex are ordered as following:

$$f(x_1) \leq f(x_2) \leq \dots \leq f(x_{n+1})$$

where  $f$  is the cost function and  $x_i \quad i = 1 \dots n$  are the vertices.

**Step 2- Reflect:** in this step the reflection point  $x_r$  as following:

$$x_r = \bar{x} + \rho(\bar{x} - x_{n+1})$$

where  $\bar{x} = \sum_{i=1}^n \frac{x_i}{n}$  is the center of gravity of the first  $n$  points, and

$\rho > 0$  is the reflection coefficient.

*Reflect condition:* if  $f(x_1) \leq f(x_r) < f(x_n)$  reflection is accepted and the answer to the reflect condition is yes and convergence check is performed. Otherwise answer is no and step 3 will be started.

**Step 3- Expand:** if the  $f(x_r) < f(x_1)$  the expansion point  $x_e$  is calculated as following:

$$x_e = \bar{x} + \chi(x_r - \bar{x})$$

where  $\chi > 1$  and  $\chi > \rho$  is the expansion coefficient.

*Expand condition:* if  $f(x_e) < f(x_r)$ ,  $x_e$  is accepted and convergence check is performed.

If  $f(x_e) \geq f(x_r)$ ,  $x_r$  is accepted and convergence check is performed.

**Step 4- Contract:** if  $f(x_r) \geq f(x_n)$  the following conditions are checked:

*Contract condition 1:* If  $f(x_n) \leq f(x_r) < f(x_{n+1})$ ,  $x_c$  is calculated as following:

$$x_c = \bar{x} + \gamma(x_r - \bar{x})$$

where  $0 < \gamma < 1$  is the contraction coefficient.

If  $f_c < f_r$   $x_c$  is accepted and convergence check is performed. Otherwise step 5 is performed.

*Contract condition 2:* if  $f_r \geq f_{n+1}$ ,  $x_{cc}$  is calculated as following:

$$x_{cc} = \bar{x} - \gamma(\bar{x} - x_{n+1})$$

If  $f(x_{cc}) < f(x_{n+1})$ ,  $x_{cc}$  is accepted and convergence check is performed. Otherwise step 5 is performed.

**Step 5- Shrink:** In this step a new simplex is generated by calculating a new set of vertices as following:

$$v_i = x_1 + \sigma(x_i - x_1) \quad i = 2, \dots, n+1$$

$$v_1 = x_1$$

where  $0 < \sigma < 1$  is the shrinkage coefficient.

**Convergence:** In every iterations a point inside the simplex is chosen randomly and the cost function associated to that point is calculated and compared to the cost function calculated from the previous iteration. If the difference between these two cost-functions is less than a predetermined value as the convergence criterion, the algorithm is converged and loop is terminated. A more detailed explanation about the Nelder-Mead algorithm can be found in [37].

MATLAB© has a function called *fminsearch* that uses the Nelder-Mead algorithm to optimize a cost function in a multi-dimensional space. The syntax of this function is:

```
x = fminsearch(fun,x0,options)
```

where:

fun is the cost function,

x0 is the vector of initial values assigned to the variables to be optimized,

x is the output vector containing the optimized variables, and

option is a structure that is set by *optimset* MATLAB© command.

*optimset* has several parameters and reader can find more explanation in MATLAB© help files. One of the important parameters of *optimset* is *TolFun* or Termination tolerance on the function value. This parameter determines the convergence condition of optimization algorithm.

## 4.5 Validation

Validating the compact model is the process of comparing its results to the detailed model results and calculating the relative error percentages. According to the criterion proposed in [4] we can consider the generated model *a valid Boundary Condition Independent Compact Thermal Model* if its relative difference with respect to the detailed model does not exceed certain agreed value for pre determined parameters such as junction temperature and heat fluxes. These relative differences (error percentages) are calculated according to the following relations:

$$\text{Max.Err. Percentage } TJ = 100 \times \max \left( \frac{T_J^c(k) - T_J^d(k)}{T_J^d(k) - T_{amb}} \right) \quad (4.5)$$

$$k = 1 \dots BC$$

$$\text{MaxErr. Percentage } Q = 100 \times \max \left( \frac{q_i^c(k) - q_i^d(k)}{q_J} \right) \quad (4.6)$$

$$i = 1 \dots N \quad , \quad k = 1 \dots BC$$

As proposed in [4], the relative errors must not exceed 10% and as long as thermal variables predicted by compact model show relative errors with respect to detailed model less than this pre determined value, the generated compact model is validated and is acceptable. Figure 4.4 shows the junction temperature relative errors for all 58 applied boundary conditions. It's clear that all of the errors are less than 10% criterion accepted in this work. The Maximum error occurs for boundary condition no. 50 at less than 1.6%.

Figures 4.5 to 4.10 also show the relative errors of heat flux variables at Top1, Top2, Lead 1, Lead2, side walls and bottom walls, respectively, for all applied 58 boundary conditions. These boundary conditions cover various scenarios such as free convection, forced convection, heat sink free convection, heat sink forced convection, cold plate. It can be observed that the error values are all less than 10% criterion for various scenarios.

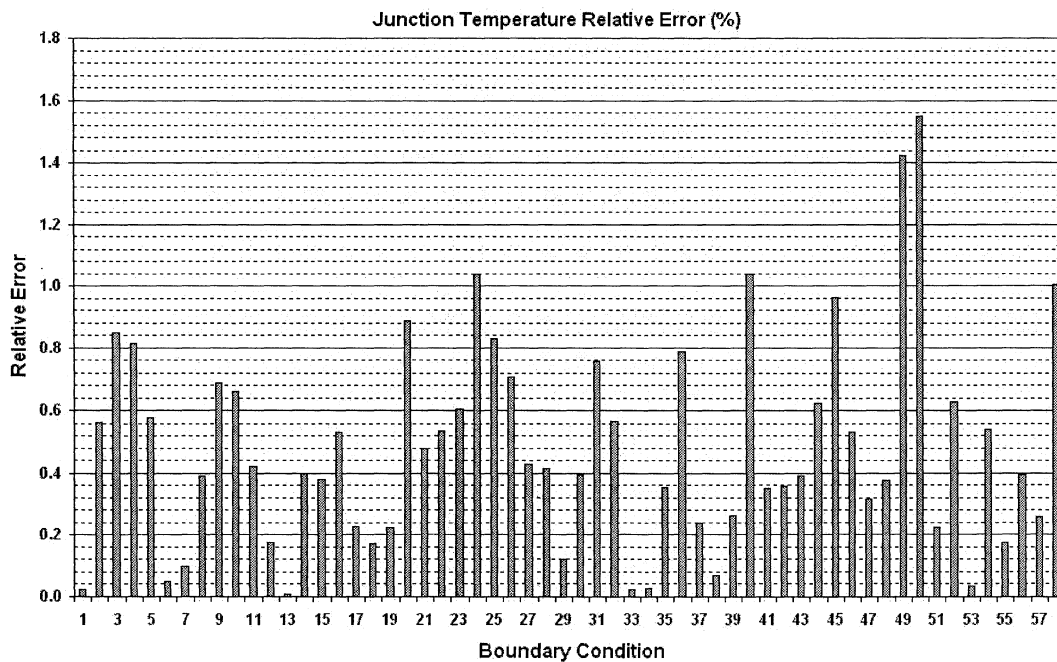


Figure 4.4: Junction temperature relative errors

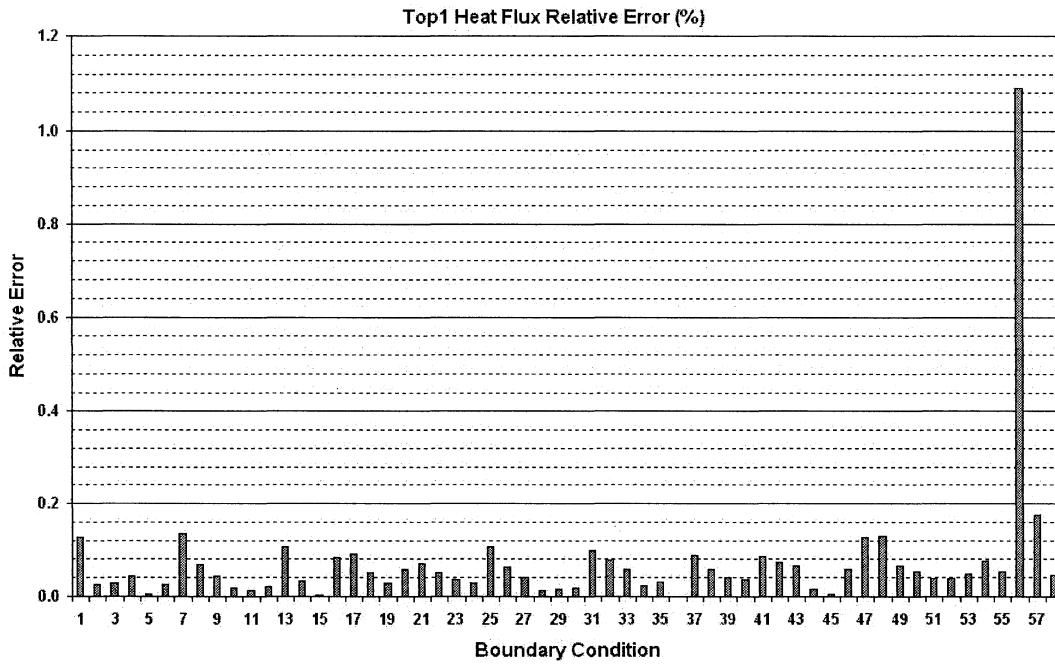


Figure 4.5: Relative errors of top1 surface.

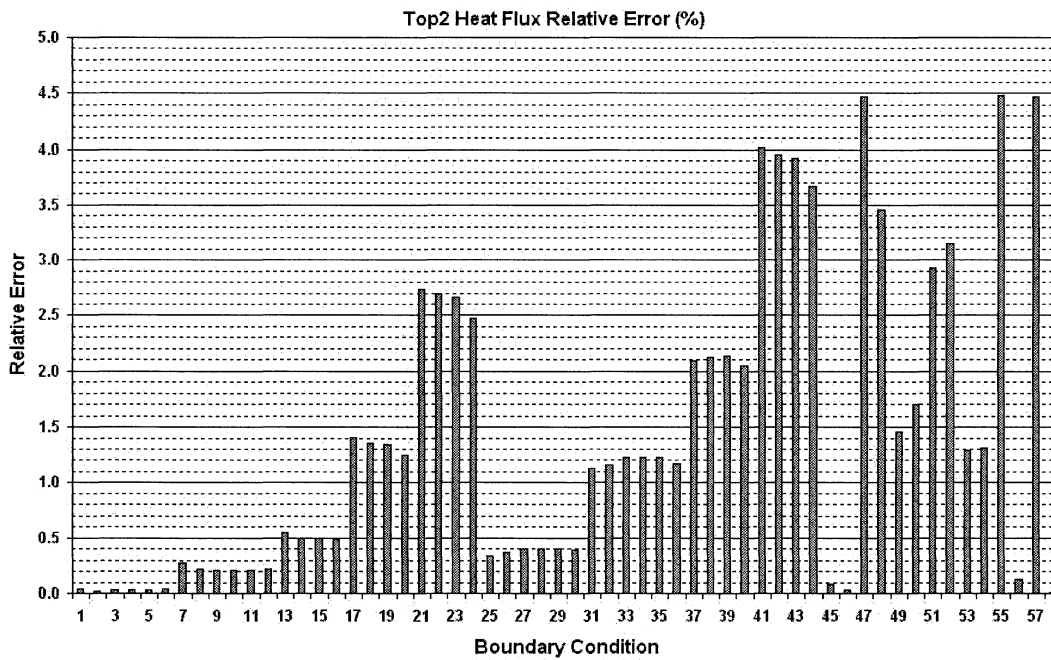


Figure 4.6: Relative errors of top2 surface.

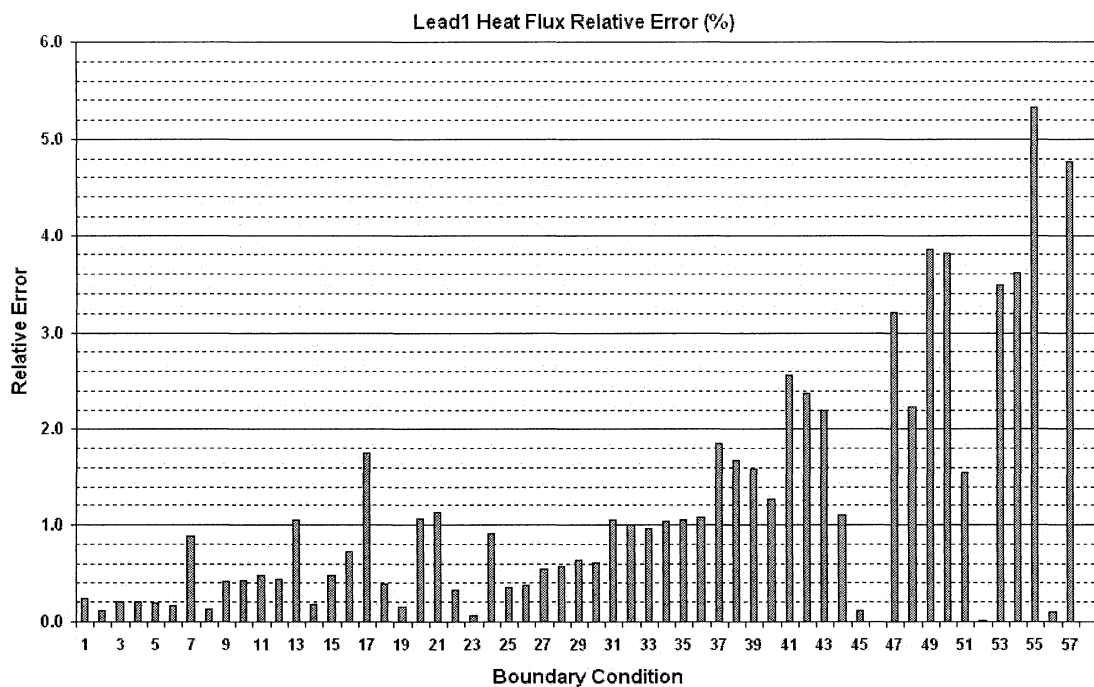


Figure 4.7: Relative errors of lead 1.

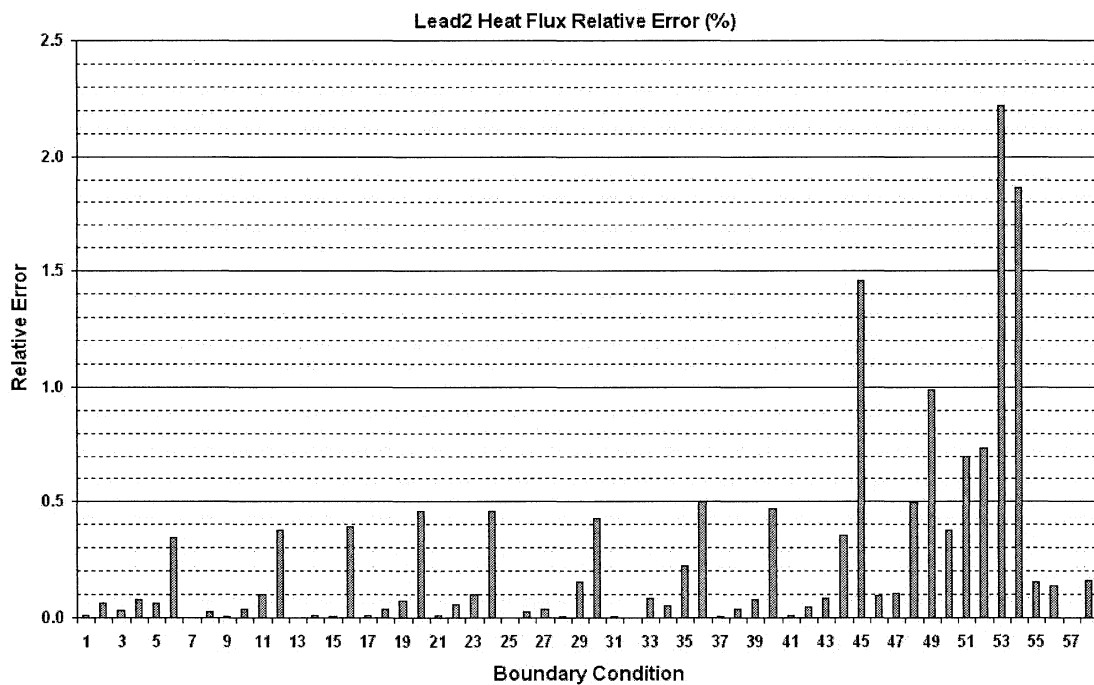


Figure 4.8: Relative errors of lead 2.

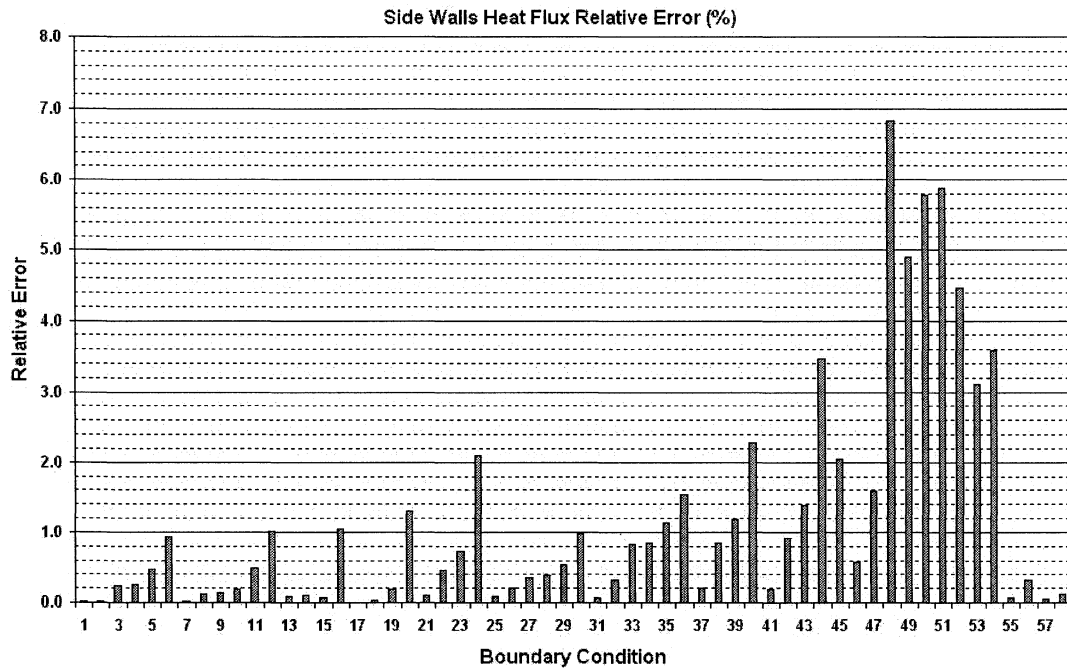


Figure 4.9: Relative errors of side walls.

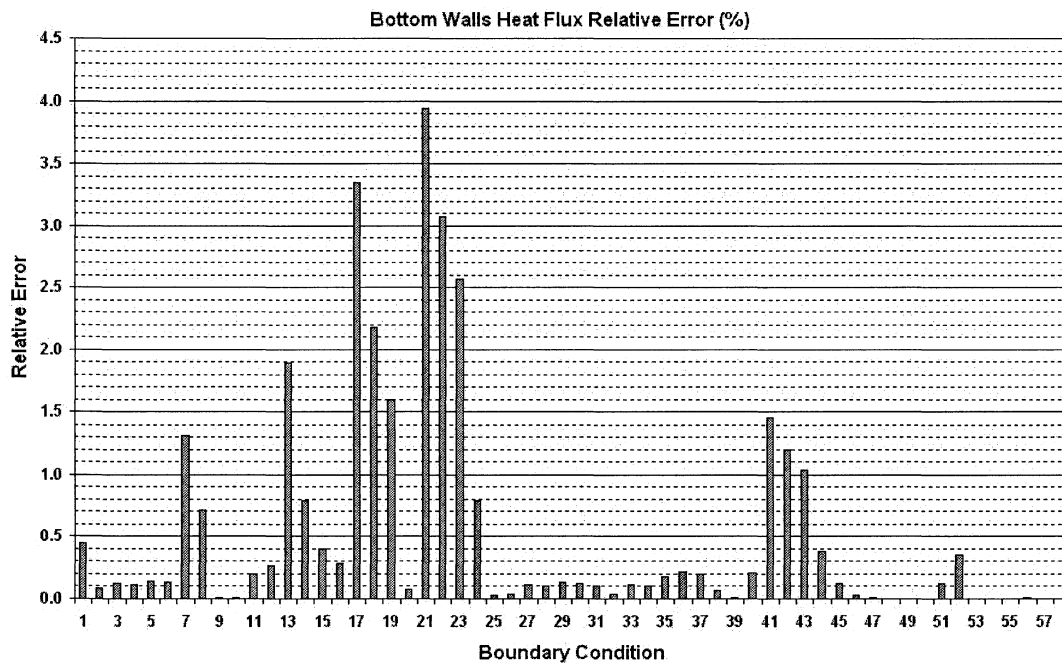


Figure 4.10: Relative errors of bottom walls.

Maximum relative errors of boundary surfaces Top1, Top2, Lead1, Lead2, Side walls, and Bottom walls occur when boundary conditions no. 51, 55, 55, 53, 48, and 21 are applied to the package, respectively. Table 4.1 contains the optimized resistor values of

compact model of BGA package. It also shows the maximum error percentage for junction temperature and heat fluxes are 1.56% and 6.83%, respectively.

<b>Table 4.1: Optimized resistor values of CTM</b>	
<b>Link</b>	<b>K/W</b>
<i>RJT1</i>	32.8
<i>RJT2</i>	66.6
<i>RJL1</i>	4.86
<i>RJB</i>	402
<i>RT2B</i>	439
<i>RT2L2</i>	3.77
<i>RT2S</i>	87.7
Err. Percentage $T_{max}$ =1.56 (BC no. 50)	
Err. Percentage $Q_{max}$ =6.83 (BC no. 48 Side walls)	
Cost Function =3.78E-5	

#### **4.6 Summary**

In this chapter the process of generating the static compact model from the detailed model simulation was investigated. The static compact thermal model consisting of resistor network based on the proposed method by DELPHI was defined. For the BGA package the topology of the network was determined which has seven resistors connecting the nodes of network. An algorithm has been developed in MATLAB to calculate the proper values for the resistors. These values are optimized by a cost function and optimization algorithm. The optimization algorithm was based on Nelder-Mead Simplex Method. Validation of the generated static compact model showed that it has good performance and meets the available criterion. The developed compact model achieved to calculate the junction temperature which is the most crucial variable in every thermal analysis of electronic system with a very good accuracy and relative error percentage equal to only 1.56% which is much smaller than available criterion which requires a relative error percentage less than 10%.

## Chapter 5

### Dynamic Compact Thermal Model

#### 5.1 Introduction

Static compact thermal model of electronic package we generated in the previous chapter was able to calculate the thermal variables only when the package had reached to its final and steady state thermal conditions. We have assumed that the package conditions do not vary with the time. However the range of practical cases in which the time dimension has to be considered is great. According to the governing equation (2.15) and boundary condition equation (2.21) if the heat generated inside the package and heat transfer coefficients applied to the package, as boundary conditions, are all constant and time invariant scalars, the solution of the equation (2.15) will be reached to a steady state condition (in which the generated steady state compact thermal model in chapter 4 is valid) after a transient period of time. There are three main reasons however that the static model may not be sufficient for thermal analysis of package and a dynamic compact thermal model of the package is necessary:

- 1- Depending on the material properties, dissipated power, and boundary condition values, it may take a considerably long time (several minutes) for a package from the moment power supplies connected to the package to the moment it reaches its steady state conditions and the package consumer needs to know what thermal behavior the package shows during this transition period.
- 2- For many electronic systems especially mobile systems such as laptop and notebook computers, mobile phones, iPods ... which use batteries, saving electrical energy is an important issue. To optimize the power usage these systems have special energy saving mechanism that gives the ability of switching between normal and low power (standby, suspend ...) modes. In each of these modes the consumed and dissipated power by an electronic package ( $q_g$ ) is different from other modes.
- 3- The boundary conditions and ambient temperature change for most mobile systems. This may cause the variation of the thermal variables of the package during transition

period. The compact model should be able to calculate the desired thermal variables during this period.

The objective of this chapter is to present the methodology on generating Dynamic Compact Thermal Model (DCTM) of the BGA package based on the steady state compact model generated and validated in chapter 4. As mentioned in chapter 4 steady state compact model approaches is based on modeling the thermal conductance of the solid materials by electrical conductance and generate a resistor network as the compact model of the package. The duality between the thermal and electrical capacitance was employed and Resistor network was expanded by adding some capacitors so it can predict the transient thermal behavior of the BGA package. The dynamic model thus is a RC network. This tool can be used to evaluate the temperatures and heat flows of BGA package during the transient periods. In the following sections of this chapter the detail of the work performed to generate the dynamic compact model is explained thoroughly.

## 5.2 Thermal Capacity

According to equation (5.1) when some heating energy is applied to a specific amount of material, the temperature of material goes up from its initial temperature to a new temperature.

$$\Delta Q = m \cdot c \cdot (T_1 - T_0) \quad (5.1)$$

where:

$\Delta Q$  (Joules) is the applied heating energy,

$m$  (Kg) is the mass of the material,

$c$  (J/Kg.Kelvin) is the thermal capacity of the material, and

$T_0$  and  $T_1$  (Kelvin) are the initial and final average temperatures respectively.

$\Delta Q$  can be expressed as:

$$\Delta Q = P \cdot \Delta t \quad (5.2)$$

where:

$P$  (watt) is the input power, and

$\Delta t$  (Second) is the time needed to apply  $\Delta Q$ .

By replacing equation (5.2) in equation (5.1):

$$\Delta t = \frac{m \cdot c \cdot \Delta T}{P} \quad (5.3)$$

where  $\Delta T = T_1 - T_0$ .

Equation (5.3) shows that for a specific amount of mass and input heating power the time needed to raise the temperature from  $T_0$  to  $T_1$  is proportional to the thermal capacity of the material or  $c$ . Equation (5.3) may be rewritten as:

$$P = m \cdot c \cdot \frac{\Delta T}{\Delta t} \quad (5.4)$$

Now considering an electrical capacitor, Equation (5.5) shows the relation between the capacitor's current and voltage.

$$I_C = C \cdot \frac{dV_C}{dt} \quad (5.5)$$

where

$V_C$  (Volt) is the voltage applied to the capacitor,

$I_C$  (Ampere) is the current flowing through the capacitor, and

$C$  (Farad) is the capacitance value.

In previous chapter we used the duality existed between the electrical and thermal characteristics and modeled thermal conductivities by electrical conductivities, heat sources by electrical current sources, and temperatures by electrical voltages. The compact thermal model thus was an electrical network consisting of current sources and resistors. Based on these dualities and comparing equations (5.4) and (5.5), it is reasonable to model the thermal capacitance of material by electrical capacitors. Therefore, an electrical network consisting of current sources, resistors, and capacitors may be used to generate the dynamic compact thermal model of the package.

### **5.3 Other Methods of Dynamic Compact Modeling**

In addition to the RC network approach we are going to use in this work for dynamic compact modeling of the package, there are several other methods of dynamic modeling

of electronic packages. Older methods were designed and able only to calculate the junction temperature of the package. It should be reminded that Junction is the region inside the package where the heat is generated and dissipated. The most well known and fully developed such methods are Network Identification by Deconvolution (NID) [38] and Asymptotic Waveform Evaluation (AWE) [39]. These two methods the goal is to model the thermal path between the junction and the environment that surrounds the package by a RC ladder. More discussion on these methods are in Appendix A.

## 5.4 Definition of a RC Dynamic Compact Thermal Model

The compact thermal model generated and validated in previous chapter showed good performance in calculating the steady state temperatures and heat flows of the BGA package. Therefore, it was desirable to extend static compact thermal model to perform transient thermal analysis of package. Static compact thermal model can be modified to the dynamic thermal model by adding capacitors to resistor network. Because the package is a distributed system each and every branch of resistor network should be replaced by a RC chain as shown in figure 5.1. The model can represent the distributed system as accurate as possible by including as many resistors and capacitors as possible.

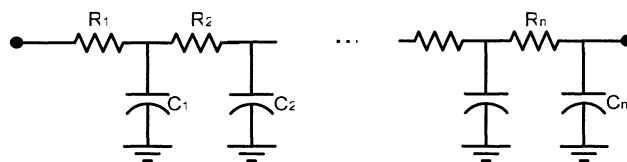


Figure 5.1: RC chain

Generation and optimization of such compact model however is almost impossible when the number of capacitors increase. In addition, during the research period and after examining several network topologies, we realize that adding only one capacitor to some and not all branches of the resistor network gives the BGA compact model sufficient accuracy to predict the transient thermal behaviors. The problem is now the location and number of the capacitors. Connecting a capacitor to the junction node is necessary because of the importance of the junction temperature as a crucial thermal variable in electrical analysis and design. A method developed by [40] where the location of the other capacitors is not predetermined and can be calculated by optimization so the highest performance of the compact model may be achieved. Based on this methodology and considering only one capacitor for every branch, we proposed the topology of the RC

network illustrated in figure 5.2. This RC network includes a total of seven resistors and seven capacitors.

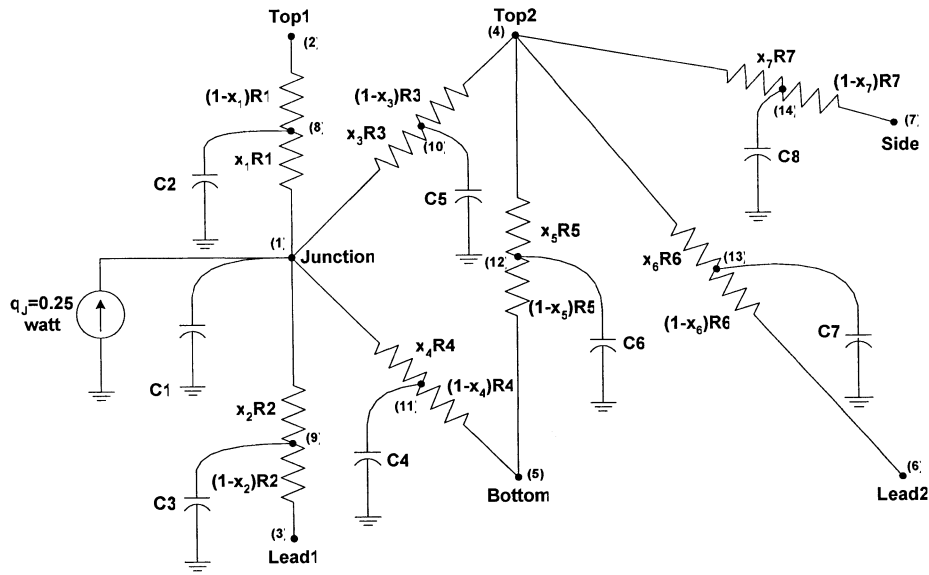


Figure 5.2: Proposed Dynamic Compact topology for BGA package

Adding these capacitors to the network increases the number of nodes from 7 to 14. The locations of capacitors are not fixed as mentioned earlier and will be determined by calculating the  $x_i$  during the optimization process.

Using node voltage analysis, the governing equation of solving network is:

$$[C] \frac{d}{dt} [T(t)] + [G][T(t)] = [P(t)] \quad (5.5)$$

where:

$$[C] = \begin{bmatrix} c_1 & 0 & 0 & 0 & 0 & 0 & 0 & 0 & 0 & 0 & 0 & 0 & 0 & 0 \\ 0 & 0 & 0 & 0 & 0 & 0 & 0 & 0 & 0 & 0 & 0 & 0 & 0 & 0 \\ 0 & 0 & 0 & 0 & 0 & 0 & 0 & 0 & 0 & 0 & 0 & 0 & 0 & 0 \\ 0 & 0 & 0 & 0 & 0 & 0 & 0 & 0 & 0 & 0 & 0 & 0 & 0 & 0 \\ 0 & 0 & 0 & 0 & 0 & 0 & 0 & 0 & 0 & 0 & 0 & 0 & 0 & 0 \\ 0 & 0 & 0 & 0 & 0 & 0 & 0 & 0 & 0 & 0 & 0 & 0 & 0 & 0 \\ 0 & 0 & 0 & 0 & 0 & 0 & 0 & 0 & 0 & 0 & 0 & 0 & 0 & 0 \\ 0 & 0 & 0 & 0 & 0 & 0 & 0 & 0 & c_2 & 0 & 0 & 0 & 0 & 0 \\ 0 & 0 & 0 & 0 & 0 & 0 & 0 & 0 & c_3 & 0 & 0 & 0 & 0 & 0 \\ 0 & 0 & 0 & 0 & 0 & 0 & 0 & 0 & 0 & c_4 & 0 & 0 & 0 & 0 \\ 0 & 0 & 0 & 0 & 0 & 0 & 0 & 0 & 0 & 0 & c_5 & 0 & 0 & 0 \\ 0 & 0 & 0 & 0 & 0 & 0 & 0 & 0 & 0 & 0 & 0 & c_6 & 0 & 0 \\ 0 & 0 & 0 & 0 & 0 & 0 & 0 & 0 & 0 & 0 & 0 & 0 & c_7 & 0 \\ 0 & 0 & 0 & 0 & 0 & 0 & 0 & 0 & 0 & 0 & 0 & 0 & 0 & c_8 \end{bmatrix}$$

is the thermal capacitance matrix,

$[T(t)] = [T_1(t) \ T_2(t) \ \dots \ T_{14}(t)]^T$  is the temperature vector,

$[G]$  is the thermal conductance matrix, and

$[P(t)]$  is the nodal loads and sources which express the heat source connected to the junction node and boundary conditions applied to the external nodes.

Equation (5.5) is a set of 14 linear differential equations. Transient time can take up to several minutes and solving these equations for such long transition period is very time consuming. To overcome this problem we transferred the equation from time domain to frequency domain by Fourier transform.

$$(j\omega[C] + [G])[T(\omega)] = [P(\omega)] \quad (5.6)$$

or

$$[T(\omega)] = (j\omega[C] + [G])^{-1} [P(\omega)] \quad (5.7)$$

Equation (5.7) is the definition of the RC network dynamic compact model. Matrix  $G$  or conductance matrix is equal to the static model generated in chapter 4 and matrix  $C$  is the additional part that upgrades the model from static to dynamic. Following sections explain how the matrix  $C$  was calculated in this research project.

## 5.5 Detailed Thermal Model

The process of generating detailed model for dynamic analysis is more complex than what has been performed for static analysis in chapter 3. There are several parameters related to transient analysis which must be calculated and set in the COMSOL simulator software before running the solver.

The first step of generating a detailed model by COMSOL is building the geometry of the subject of analysis (i.e. BGA package). The size and physical properties of the package layers are according to Table 3.1. Figure 5.3 shows the geometry built by COMSOL CAD tool.

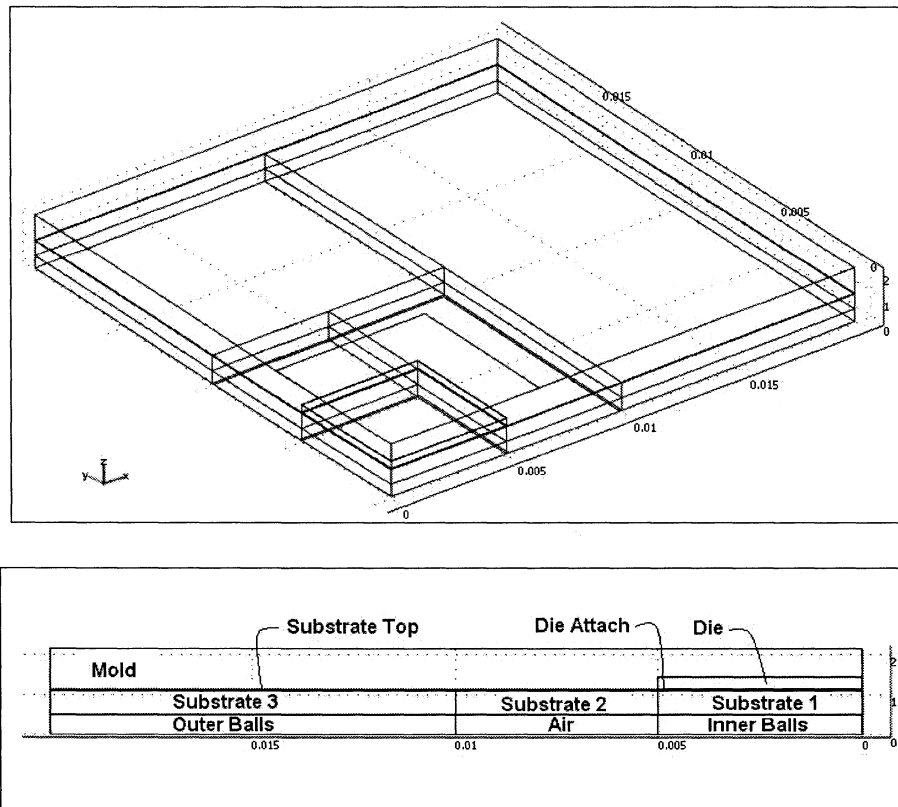


Figure 5.3: Quarter symmetric Geometry of BGA Package

Next step after building geometry is meshing process. In this process the geometry is divided into small elements and will be used by solver to solve the partial differential heat equation by finite elements method. There is not a straight forward method of calculating the optimum number of elements or mesh density. While it's very desirable to have as few as possible elements because of the computation costs, it can not be less than a specific number in order to preserve the minimum accuracy. One heuristic method of finding the minimum number of elements used during this project was starting from a very coarse meshing (low number of elements) and solving the package. When the number of elements is too small and meshing is too coarse after solving the package, the total amount of outward heat flux obtained from detailed model had a large relative error with respect to the real value which was 0.25 watt. After several steps of trial and error and increasing the number of elements, the final meshing parameters were accepted only when the relative error between measured outward heat flux and the real value dropped below 0.5%. Table 5.1 shows the meshing parameters used by COMSOL software and table 5.2 shows the mesh statistics. The BGA package was modeled using approximately 225000 elements. Figure 5.4 shows the meshed BGA package by COMSOL©.

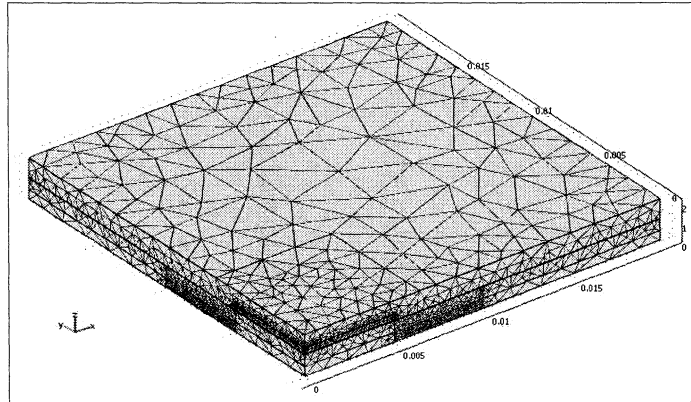


Figure 5.4: Finite element model of the BGA package

Table 5.1: Free Mesh parameters			
Pre defined mesh sizes	Extremely coarse	Maximum element size	
Maximum element size scaling factor	5	Air layer	0.0002
Element growth rate	2	Substrate 2	0.0003
Mesh curvature factor	1		
Mesh curvature cutoff	0.07		
Resolution of narrow regions	0.1		
Refinement method	Longest		

Table 5.2: Mesh statistics			
Number of degrees of freedom	312717	Minimum element quality	0.0103
Number of mesh points	41100	Element volume ratio	2.63e-6
Number of elements	224959		
Number of boundary elements	52082		
Number of edge elements	2005		
Number of vertex elements	70		

Table 5.3 contains the boundary conditions (BC's) used for detailed simulation. These boundary conditions are equal to the values used in previous chapter for steady state analysis. An important point here is that for some of boundary conditions transient time is very short and for the rest of boundary conditions this time is considerable long. Therefore, these boundary conditions have been divided into two different groups. When boundary conditions of group one are applied to the package, the transient time is longer than 50 seconds. Therefore, the solver was run from time 0 to time 511 seconds and every one second the desired temperatures and inward/outward heat flows were obtained.

As a result, for each of boundary conditions belongs to this group desired measurements are vectors with 512 elements. 512 was chosen because it's a complete binary number and running Fast Fourier Transform or FFT is optimized for such numbers. Boundary conditions with higher values (heat sink, cold plate, fluid bath, Infinite h.t.c, and DCPs) belong to the second group and when applied to the package, transient time is less than 50 seconds. For this group the solver was run from 0 to 51.1 seconds and every 0.1 second the desired temperatures and heat fluxes were measured. Similar to first group measured variables are vectors with 512 elements. Boundary conditions belong to this group are specified by color gray in table 5.3. Figure 5.5 show the magnitude of junction temperature measured from detailed model in frequency domain for BC no. 20 form the first group and BC no. 45 from the second group.

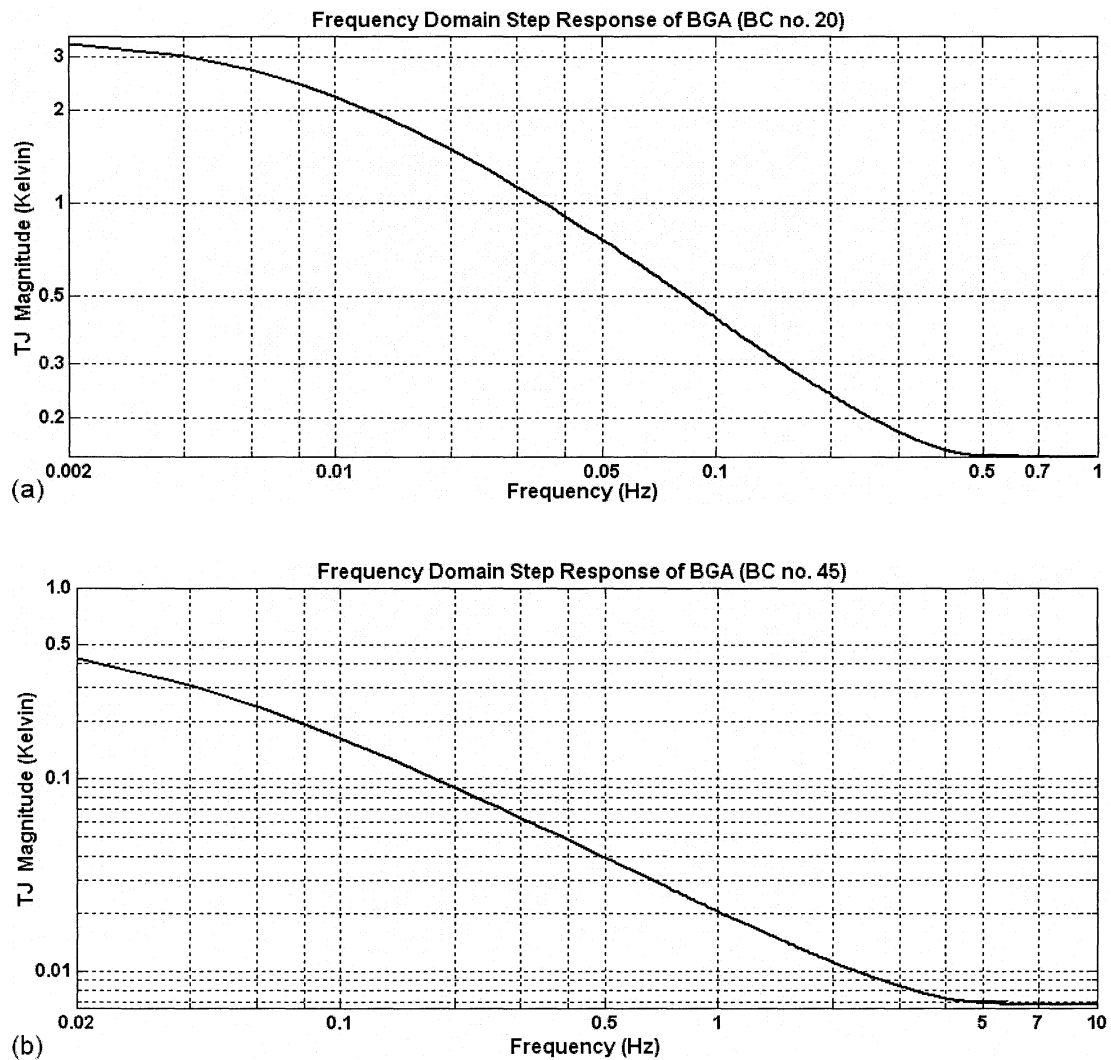


Figure 5.5: Frequency responses of junction temperatures for BC no. (a) 20 and (b) 45

Figure 5.5 (a) shows clearly that for boundary conditions of group 1 most of the signal energy is in the frequency band below the 0.5 Hz according to the Nyquist sampling theorem thus the signal can be fully sampled without no information loss by sampling frequency not more than 1 Hz or sampling period not smaller than 1 second. This is the reason that for the first group of boundary conditions, thermal parameters were obtained from detailed model by sampling frequency  $F_s=1$  Hz. Figure 5.5 (b) shows that for boundary conditions of group 2 most of the signal energy is in the frequency band below the 5 Hz according to the Nyquist sampling theorem thus the signal can be fully sampled without no information loss by sampling frequency not more than 10 Hz or sampling period not smaller than 0.1 second. This is the reason that for the second group of boundary conditions, thermal parameters were obtained from detailed model by sampling frequency  $F_s=10$  Hz.

**Table 5.3: Boundary Conditions**

No	$h_{TOP}$	$h_{BOT}$	$h_{SIDE}$	$h_{LEADS}$
1	5	1	5	1
2	5	10	5	10
3	5	25	5	50
4	5	50	5	50
5	5	50	5	100
6	5	100	5	200
7	15	1	15	1
8	15	10	15	10
9	15	25	15	50
10	15	50	15	50
11	15	50	15	100
12	15	100	15	20
13	30	5	30	5
14	30	30	30	30
15	30	50	30	50
16	30	200	30	200
17	80	5	80	5
18	80	30	80	30
19	80	50	80	50
20	80	200	80	200
21	200	5	200	5
22	200	30	200	30
23	200	50	200	50
24	200	200	200	200
25	25	1	5	1
26	25	10	5	10
27	25	25	5	50
28	25	50	5	50

29	25	50	5	100
30	25	100	5	200
31	75	1	15	1
32	75	10	15	10
33	75	25	15	50
34	75	50	15	50
35	75	50	15	100
36	75	100	15	200
37	150	5	30	5
38	150	30	30	30
39	150	50	30	50
40	150	200	30	200
41	500	5	200	5
42	500	30	200	30
43	500	50	200	50
44	500	200	200	200
45	10	50	10	1000
46	10	1000	10	10000
47	1000	5	10	50
48	10000	50	10	500
49	10000	10000	10000	10000
50	5000	5000	5000	5000
51	1000	1000	1000	1000
52	500	500	500	500
53	$10^9$	$10^9$	$10^9$	$10^9$
54	50000	50000	50000	50000
55	10000	10000	1	1
56	10	10000	1	1
57	10000	10	1	1
58	1	1	1	10000

The measurements include junction average temperature, Top1 average temperature and total heat flux, Top2 average temperature and total heat flux, Lead1 (inner balls) average temperature and total heat flux, Lead2 (outer balls) average temperature and total heat flux, Bottom (air) average temperature and total heat flux, and Side average temperature and total heat flux.

In order to provide the reader a better understanding of transient thermal simulation by detailed model of package, boundary condition no. 20 was taken as a case study. The sequential views of the temperature profile obtained from FE simulation is shown in Figure 5.6. The temperature variation is illustrated in the five figures representing the temperature at  $t=0$ , 5, 10, 50, 100 and 150 seconds. While the package becomes hotter during the transient time, its color becomes brighter. It is also expected that the junction area is hotter and must be shown with brighter color. Figure 5.6 (g) shows the Junction temperature variation during the transition period for the applied boundary condition no. 20. Similar images and curves can be obtained for other thermal parameters and boundary conditions. COMSOL has the capability of generating a movie file that shows the variation of any desired thermal variable during the transition period.

Looking at figure 5.6, it is clear that at  $t=0$  or just before starting simulation time when the input power is off, the package is in a steady state condition and the temperature of any location inside or on the surfaces is equal to room temperature:  $T=300$  (K). This has been shown in figure 5.6 (a). The next 5 snapshots show that while the input heating source is on and transient time passes, the package becomes hotter until it gets to its final thermal conditions. In other words transition period is finished and package is again in a steady state thermal condition. This new steady state however is different from the steady state conditions showed in figure 5.6 (a) because heat source is on inside the package in Junction region. This also explains why the Junction region and its surrounding areas are looking brighter which means hotter than other regions of package.

Finally it should be noted that these curves and snapshot images are only available for transient analysis. Thermal variables for steady state analysis are expressed only by scalar numbers and static images as explained and shown in previous chapter.

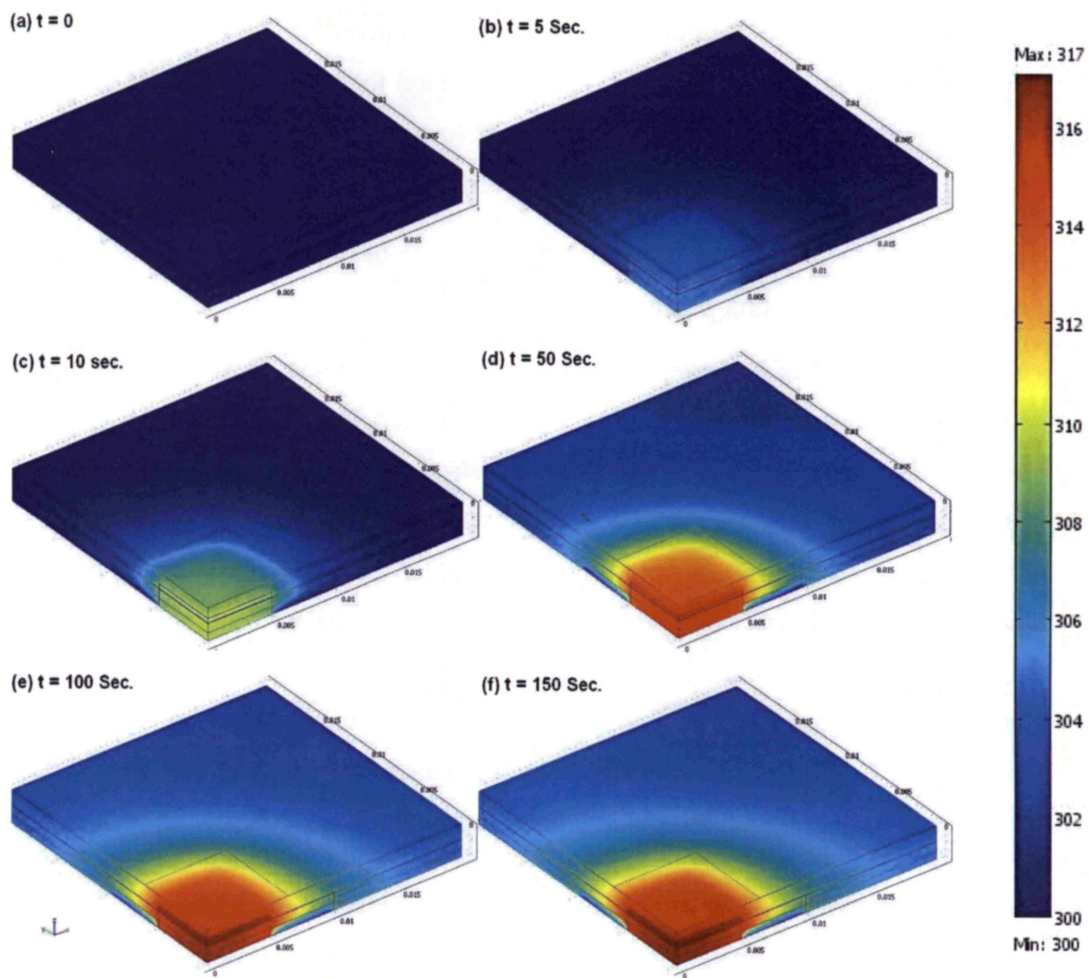


Figure 5.6: Graphical representation of package temperature variation during transitions period

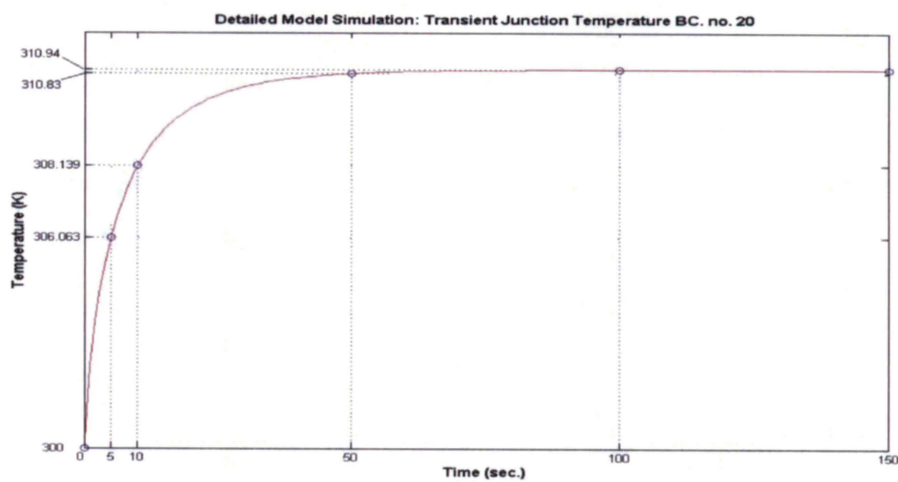


Figure 5.6 (g): Detailed model simulation results: Junction temperature of BGA package for boundary condition no. 20

## 5.6 Compact Model Generation

Dynamic thermal model must be able to predict the thermal behavior of package in both transient and steady state conditions. In steady state conditions all capacitors are fully charged and model is only a resistor network like the model generated in previous chapter. This means we don't need to calculate and optimize new values for resistors of dynamic model because they are equal to what we calculated and optimized for static model which are repeated in table 5.4.

<b>Resistor Name</b>	<b>Value (K/W)</b>	<b>Description</b>
<b>R<sub>J-T1</sub></b>	<b>32.8</b>	<b>Junction to Top1</b>
<b>R<sub>J-L1</sub></b>	<b>4.86</b>	<b>Junction to Lead1</b>
<b>R<sub>J-T2</sub></b>	<b>66.6</b>	<b>Junction to Top2</b>
<b>R<sub>J-B</sub></b>	<b>402</b>	<b>Junction to Bottom</b>
<b>R<sub>T2-B</sub></b>	<b>439</b>	<b>Top2 to Bottom</b>
<b>R<sub>T2-L2</sub></b>	<b>3.77</b>	<b>Top2 to Lead2</b>
<b>R<sub>T2-S</sub></b>	<b>87.7</b>	<b>Top2 to Side</b>

The method of calculating the capacitors is fitting by optimization. A Nelder-Mead Simplex multidimensional optimization algorithm tries to find the best values of capacitors that minimize a cost function representing the deviation between the compact and detailed model is minimized.

$$COST = \sum_{i=1}^N \sum_{k=1}^n \left( \frac{|T_{j_i}^d(\omega_k)| - |T_{j_i}^c(\omega_k)|}{|T_{j_i}^d(\omega_k)|} \right)^2 \quad (5.8)$$

where:

N=58 is the number of boundary conditions,

n=512 is the number of samples in time domain or frequency domain,

$|T_{j_i}^d(\omega_k)|$  is the magnitude of the Fourier transform of the  $i^{\text{th}}$  Junction temperature measured from detail model, and

$|T_{j_i}^c(\omega_k)|$  is the magnitude of the Fourier transform of the  $i^{\text{th}}$  Junction temperature calculated by compact model.

This cost function adopted from [40] and optimizes the compact model for junction temperature because of its importance and crucial effect on electrical operating point but showed acceptable results (error percentages less than 10%) for inward/outward heat fluxes. The detail of compact model results will be explained in section 5.6 of this chapter. Equation (5.8) however can be customized so the model will be optimized for any desired temperature or heat flux.

Figure 5.7 shows the different steps of generating dynamic compact thermal model.

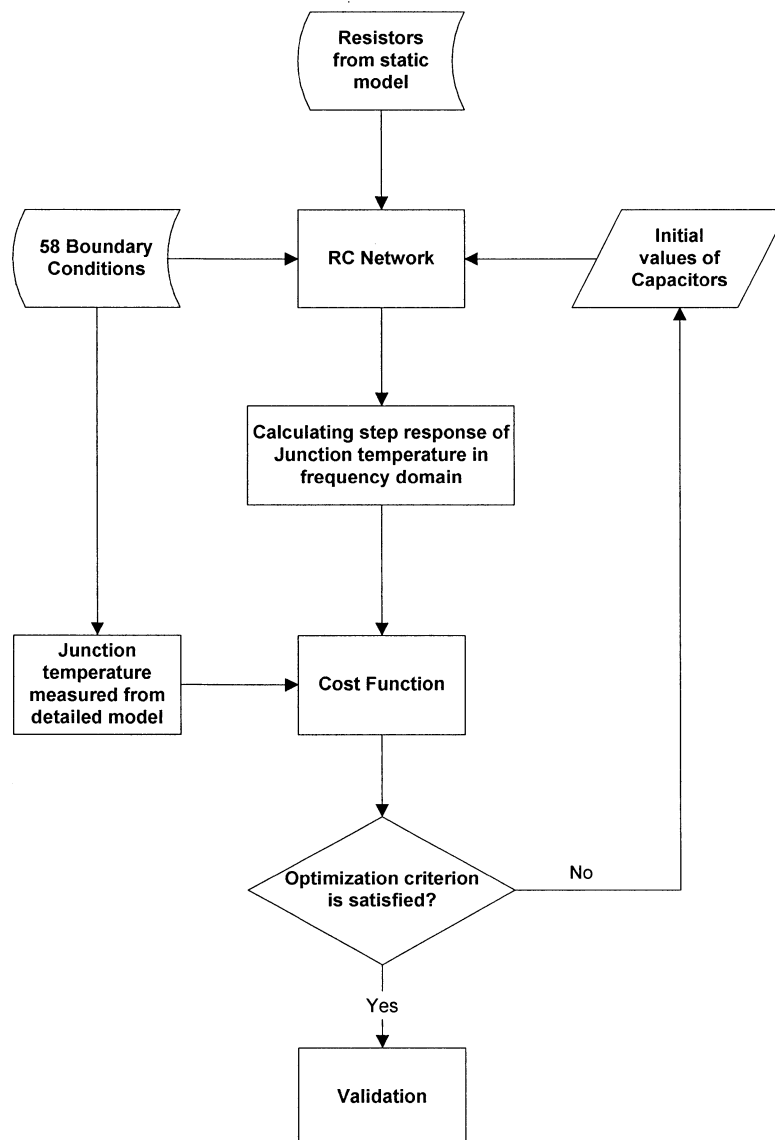


Figure 5.7: Different steps of generating dynamic compact model

At first step some predetermined values is considered as initial values for capacitors and the step response of RC network is calculated in frequency domain. The range of frequency is from 0 to 1 Hz or 0 to 10 Hz depends on the boundary condition. This is because detailed model was measured with two different sampling times: 1 second or 0.1 second. The frequency range is divided to 512 frequencies because 512 samples of temperatures and heat fluxes were measured from detailed model for each boundary condition and their FFT vectors of have also 512 elements.

Next step 2 is calculating equation (5.8) as cost function using the junction temperatures calculated from RC network and obtained from detailed model. If this cost function satisfies the Nelder-Mead Simplex optimization criterion, the capacitor values are accepted and the last step which is validation will be performed. Otherwise new values for capacitors will be chosen based on what Nelder-Mead Simplex method suggested and the process will be repeated. The validation process will be explained in section 5.6 of this chapter. Nelder-Mead Simplex optimization method was explained in previous chapter.

For this work initial values for  $x_i$ ,  $i=1 \dots 7$  was set to 1. The RC network thus was reduced to configuration shown in figure 5.8. After optimization process, validation showed that this simplified model can predict the thermal variables with acceptable accuracies.  $x_i$  however can be optimized to increase the performance of model. Table 5-5 contains the optimized values of capacitors.

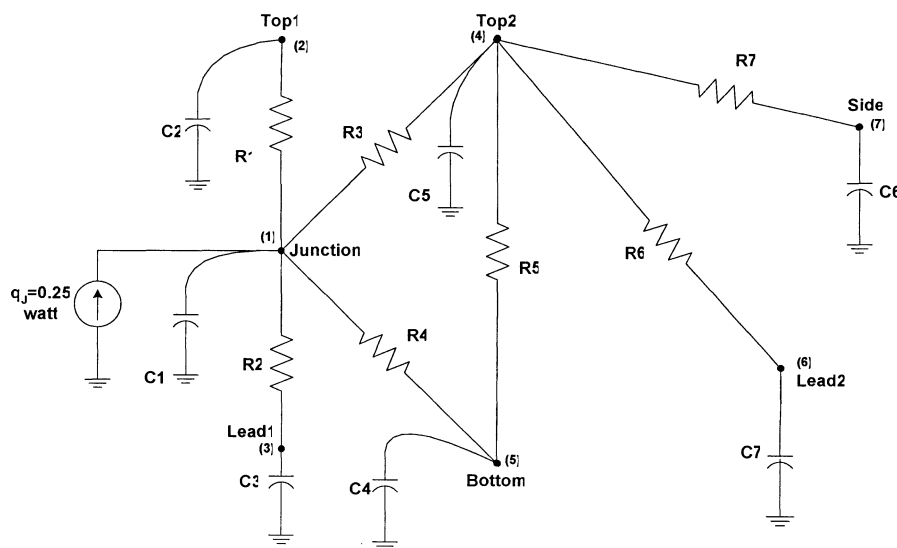


Figure 5.8: RC network of dynamic compact model.

Table 5.5: Capacitors' value of Dynamic Compact Thermal Model		
Capacitor	Value (J/K)	Description
$C_1$	0.10284	Junction Capacitor
$C_2$	0.0415	Top1 Capacitor
$C_3$	0.0015	Lead1 Capacitor
$C_4$	1.8057	Bottom Capacitor
$C_5$	0.00042	Top2 Capacitor
$C_6$	0.0327	Side Capacitor
$C_7$	0.00024	Lead2 Capacitor

It can be observed that  $C_5$  and  $C_7$  are considerable small with respect to other capacitors. It would be an educated try thus to eliminate these two capacitors and investigate the performance of modified and reduced DCTM which has been illustrated in figure 5.9.

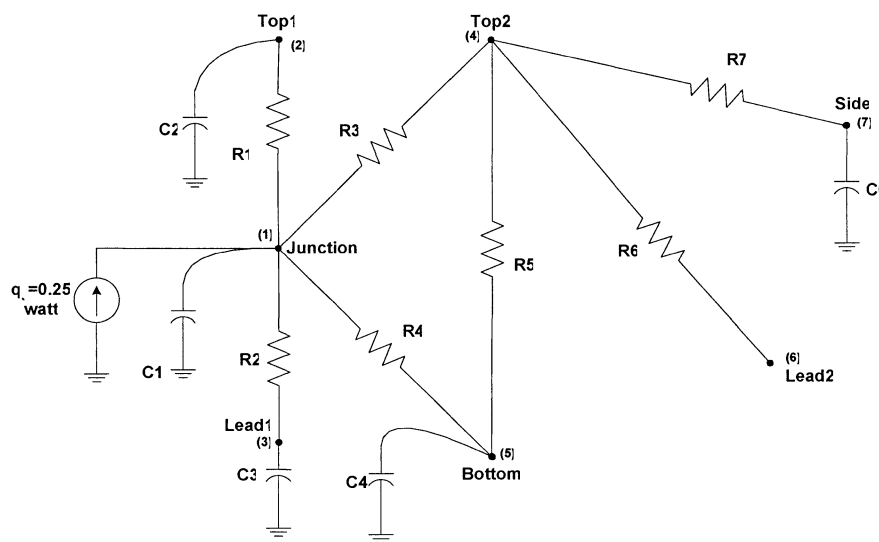


Figure 5.9: Reduced RC network of dynamic compact model.

Figure 5.10 shows the transient Junction temperature for boundary condition no. 35 predicted by the optimized compact thermal model of BGA package. Comparing this figure to figure 5.6 (g) that shows the detailed model results, it can be observed that the compact model has predicted the junction temperature with very good accuracy. The generated compact model however can not be accepted unless it pass validation step and its results examined thoroughly.

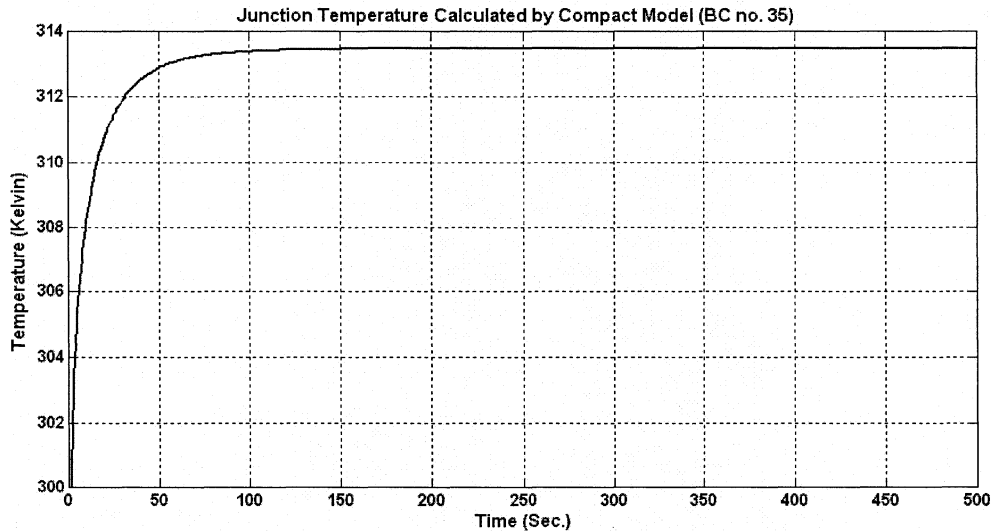


Figure 5.10: Compact model prediction results: Junction temperature of BGA package for boundary condition no. 20

### 5.7 Validation

The final step of dynamic compact thermal modeling is validation. In this step the performance of compact model is evaluated by comparing its output to the detailed model. First step of compact model evaluation is applying the same boundary conditions and power dissipation to the compact model that applied to the detailed model. Boundary conditions are listed in Table 5.3. Power dissipation is a step function with magnitude equal to 0.25 watts. The compact model thus is RC network shown in figure 5.11.

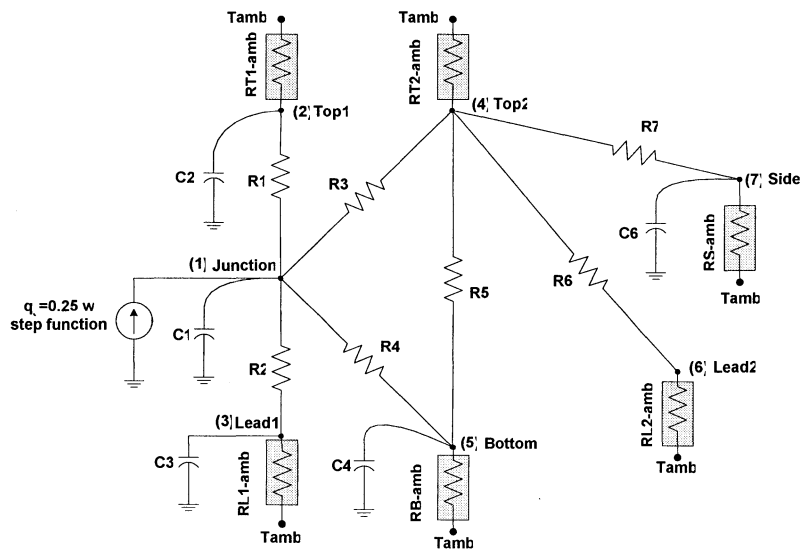


Figure 5.11: Compact model when boundary conditions are applied

$R_i$  and  $C_i$   $i=1\dots7$  values are presented in Tables 5.4 and 5.5, respectively. Resistors shown inside the gray boxes model the boundary conditions which are heat transfer conditions by convection and calculated as following:

$$\begin{aligned}
 R_{T1-amb} &= \frac{1}{h_{TOP} \cdot A_{TOP1}} & (K/W) \\
 R_{T2-amb} &= \frac{1}{h_{TOP} \cdot A_{TOP2}} & (K/W) \\
 R_{L1-amb} &= \frac{1}{h_{LEADS} \cdot A_{LEAD1}} & (K/W) \\
 R_{L2-amb} &= \frac{1}{h_{LEADS} \cdot A_{LEAD2}} & (K/W) \\
 R_{S-amb} &= \frac{1}{h_{SIDE} \cdot A_{SIDE}} & (K/W) \\
 R_{B-amb} &= \frac{1}{h_{BOTTOM} \cdot A_{BOTTOM}} & (K/W)
 \end{aligned} \tag{5.9}$$

where:

$R_{T1-amb}$  is Top1 to ambient thermal resistance,

$R_{T2-amb}$  is Top2 to ambient thermal resistance,

$R_{L1-amb}$  is Lead1 to ambient thermal resistance,

$R_{L2-amb}$  is Lead2 to ambient thermal resistance,

$R_{S-amb}$  is Side to ambient thermal resistance,

$R_{B-amb}$  is Bottom to ambient thermal resistance,

$A_{TOP1}$ ,  $A_{TOP2}$ ,  $A_{LEAD1}$ ,  $A_{LEAD2}$ ,  $A_{SIDE}$ , and  $A_{BOTTOM}$  are the areas of Top1, Top2, Lead1, Lead2, Side, and Bottom respectively, and

$h_{TOP}$ ,  $h_{LEADS}$ ,  $h_{BOTTOM}$ , and  $h_{SIDE}$  are boundary conditions applied to Top1, Leads, Bottom, and Side walls of package respectively.

Note that equation (5.9) can be calculated easily from equations (2.2).

RC network shown in figure 5.11 can be analyzed by any electric circuit simulator. We preferred to write a MATLAB® code which use node analysis method to calculate the voltages (average temperatures) of nodes and inward/outward currents (heat fluxes) to/from each node in frequency domain and transform the results into time domain.  $T_{amb}$  is ambient temperature or temperature of the room in which the package is located and measurements are performed. For this research work we assumed  $T_{amb} = 300$  K, but it can have any other value.

After calculating the output of RC network compact model next step is comparing them to the results already obtained from detailed model and calculating the relative errors. These relative errors are calculated by the following equations:

$$\text{Err. Percentage of Junction Temperature} = 100 \times \text{abs} \left( \frac{T_J^c(k, t) - T_J^d(k, t)}{T_J^d(k, t) - T_{amb}} \right) \quad (5.10)$$

$$\text{Err. Percentage of Top1 Heat Flux} = 100 \times \text{abs} \left( \frac{q_{TOP1}^c(k, t) - q_{TOP1}^d(k, t)}{q_g} \right) \quad (5.11)$$

$$\text{Err. Percentage of Top2 Heat Flux} = 100 \times \text{abs} \left( \frac{q_{TOP2}^c(k, t) - q_{TOP2}^d(k, t)}{q_g} \right) \quad (5.12)$$

$$\text{Err. Percentage of Lead1 Heat Flux} = 100 \times \text{abs} \left( \frac{q_{LEAD1}^c(k, t) - q_{LEAD1}^d(k, t)}{q_g} \right) \quad (5.13)$$

$$\text{Err. Percentage of Lead2 Heat Flux} = 100 \times \text{abs} \left( \frac{q_{LEAD2}^c(k, t) - q_{LEAD2}^d(k, t)}{q_g} \right) \quad (5.14)$$

$$\text{Err. Percentage of Side Heat Flux} = 100 \times \text{abs} \left( \frac{q_{SIDE}^c(k, t) - q_{SIDE}^d(k, t)}{q_g} \right) \quad (5.15)$$

$$\text{Err. Percentage of Bottom Heat Flux} = 100 \times \text{abs} \left( \frac{q_{BOTT}^c(k, t) - q_{BOTT}^d(k, t)}{q_g} \right) \quad (5.16)$$

where

$k=1 \dots 58$  is the boundary condition number,

$q_g=0.25$  watts is the dissipated power, and

$c$  and  $d$  superscripts determine the variable is either measured from detailed model or calculated from compact model.

The compact models results were compared to the detailed FE simulation results for the cases with boundary conditions no. 6, 20, and 43, to verify the accuracy of the compact model. Additional cases were simulated for different boundary conditions to provide additional information on the trend of data over a range of parameters. These cases were presented in the appendix B.

It should be reminded one more time the desired areas of the BGA package are TOP1, TOP2, LEAD1, LEAD2, SIDE, and BOTTOM of the package as illustrated in figure 5.12. Junction is the top region of the die and located inside the package.

The 10% criterion proposed by Clemens in [30] is accepted here to evaluate the performance of dynamic model. Figures 5.13 to 5.18 show the transient Junction temperature and outward heat fluxes of BGA package measured from detailed model and calculated by compact model and their relative error for boundary conditions no. 6, 20, and 45 as the cases study. The performance of compact model can be observed by comparing its result with the detailed model results. Note that dashed curves represent the detailed model results and solid curves represent the compact model results.

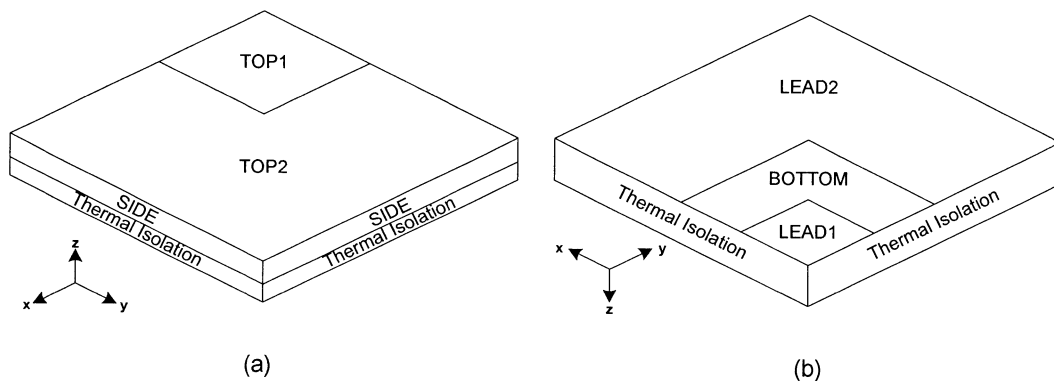


Figure 5.12: (a) TOP1, TOP2, and SIDE areas, (b) LEAD1, LEAD2, and BOTTOM areas of the BGA package.

### 5.7.1 Case Study 1: Boundary condition no. 6

The first example shows the performance of compact model when the boundary condition applied to the package is free convection. BC no. 6 was selected as the case study. The variation of junction temperature as a function of time has been illustrated in figure 5.13 (a) for the first 500 seconds for both detailed and compact model analysis. The relative error percentage of these two models is illustrated in a semi-logarithmic scale in figure 5.13 (b).

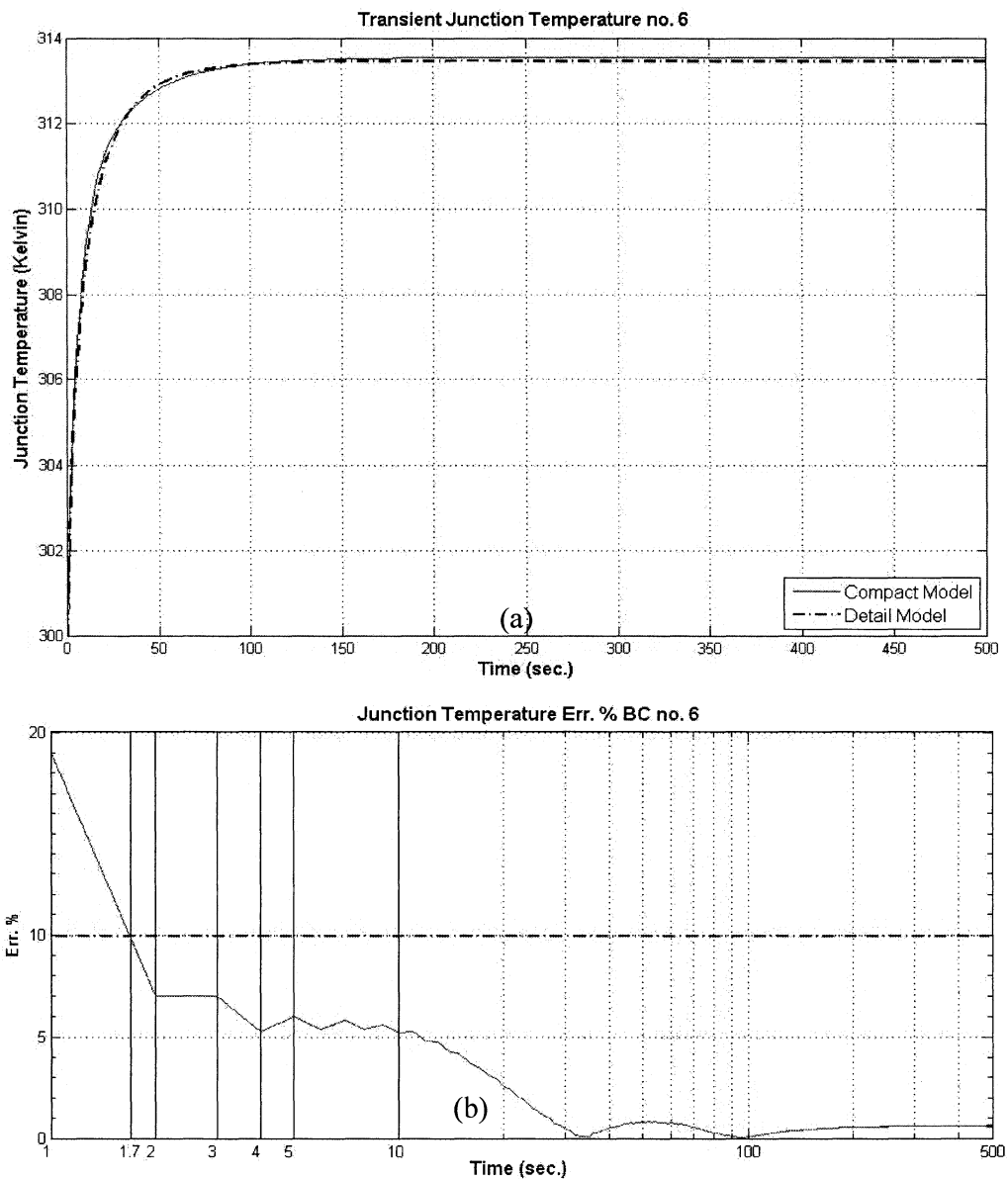


Figure 5.13: (a) Detailed and Compact model junction temperature for boundary condition no. 6, (b) Their relative error percentage.

figure 5.13 (a) shows the transition time before package reaches its thermal steady state condition is approximately 150 seconds and figure 5-13 (b) shows from  $t=1.7$  sec. the error percentage drops below 10%. This means compact model gives acceptable result for almost 98.9% of transient time. In addition, it can be noted that the results of the compact model yielded conservative estimates of the junction temperature over the simulation time compared to the detailed model.

Note that the Junction temperature relative error is calculated using equation (5.10). According to this formula the relative error percentage is equal to the absolute difference of the average junction temperature obtained from detailed model and temperature calculated from compact model (node 1 potential of RC network shown in figure 5.10) divided by the difference of average temperature measured from detailed model and ambient temperature, multiplied by 100.

Another point should be discussed is that in figure 5.13 (a) it can be observed that as already mentioned the transient period takes some 150 seconds and after this period the package reaches to its steady state thermal condition. Figure 5.13 (b) also shows that the relative error varies during this transient period and after that it remains constant which is equal to what we calculated in chapter 4 by static compact model.

In order to explain why error percentage starts from a considerable large value we should take a look at figure 5.13 (c). This figure is a zoomed in version of figure 5.13 (a) and shows the Junction temperatures for the first 2 seconds.

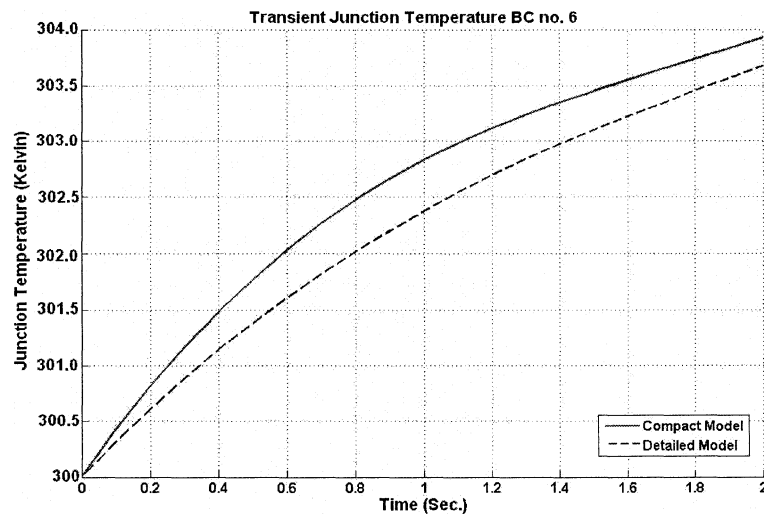
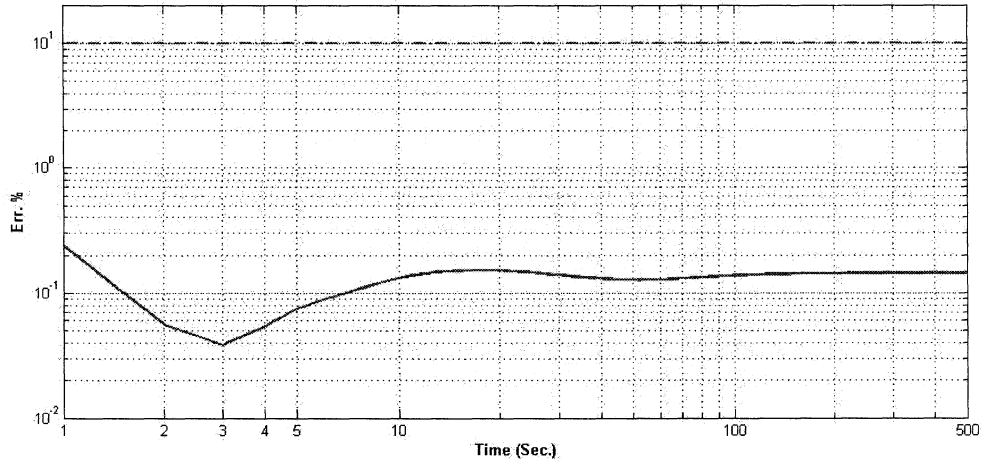


Figure 5.13: (c) Junction temperature of BGA for the first 2 seconds of transition period

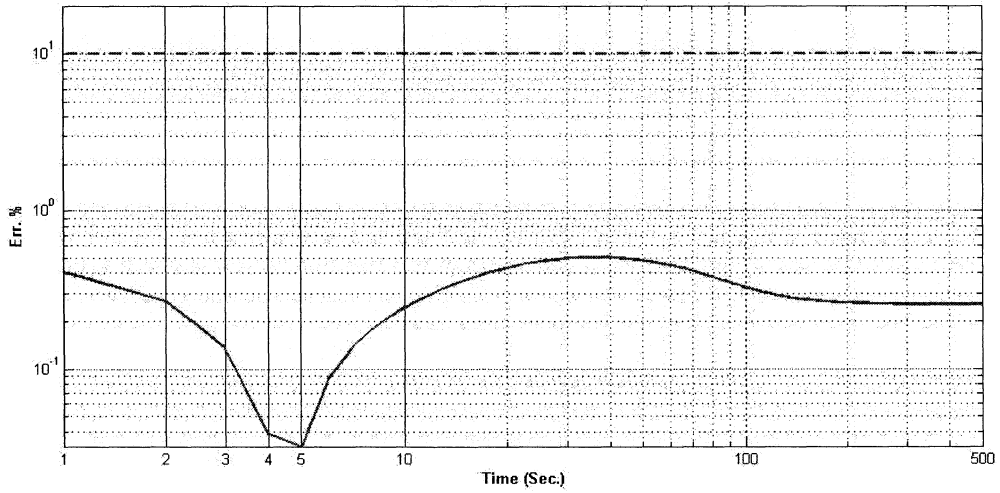
It can be seen clearly in figure 5.13 (c) that the solid curve representing the compact model output is increasing more quickly than dashed line representing the detailed model. The reason behind this phenomenon is that the BGA package is a distributed thermal system and heat wave needs some time to propagate from its originating location to the surrounding locations. The compact model however is a lumped RC network in which the wave propagation time is considered to be zero. In other word it's assumed that any change in any node or branch of network will affect other nodes and branches immediately. The heat wave propagation time is small but still effective in calculating the thermal variables especially at the beginning of analysis. This error may be reduced thus by considering the fact that package is a distributed thermal system and modifying the compact model so this characteristic of package is taken into consideration. One solution could be using RC ladders instead of single resistors and capacitors. This idea comes from the RF and microwave theory where transmission lines are modeled by RC ladders. Other models of transmission lines may also be helpful.

Figure 5.14 shows the relative error percentages between compact model results and detailed model results for transient outward heat fluxes from Top1, Top2, Bottom, Lead1, Lead2, and side walls in a logarithmic scale. These relative errors are calculated using equation (5.11) to (5.16). According to these formulas the heat flux relative error percentages are equal to the absolute difference of the outward heat fluxes measured from detailed model and heat fluxes calculated from compact model (currents flowing through the  $R_{T1-amb}$ ,  $R_{T2-amb}$ ,  $R_{L1-amb}$ ,  $R_{L2-amb}$ ,  $R_{S-amb}$ , and  $R_{B-amb}$  of RC network shown in figure 4-14) divided by the difference of average temperature measured from detailed model and ambient temperature, multiplied by 100. It's clearly illustrated that all of these error curves are below 10% line during the whole period of analysis time. The performance of compact model thus is acceptable.

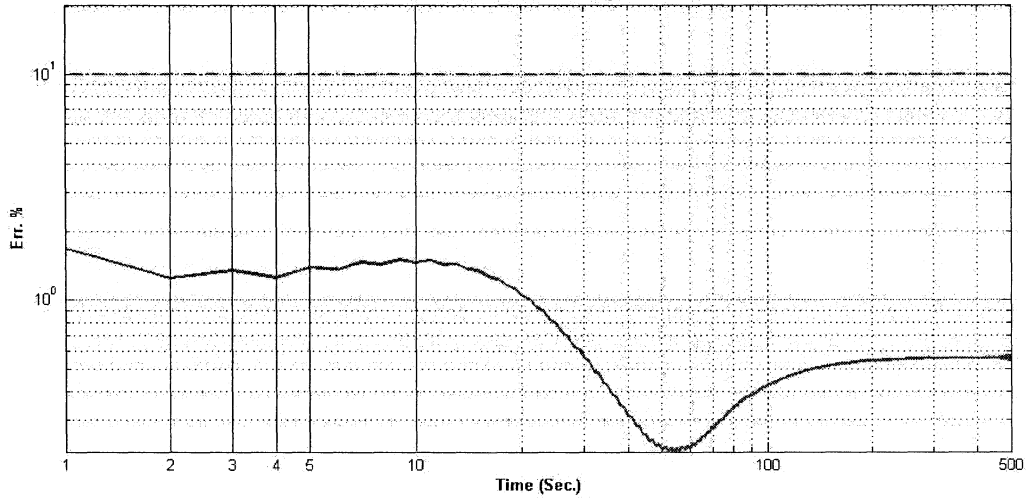
Top1 Heat Flux Err.% Boundary Condition no. 6



Top2 Heat Flux Err.% Boundary Condition no. 6



Lead1 Heat Flux Err.% Boundary Condition no. 6



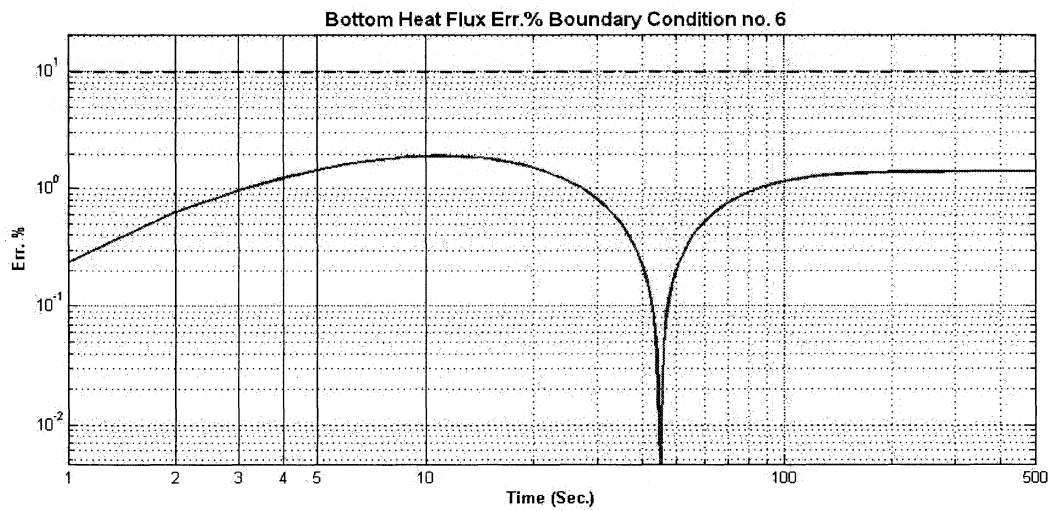
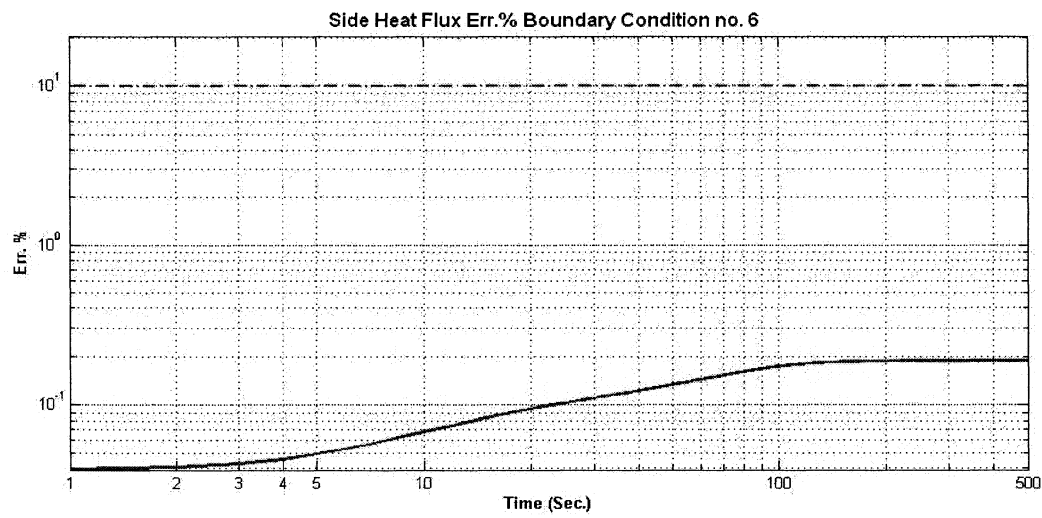
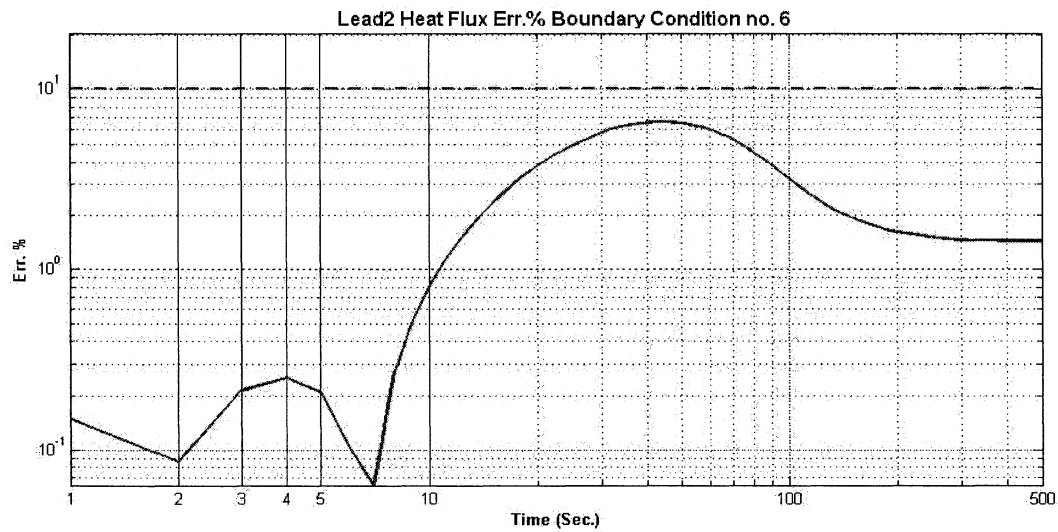
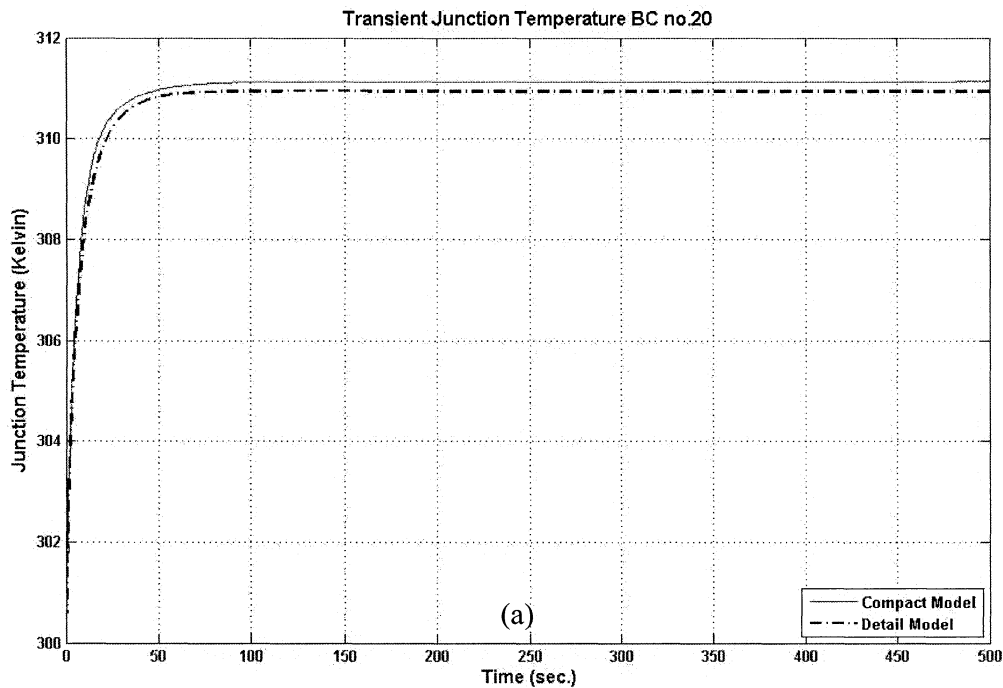


Figure 5.14: Relative error percentages of outward heat fluxes from Top1, Top2, Lead1, Lead2, Side, and bottom of BGA package for BC no. 6.

## 5.7.2 Case Study 2: Boundary condition no. 20

To investigate the performance of compact model when forced convection boundary condition is applied to the package BC no. 20 of table 5-3 is selected. Similar to previous example the variation of junction temperature as a function of time is shown in figure 5.15 (a) for the first 500 seconds. The solid line represents the junction temperature predicted by compact model and the dashed line represents the junction temperature measured from detailed model analysis. It can be noted that the results of the compact model yielded conservative estimates of the junction temperature over the simulation time compared to the detailed model. The relative error percentage of these two models is calculated by equation (5.10) and showed in a semi-logarithmic scale in figure 5.15 (b).



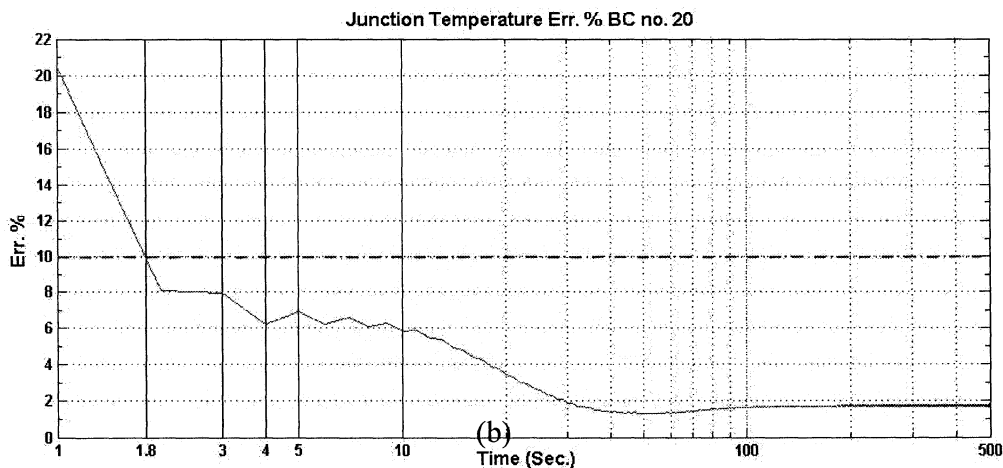
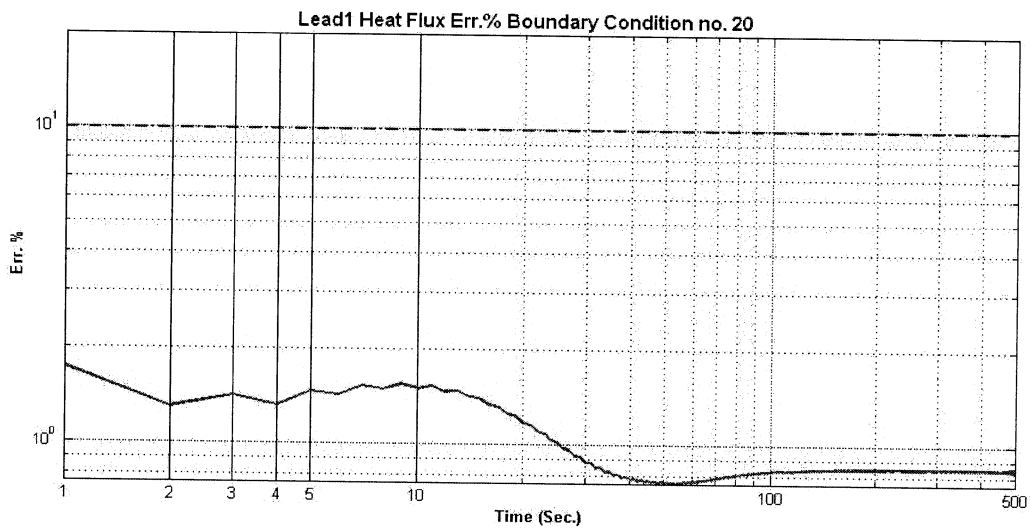
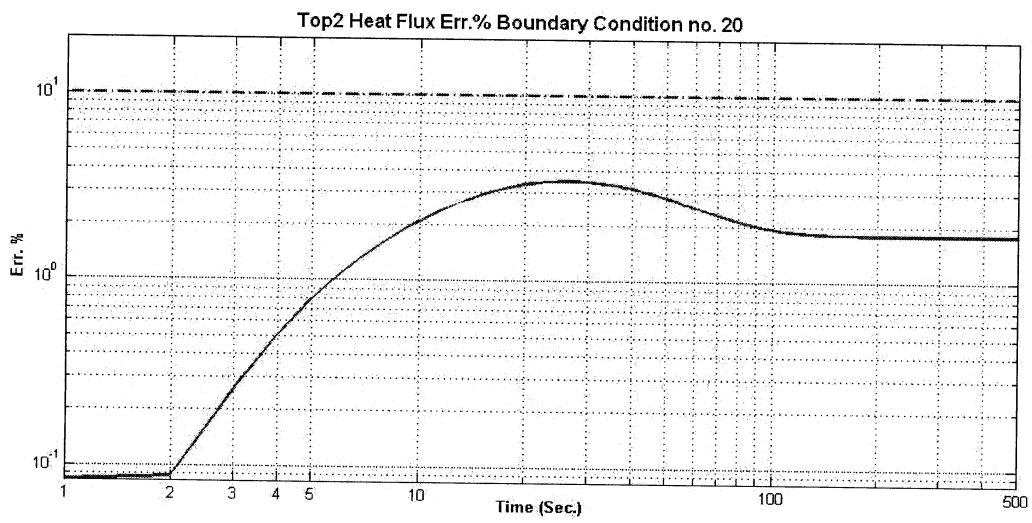
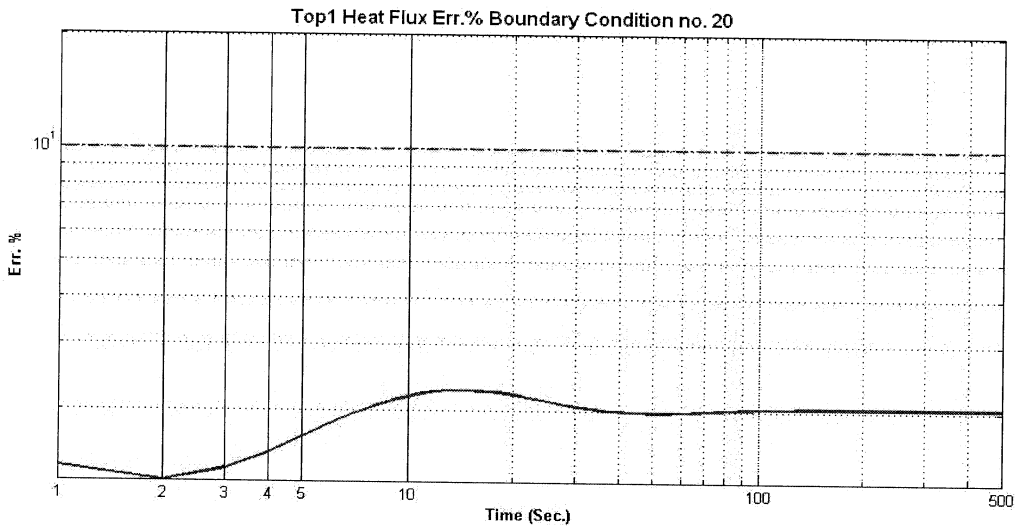


Figure 5.15: (a) Detailed and Compact model junction temperature for BC no. 20, (b) Their relative error percentage.

Figure 5.15 (a) shows the transition time before package reaches its steady state condition is approximately 100 seconds and figure 5.15 (b) shows from  $t=1.8$  sec. the error percentage drops below 10%. This means compact model gives acceptable result for almost 98.2% of transient time.

Similar to Case Study 1 the error percentage graph starts from a large value because of the distributed quiddity of package as a thermal system and after transition period it gets into a constant value which is equal to the relative error calculated in previous chapter from static model.

In this example also the relative error percentages between compact model results and detailed model results for transient outward heat fluxes from Top1, Top2, Bottom, Lead1, Lead2, and side walls area are illustrated in figure 5.16 in a logarithmic scale. These relative errors are also calculated using equation (5.11) to (5.16). For this example also we can see that all of these error curves are below 10% line during the whole period of analysis time. The performance of compact model thus is acceptable.



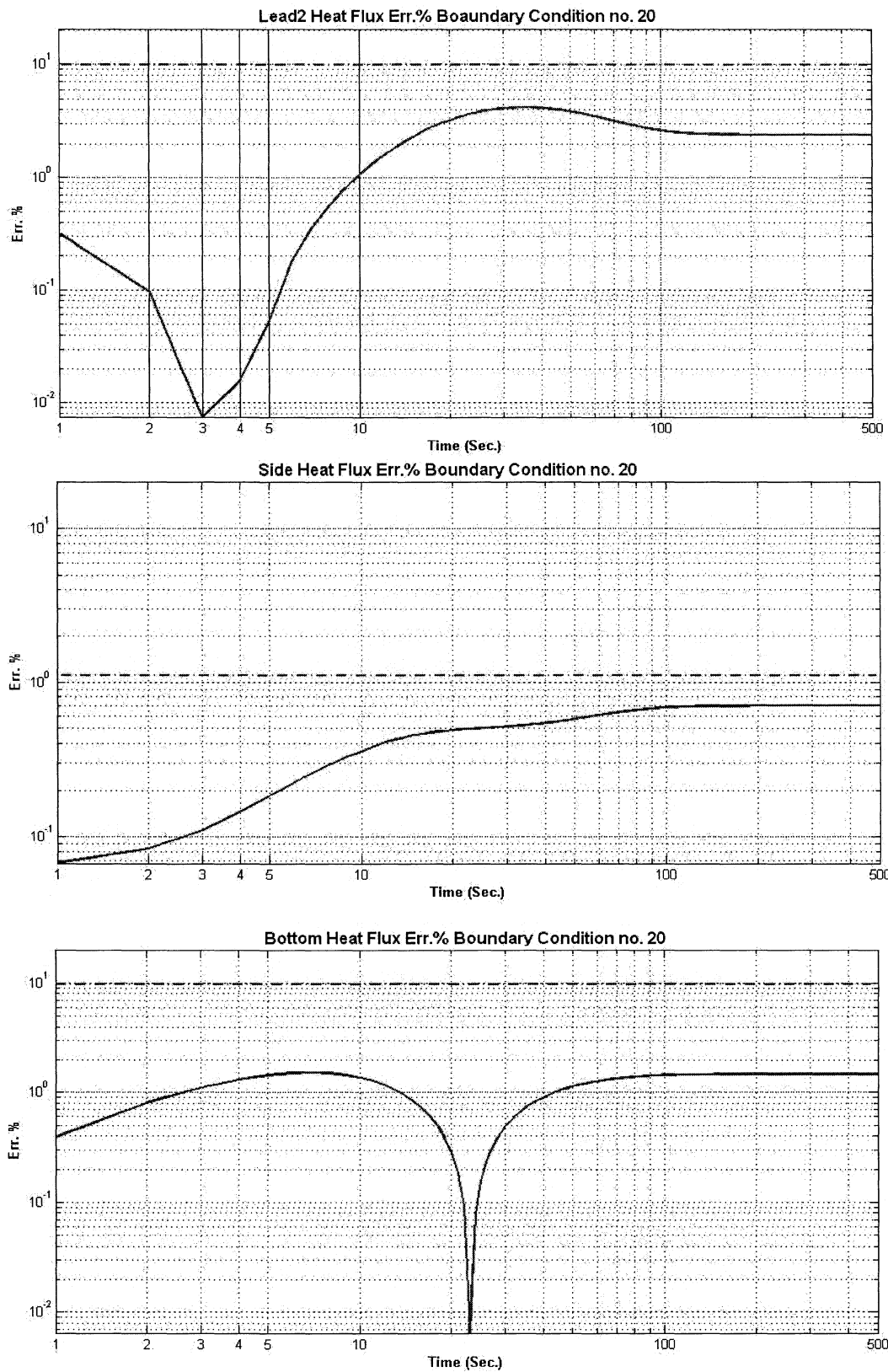
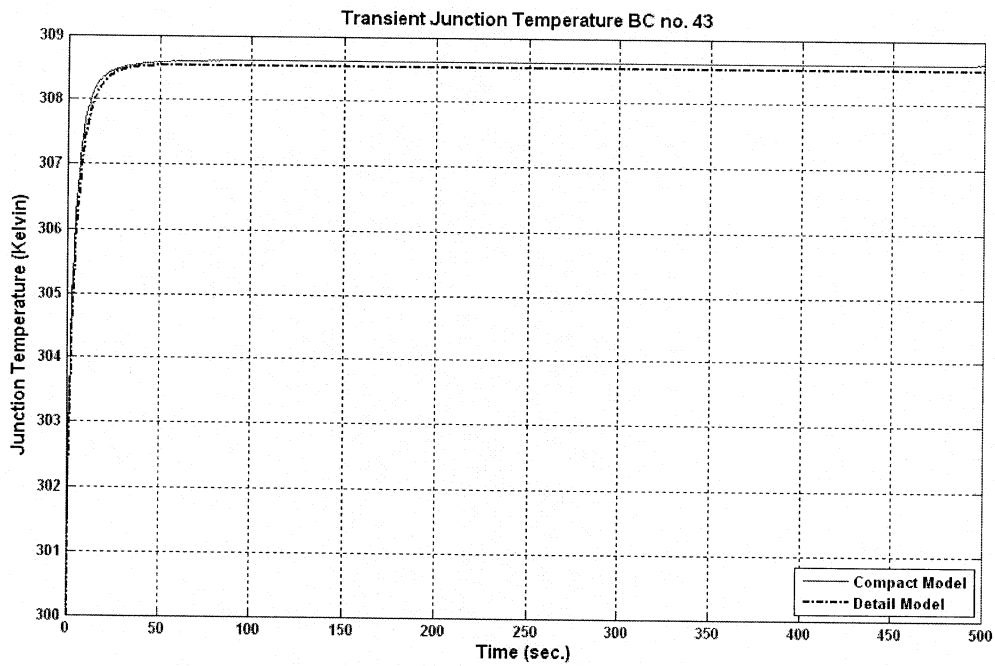


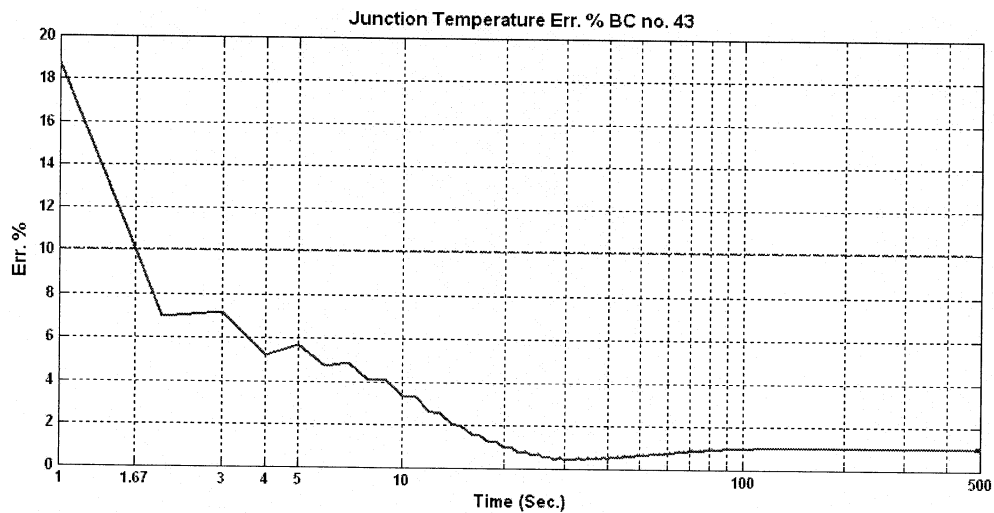
Figure 5.16: Relative error percentages of outward heat fluxes from Top1, Top2, Lead1, Lead2, Side, and bottom of BGA package for boundary condition no. 20.

### 5.7.3 Case Study 3: Boundary condition no. 43

For the last case study, BC number 43 which is a mixed heat sink and forced convection boundary condition has been investigated. The variation of junction temperature as a function of time is shown in figure 5.17 (a) for the first 50 seconds. Similar to previous example solid line shows the junction temperature predicted by the compact model and dashed line shows the junction temperature measured from detailed model.



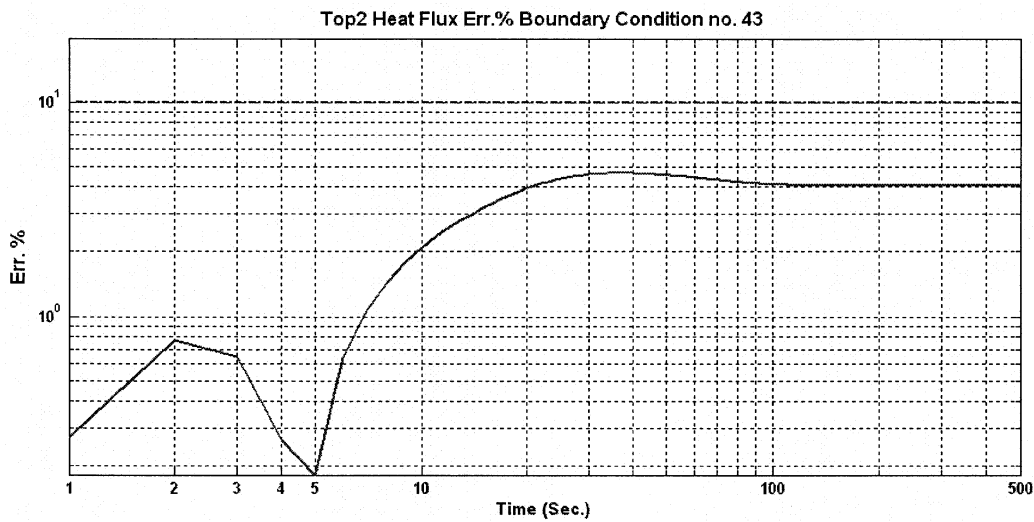
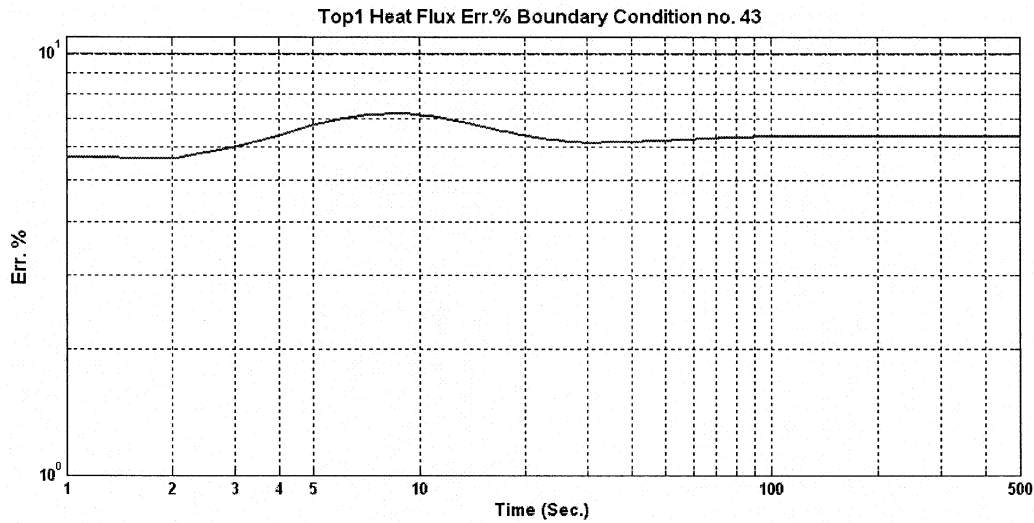
(a)



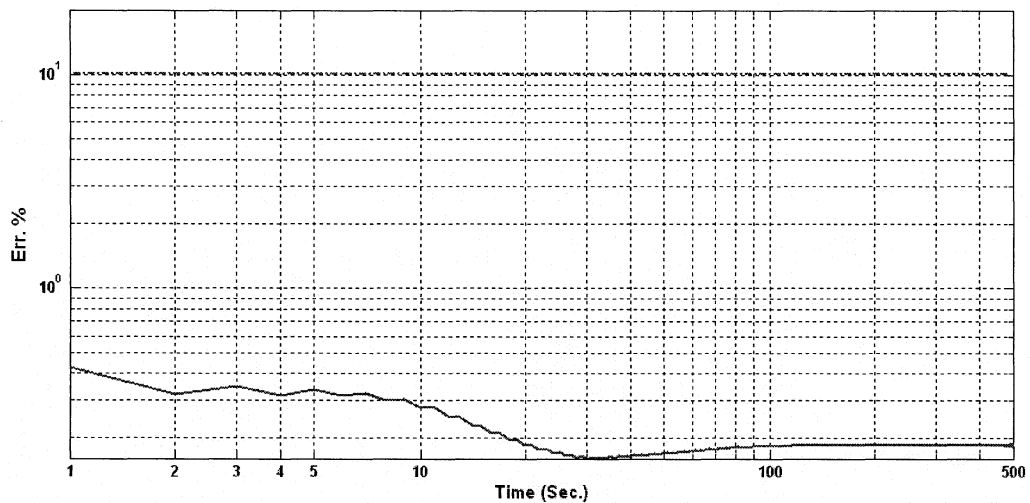
(b)

Figure 5.17: (a) Detailed and Compact model junction temperature for BC no. 43, (b) Their relative error percentage.

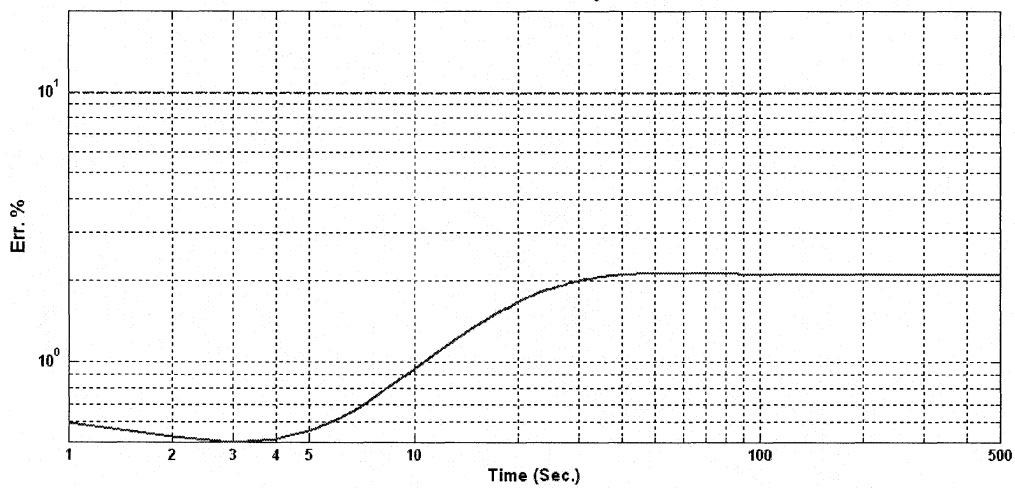
The relative error percentage of these two models is illustrated in a semi-logarithmic scale in figure 5.17 (b). figure 5.17 (a) shows the transition time before package reaches its steady state thermal condition for is approximately 40 seconds and figure 5.17 (b) shows from  $t=1.7$  sec. the error percentage drops below 10%. This means compact model gives acceptable result for almost 96% of transient time.



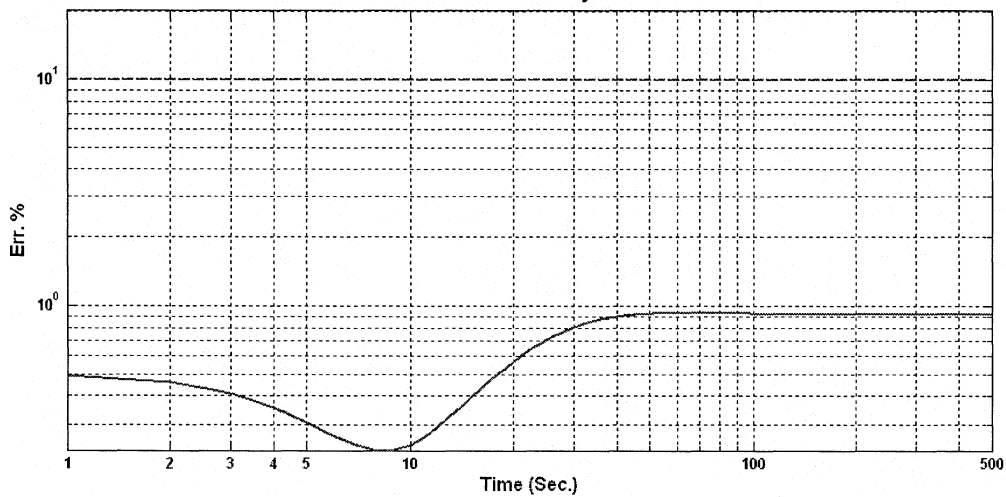
Lead1 Heat Flux Err.% Boundary Condition no. 43



Lead2 Heat Flux Err.% Boundary Condition no. 43



Side Heat Flux Err.% Boundary Condition no. 43



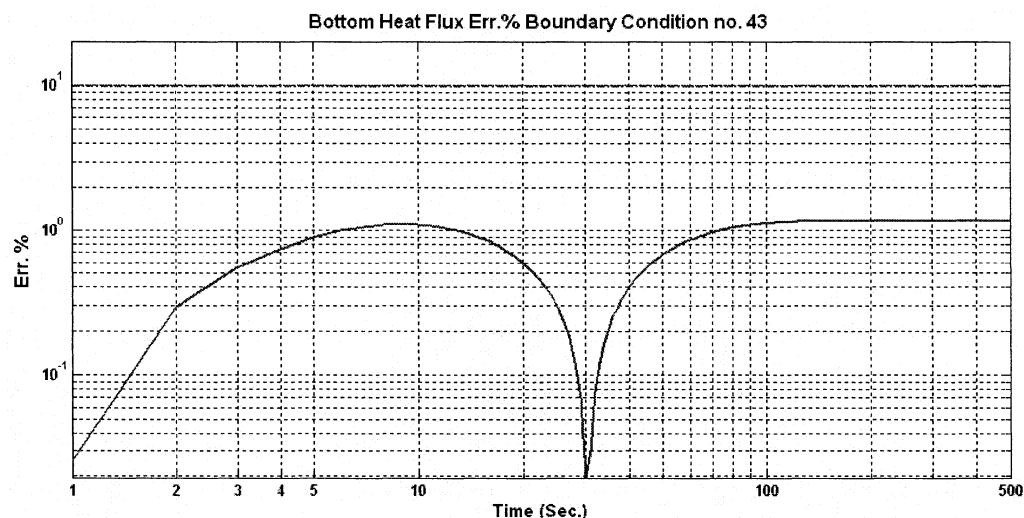


Figure 5.18: Relative error percentages of outward heat fluxes from Top1, Top2, Lead1, Lead2, Side, and bottom of BGA package for BC no. 43.

Figure 5.18 shows the relative error percentages between compact model results and detailed model results for transient outward heat fluxes from Top1 area, Top2 area, Bottom are, Lead1 area, Lead2 area, and side walls area in a logarithmic scale. It's clear that all of these error curves are below 10% line during the whole period of analysis time. The performance of compact model thus is acceptable.

As noted earlier, dynamic compact model results for all cases considered are included in the appendices B to this thesis where they are compared to detailed FE model data. In all cases evaluated, the results predicted from the dynamic compact model compared favorably to the detailed model results. The agreement between the compact model results and detailed model data for different boundary conditions showed that the compact model has the capacity to predict junction temperature, heat fluxes from various sections.

The similar results for junction temperature, heat fluxes from various sections would suggest that the dynamic compact model of the BGA package provides a very good representation of this detailed dynamic model. Although differences were shown to exist between DCTM data and detailed model results, these differences were generally of the same order of magnitude. Moreover, it can be noted that the results of the dynamic compact model yielded more conservative estimates of the junction temperature over the simulation time compared to the detailed model.

## 5.8 Summary

In this chapter the static compact model generated in previous chapter was extended and modified so it can predict the desired temperatures and heat fluxes during the thermal transient period. This model is called dynamic compact thermal model and is a necessary tool for thermal analysis of the systems that expose to boundary condition variation and/or power consumption (dissipation) mode switching such as mobile systems and battery powered system. The duality between the thermal and electrical capacitance was employed and Resistor network was expanded by adding some capacitors so it can predict the transient thermal behavior of the BGA package. The dynamic model thus is a RC network. Other types of dynamic compact modeling approaches were also introduced briefly.

Detailed model transient simulation was performed using COMSOL for all 58 boundary conditions and the results were saved. These results then were used by an optimization algorithm that calculates the optimum capacitors values so the cost function representing the deviation between the detailed and compact model was minimized. The optimization results suggested that it was possible to eliminate two capacitors and make the dynamic model even more compact. This reduced compact model was validated by calculating the relative errors of compact model results with respect to the detailed model results. These relative errors have been verified to be less than 10% criterion. The performance of compact model were investigated for three different boundary conditions at the end of this chapter as case studies and 6 more boundary conditions are presented in appendix B. These 9 case studies cover all types of boundary conditions proposed in [30] and listed in table 5.3. Our primary decision to eliminate 2 capacitors thus proved to be correct and reduced DCTM consisting of seven resistors and five capacitors considered as the final result of compact model generation.

## Chapter 6

### Conclusion and Future Work

In this thesis the theory and practice of compact thermal modeling (CTM) of the electronic packages were discussed and a new dynamic compact thermal model was developed and proposed for Ball Grid Array (BGA) package. BGA is a modern and increasingly popular technology of packaging the complex single chip and multi chips VLSI integrated circuits and was selected as the case study to keep this work up-to-dated. COMSOL Multiphysics© which is a very powerful finite element analysis tool and adopted by some well known and reputable high tech industries and educational institutes was used to perform the thermal simulation of the BGA package. This simulation then used as the input of compact model generation algorithms. The approach proposed by the European Union funded DELPHI project for static compact modeling which is based on thermal modeling by resistor network was adopted as the starting point and based on this approach CTM generation algorithms necessary for the new dynamic compact thermal model of the BGA were developed and validated using MATLAB© programming.

The present work was done in 2 major steps: Static or steady state CTM generation, and Dynamic CTM generation. First the steady state simulation was performed for BGA. The output of this simulation is called the detailed thermal model from which the static CTM was generated by optimization method and validated by comparing its outputs to the detailed thermal model. An optimization algorithm based on Nelder-Mead multidimensional optimization method was developed by MATLAB© programming and used for optimization process. According to the validation results the static CTM generated in this work can calculate the Junction temperature with the maximum relative error equal to 1.5% with respect to the detailed model. Steady state outward heat fluxes are also calculated by the CTM with maximum relative error equal to 6.8% with respect to the detailed model. Considering the fact that maximum 10% relative error is a validation criterion commonly accepted in many works and this project, it is clear that our static CTM shows a very high performance in terms of calculating Junction temperature which is usually the most crucial parameter in thermal analyses. Performance of the model in terms of calculating the heat fluxes can also be accepted confidently.

Second and more important of the research presented by this thesis was dedicated to dynamic CTM generation. In this work we tried to generalize the DELPHI methodology and expanded the resistor network into a resistor capacitor network which is able to model the transient thermal behavior of the BGA package. Time dependent detailed thermal simulation of the BGA package was performed using COMSOL© and its output was saved as the dynamic detailed model of the package. Resistor network generated previously was updated by adding seven capacitors and their values were optimized. Similar to static model generation a Nelder-Mead optimization algorithm was developed by using MATLAB© programming and applied for optimization process. The optimization results showed that it is possible that two capacitors may be eliminated without any considerable harm to the performance of the dynamic model.

Dynamic compact model results for all cases considered are compared to detailed finite element model data. In all cases evaluated, the results predicted from the dynamic compact model compared favorably to the detailed model results. The agreement between the compact model results and detailed model data for different boundary conditions showed that the compact model has the capacity to predict junction temperature, heat fluxes from various sections. The similar results for junction temperature, heat fluxes from various sections would suggest that the dynamic compact model of the BGA package provides a very good representation of this detailed dynamic model. Although differences were shown to exist between dynamic compact model data and detailed model results, these differences were generally of the same order of magnitude. Moreover, it was noted that the results of the dynamic compact model yielded more conservative estimates of the junction temperature over the simulation time compared to the detailed model.

Electronic package thermal analysis and compact modeling is an increasingly popular research area in the fields of electronic packaging, MEMS, and consumer electronics. The future works in this area is trying to improve the performance of dynamic CTM for the first couple of seconds of the transition time. This may be done by modeling the package using transmission lines rather than lumped resistors and capacitors. Another suggestion is investigating on the effect of surface allocation to the compact model nodes. We would also like to perform more evaluation on the proposed static and dynamic compact thermal models by comparing their results to experimental results and improve their efficiency.

## References

- [1] F.A. Mohammadi, K. Meres and M.C.E. Yagoub, "Rigorous thermal treatment of heat generation and heat transfer in GaAs-based HBT device modeling", Proceedings of EuroSIME2005, pp. 604-608, April 17-20, 2005, Berlin/Germany.
- [2] S. Sharifian Attar, M.C.E. Yagoub, F.A. Mohammadi, "Electro-thermal simulation of device and circuit," WSEAS Trans. on Circuits and Systems, Vol. 5, No 7, pp. 926-930, July 2006.
- [3] S. Sharifian Attar, M.C. E. Yagoub and F. Mohammadi, "New Electrothermal Integrated Circuit Modeling Using Coupling of Simulators," Proceeding of the 19th Canadian Conference on Electrical and Computer Engineering, MAY 2006.
- [4] Rosten H., Parry J., Lasance C. J. M. et al, "Final Report to SEMI-THERM XIII on the European-Funded Project DELPHI - The Development of Libraries and Physical Models for an Integrated Design Environment," Proc. of the Thirteenth IEEE SEMI-THERM Symposium, Austin, TX USA, January 28-30, 1997.
- [5] Rosten H., Clemens J. M. Lasance, and John D. Parry, " The World of Thermal Characterization According to DELPHI – Part I: Background to DELPHI," IEEE Transactions on Components, Packaging, and Manufacturing Technology-Part A, Vol. 20, No. 4, December 1997.
- [6] Eric G. T. Bosch, "Thermal Compact Models: An Alternative Approach," IEEE Transactions on Components and Packaging Technologies, VOL. 26, No. 1, March 2003.
- [7] M. Asghar Bhatti, *Fundamental Finite Element Analysis and Applications: with Mathematica and Matlab Computations*, Wiley, 2005.
- [8] G. E. Myers, *Analytical Methods in Conduction Heat Transfer*, 2nd Edition , AMCHT Publications, 1998.
- [9] D. Celso, X. Guo, P. Gunupudi, R. hazaka, D. J. Walkey, T. Smy, and M. nakhla, "The Creation of Compact Thermal Models of Electronic Components Using Model Reduction," *IEEE Transactions on Advanced Packaging*, vol. 28, no. 2, May 2005.

- [10] M. N. Sabry, "High-Precision Compact-Thermal Models," *IEEE Transactions on Components and packaging Technologies*, vol. 28, no. 4, Dec. 2005.
- [11] M. R. Stan, K. Skadron, M. Barcella, W. Huang, K. Sankaranarayanan, and S. Velusamy, "HotSpot: a Dynamic Compact Thermal Model at the Processor-Architecture Level," *Special issue on Thermnic*, T02MEJ 14, 2002.
- [12] F. Chrstanes, B. Vandavelde, E. Beyne, R. Mertens, and J. Berghmans, "A Generic Methodology for Deriving Compact Dynamic Thermal Models, Applied to the SGA Package," *IEEE Transactions on Components, Packaging, and Manufacturing Technology Part A*, vol. 21, no. 4 Dec. 1998.
- [13] Incropera, Frank P. : *Introduction to heat transfer*, John Wiley Hobokenm NJ, 5<sup>th</sup> edition, 2007.
- [14] Kutz, M.: *Heat-transfer calculations*, McGraw-Hill, New York, 2006.
- [15] Thomas, George B. Jr.; Finney, Ross L. : *Calculus and Analytic Geometry (9th ed.)*. Addison Wesley, 1996.
- [16] Eriksson, K.; Estep, D.; Johnson, C. : *Applied mathematics, body and soul*. Berlin; New York: Springer, 2004.
- [17] K. J. Bathe, *Finite Element Procedures in Engineering Analysis*. Prentice-Hall, 1982.
- [18] Dacorogna, B.: *Introduction to calculus of variations*, Imperial College Press, London, 2004.
- [19] George R. Buchanan : *Finite Element Analysis*, Schaum's Outline Series, McGraw-Hill Companies, Inc. Ney York, 1995.
- [20] Brown, William D. *Advanced Electronic Packaging*, Hoboken, NJ Wiley ; Piscataway, 2<sup>nd</sup> edition, 2006.
- [21] James J. Licari and Dale W. Swanson, *Adhesives technology for electronic applications: materials, processes, reliability*, Norwich, NY, William Andrew Pub., 2005.

- [22] <http://www.educyclopedia.be/electronics/Images/dip.gif>
- [23] <http://www.topline.tv/images/soic.jpg>
- [24] <http://www.topline.tv/images/soj.jpg>
- [25] <http://www.topline.tv/images/soj.jpg>
- [26] [http://www.analog.com/UploadedFiles/Packages/60734SU\\_100.jpg](http://www.analog.com/UploadedFiles/Packages/60734SU_100.jpg)
- [27] <http://ashmorsystems.com/images/BX80552631.jpg>
- [28] <http://www.statschippac.com/en-US/STATSChipPAC/IntegratedServices/Packaging/Array/pbga.htm>
- [29] [http://www.intel.com/design/packtech/ch\\_14.pdf](http://www.intel.com/design/packtech/ch_14.pdf)
- [30] Clemens J. M. Lasance, "Two Benchmarks to Facilitate the Study of Compact Thermal Modeling Phenomena," IEEE Transactions on Components and Packaging Technologies, VOL. 24, No. 4, December 2001
- [31] COMSOL multiphysics user's guide, © COPYRIGHT 1994-2006 by COMSOL AB.  
<http://www.comsol.com/products/multiphysics/>
- [32] E. G. T. Bosch and M. N. Sabry, "Thermal Compact Models for Electronic Systems," 18<sup>th</sup> IEEE SEMI-THERM Symposium, 2002
- [33] The MathWorks Inc., MALAB R2006b Copyright 1984-2006  
<http://www.mathworks.com/>
- [34] J. A. Nelder and R. Mead, *A simplex method for function minimization*, Computer Journal 7, 1965.
- [35] V. Torczon, *On the convergence of pattern search algorithms*, SIAM J. Optim., 7 (1997).
- [36] M. H. Wright, *Direct search methods: Once scorned, now respectable*, in Numerical Analysis 1995: Proceedings of the 1995 Dundee Biennial Conference in

- Numerical Analysis, D. F. Gri\_ths and G. A. Watson, eds., Addison Wesley Longman, Harlow, UK, 1996.
- [37] Lagarias, J.C., J. A. Reeds, M. H. Wright, and P. E. Wright, "Convergence Properties of the Nelder-Mead Simplex Method in Low Dimensions," *SIAM Journal of Optimization*, Vol. 9 Number 1, pp. 112-147, 1998.
- [38] V. Szekely: Identification of RC Networks by Deconvolution: Chances and Limits, *IEEE Trnnscriptions on Circuits and Systems-I. Theory and Applications*, CAS-45(3):244-258, 1998.
- [39] Y. K. Chang, C. Tsai, C. Teng, S. Kang, "*Electrothermal analysis of VLSI systems*," Kluwer Academic Publishers, 2000.
- [40] Filip Charistiaens, Bart Vandavelde, Eric Beyne, Robert Mertens, and Jan Berghmans: A Generic Methodology for Deriving Compact Dynamic Thermal Models, Applied to PSGA Package, *IEEE Transactions on Components, Packaging, and manufacturing Technology*, Part A, Vol. 21, No. 4, December 1998.
- [41] Hun H. Sun, "*Synthesis of RC Networks*," Hayden book company, Inc. 1967.
- [42] Shlomo Karni, "*Network Theory: Analysis and Synthesis*," Allyn and Bacon, Inc. 1966.
- [43] V. Szekely, A. Poppe, M. Rencz, A. Csendes, and A. Pahi, "Electro-thermal simulation: A realization by simultaneous iteration," *Microelectronics J.*, vol. 28, no. 3, pp. 247-262, Mar. 1997.
- [44] V. Szekely and T. Van Bein, "Fine structure of heat flow path in semiconductor devices: A measurement and identification method," *Solid-State Electron.*, vol. 31, no. 9, pp. 1363-1368, 1988.
- [45] V. Szekely, "A new evaluation method of thermal transient measurement results," *Microelectronics J.*, vol. 28, no. 3, pp. 277-292, Mar. 1997.
- [46] E. Kreyszig, "*Advanced Engineering Mathematics*," 9<sup>th</sup> edition. John Wiley & Sons, Inc. 2006.

- [47] E. S. Ochotta, T. Mukherjee, R. A. Rutenbar, L. R. Carley, "*Practical synthesis of high-performance analog circuits*," Kluwer Academic Publishers, 1998.
- [48] L.T. Pillage, R.A. Rohrer: Asymptotic waveform evaluation for timing analysis, *IEEE Transactions on Computer-Aided Design*, CAD-9(4):352-366, 1990.
- [49] P. K. Chan: Comments on "Asymptotic Waveform Evaluation for Timing Analysis", *IEEE Transactions on Computer-Aided Design*, vol. 10, no. 8. August 1991.
- [50] V. Raghavan, R. A. Rohrer, M. M. Alabeyi, J. E. Bracken, J. Y. Lee, and L.T.Pillage: AWE Inspired. *IEEE Custom Integrated Circuit Conference*, pages 18.1/1-8. San Diego, May, 1993.
- [51] S.S. Lee. D.J. Allstot: Electrothermal simulation of integrated circuits, *IEEE Journal of Solid-State Circuits*, SSC-28(12):1283-1293, 1993.
- [52] D.Liu, V. Phanilatha, Q. Zhang, and M. S. Nakhla: Asymptotic Thermal Analysis of Electronic Packages and Printed-Circuit Boards, *IEEE Transactions on Components, Packaging, and Manufacturing Technology*, PART A, vol. 18, no. 4, December 1995.

## **Publications**

1- M. Marami, F. Mohammadi, "A New Approach for Generation of Compact Thermal Model of a Package" Submitted to the 2008 IEEE International Symposium on Circuits and Systems (ISCAS 2008)

2- M. Marami, F. Mohammadi, "Generation and Evaluation of Compact Thermal Model of a Package," The International Conference for Upcoming Engineers (ICUE), 2007.

## Appendix 1

# NID and AWE methods of Dynamic Compact Thermal Modeling

### A.1 Network Identification by Deconvolution (NID)

NID is a method of synthesizing RC network from its time constant distribution function. Figure A.1.1 shows a single time constant RC network stimulated by a step function current source.

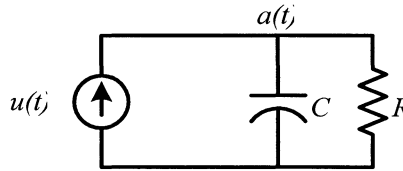


Figure A.1.1: Single time constant system.

Transient response of this system is:

$$a(t) = R(1 - \exp(-t/\tau)) \quad (\text{A.1})$$

where  $R$ ,  $C$ ,  $u(t)$ , and  $a(t)$  model thermal conduction resistance, thermal capacity, heat injected to thermal point, and temperature of node, respectively.

For a system with multiple time constants transient response is:

$$a(t) = \sum_i R_i(1 - \exp(-t/\tau_i)) \quad (\text{A.2})$$

and transient response of distributed system such as a package to  $u(t)$  is:

$$a(t) = \int_0^{\infty} R(\tau)(1 - \exp(-t/\tau))d\tau \quad (\text{A.3})$$

Now introducing new variables:

$$z = \ln t \quad \text{and} \quad \zeta = \ln \tau \quad (\text{A.4})$$

Equation (A.3) will be changed to:

$$a(z) = \int_{-\infty}^{\infty} R(\zeta)(1 - \exp[-\exp(z - \zeta)])d\zeta \quad (\text{A.5})$$

After differentiating equation (A.5) with respect to  $z$ :

$$\frac{d}{dz}a(z) = \int_{-\infty}^{\infty} R(\zeta) \exp(z - \zeta) \exp[-\exp(z - \zeta)]d\zeta \quad (\text{A.6})$$

or:

$$\frac{d}{dz}a(z) = R(z) \otimes W(z) \quad (\text{A.7})$$

where:

$$W(z) = \exp[z - \exp(z)] \quad (\text{A.8})$$

Taking  $a(t)$  as the input of process RC model is prepared by the following steps:

- $a(z)$  is generated using transformations shown by equation (A.4).
- $\frac{d}{dz}a(z)$  is calculated.
- using equations (A.6) and (A.7),  $R(z)$  is calculated.
- based on number of desired complexity of model  $R(z)$  is discretized into  $n$  regions along  $z$  axis. Each region is then modeled by a parallel RC as shown in figure A.1.2.

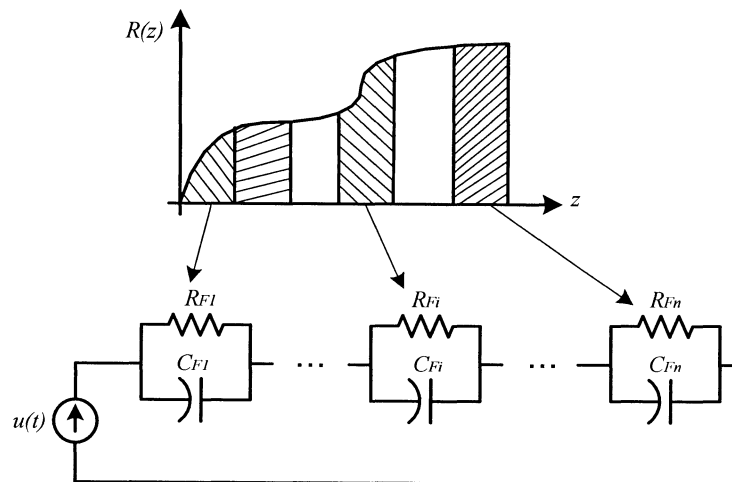


Figure A.1.2: Foster RC network

- Average value of  $R(z)$  for each region is the value of resistance and its corresponding  $z$  will be used for calculating capacitance.

$$R_{Fi} = R(z_i) \quad , \quad C_{Fi} = \frac{1}{R_{Fi}} \exp(z_i) \quad (\text{A.9})$$

- RC network shown in figure A.1.2 is a foster network and has no physical meaning. It must be converted into Cauer form which represents a model of physical properties and shown in figure A.1.3.

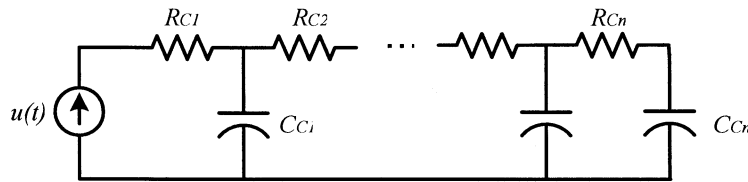


Figure A.1.3: Cauer RC network

The Foster to Cauer transformation method can be found in most electrical network text books such as [41, 42].

A detailed discussion of NID may be found in [38]. A good example of NID used for CTM extraction can be found in [43]. NID can also be used as a non-destructive measuring method to investigate internal structure of a package by its thermal characteristics. Examples are [44, 45].

## A.2 Asymptotic Waveform Evaluation (AWE)

RC network shown in figure A.1.3 is a Single-Input, Single-Output (SISO) linear, time invariant, lumped circuit modeling thermal characteristics of chip. Transfer function of a circuit with these characteristics is a rational fraction and can be expressed by partial fraction expansion.

$$H(s) = \sum_{l=1}^L \frac{k_l}{s - p_l} \quad (\text{A.10})$$

which has  $L$  poles and  $L$  residues.

Equation (A.10) has a Maclaurin series expansion [46] as:

$$H(s) = m_0 + m_1 s + m_2 s^2 + \dots \quad (\text{A.11})$$

where  $m_i$  is called the  $i^{\text{th}}$  moment.

An approximate transfer function can be expressed by only the first  $q$  partial fractions of equation (A.10):

$$\hat{H}(s) = \sum_{l=1}^q \frac{k_l}{s - p_l} \quad (\text{A.12})$$

or

$$\hat{H}(s) = -\sum_{l=1}^q \frac{k_l/p_l}{1 - s/p_l} \quad (\text{A.13})$$

setting equation (A.12) equal to equation (A.11):

$$\begin{aligned} \frac{k_1}{p_1} + \frac{k_2}{p_2} + \dots + \frac{k_q}{p_q} &= -m_0 \\ \frac{k_1}{p_1^2} + \frac{k_2}{p_2^2} + \dots + \frac{k_q}{p_q^2} &= -m_1 \\ &\vdots \\ \frac{k_1}{p_1^{2q-1}} + \frac{k_2}{p_2^{2q-1}} + \dots + \frac{k_q}{p_q^{2q-1}} &= -m_{2q-2} \end{aligned} \quad (\text{A.14})$$

which provides us  $2q$  unknowns ( $q$  poles and  $q$  residues) and  $2q-1$  equations! Supplementary equation can be obtained from initial conditions. Transforming equation (A.13) to time domain, impulse response of network is:

$$\hat{h}(t) = -\sum_{l=1}^q k_l e^{p_l t} \quad (\text{A.15})$$

and

$$y(t) = \hat{h}(t) * u(t) \quad (\text{A.16})$$

where  $u(t)$  and  $y(t)$  are input and output signals respectively. Initial condition is:

$$y(0) = \hat{h}(0) * u(0) = \left( -\sum_{l=1}^q k_l \right) * u(0) \quad (\text{A.17})$$

or

$$(k_1 + k_2 + \dots + k_q) * u(0) = -y(0) \quad (\text{A.18})$$

Next step is determining  $m_0, m_1, \dots,$  and  $m_{2q-2}$  so equation 4-19 and equation (A.18) can be used to find poles and residues. To find  $m_0, m_1, \dots,$  and  $m_{2q-2}$  state-space equations of a SISO linear system are used:

$$\begin{aligned} \dot{X} &= AX + Bu \\ y &= CX \end{aligned} \quad (\text{A.19})$$

where  $X$  is a  $n$  by  $1$  state vector,  $u$  and  $y$  are scalars representing Input and Output,  $A$  ( $n \times n$  matrix) and  $B$  ( $n \times 1$  vector) determine relationship between the state variables and input, and  $C$  ( $1 \times n$  vector) determine the relationship between the state variables and output.

Assuming network was at rest at time zero, Laplace transform of equation (A.19) is:

$$\begin{aligned} sX(s) &= AX(s) + Bu(s) \\ y(s) &= CX(s) \end{aligned} \quad (\text{A.20})$$

and transfer function:

$$H(s) = \frac{y(s)}{u(s)} = C(sI - A)^{-1}B \quad (\text{A.21})$$

Equation (A.21) can be expanded in a Maclaurin series:

$$H(s) = -CA^{-1}B - sCA^{-2}B - s^2CA^{-3}B - \dots \quad (\text{A.22})$$

Setting equation (A.11) and equation (A.22) equal, the moments can be calculated as following:

$$\begin{aligned} m_0 &= -CA^{-1}B \\ m_1 &= -CA^{-2}B \\ m_2 &= -CA^{-3}B \\ &\vdots \\ m_{2q-2} &= -CA^{-2q+1}B \end{aligned} \quad (\text{A.23})$$

which are equal to the right side of equation (A.14).

Some basic explanation about AWE method is in [39, 47, 48, 49, 50] offer detail information and different techniques of solving equations with different cost and accuracy. Examples of using AWE method to solve a compact thermal model can be found in [51, 52] and many other works. It must be mentioned at the end of this part that AWE method is not restricted to RC networks and has also been used vastly for RLC circuits.

## Appendix B

### Dynamic CTM - Case studies

As mentioned earlier in chapter 5 six other boundary conditions are presented here as case studies to provide more information on the trend of data over a range of parameters. Boundary conditions 12, 23, 35, 40, 46, and 52 of table 5.3 which are Free convection, Forced convection, Heat sink Free convection, Heat sink Forced convection, Cold Plate, and Fluid Bath types of boundary condition respectively will be presented in case studies 4 to 9. The applied boundary conditions are repeated in table B.1.

No	$h_{TOP}$	$h_{BOT}$	$h_{SIDE}$	$h_{LEADS}$
12	15	100	15	20
23	200	50	200	50
35	75	50	15	100
40	150	200	30	200
46	10	1000	10	10000
52	500	500	500	500

For each case study the transient junction temperature obtained from detailed model simulation and calculated from compact model, their relative error, and relative errors of compact model with respect to the detailed model for outward heat fluxes from TOP1, TOP2, LEAD1, LEAD2, SIDE, and BOTTOM of the package are presented. Figure B.1 shows these locations on the surfaces of the BGA package.

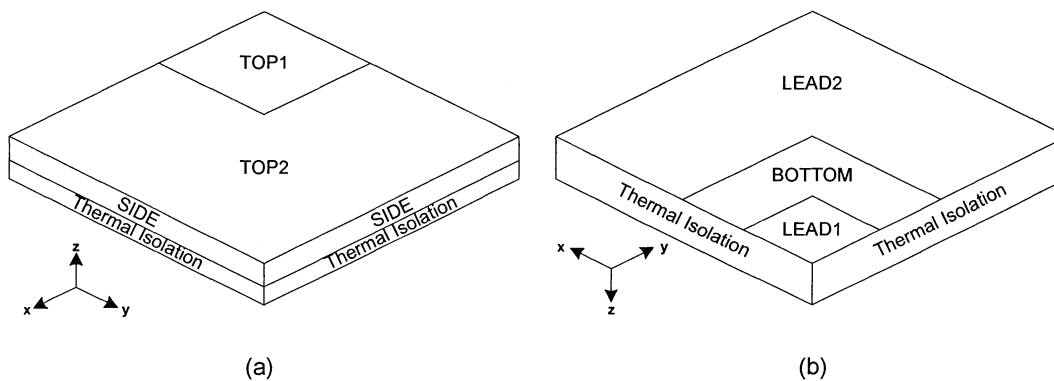


Figure B.1: (a) TOP1, TOP2, and SIDE areas, (b) LEAD1, LEAD2, and BOTTOM areas of the BGA package.

Note that all heat flux relative errors are below the 10% margin and junction temperature relative errors drop below the margin during the first 2 seconds of transient time. More explanation about figures B.1.1 to B.6.8 has been provided in chapter 5.

### B.1 Case study 4 - BC no. 12 - Free convection boundary condition

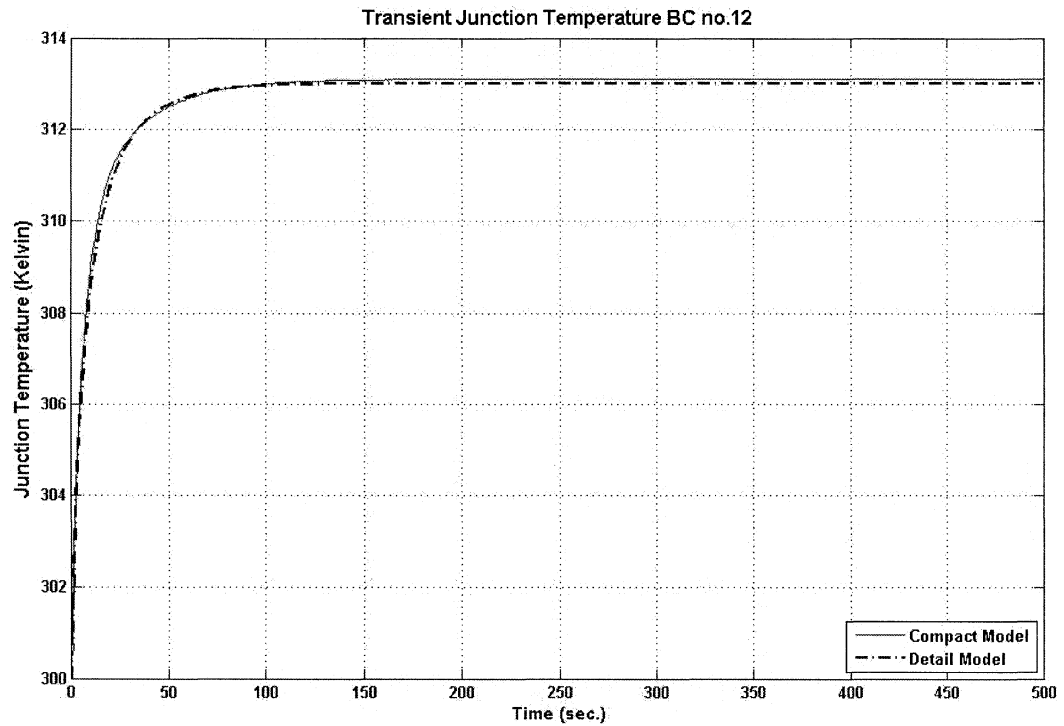


Figure B.1.1: Detailed and Compact model junction temperature for BC no. 12

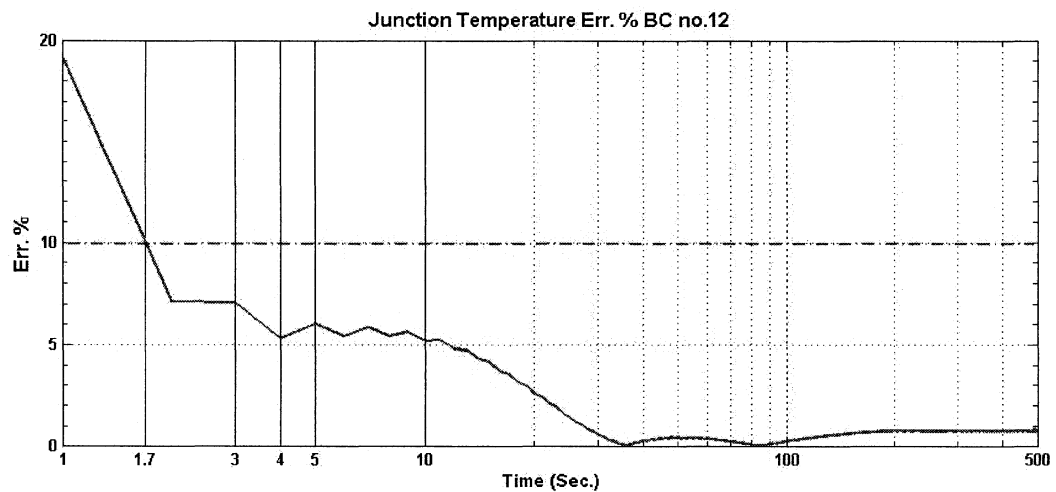


Figure B.1.2: Junction temperature relative error for BC no. 12

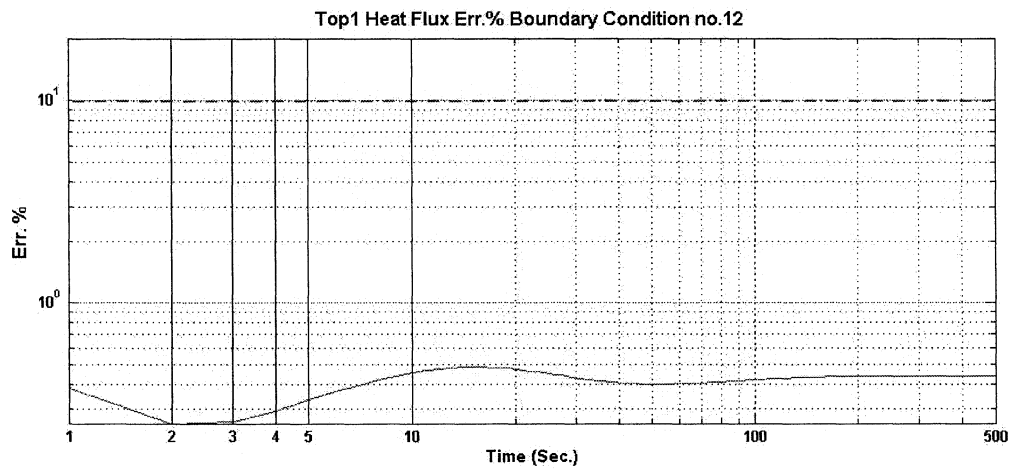


Figure B1.3: Top1 heat flux relative error for BC no. 12

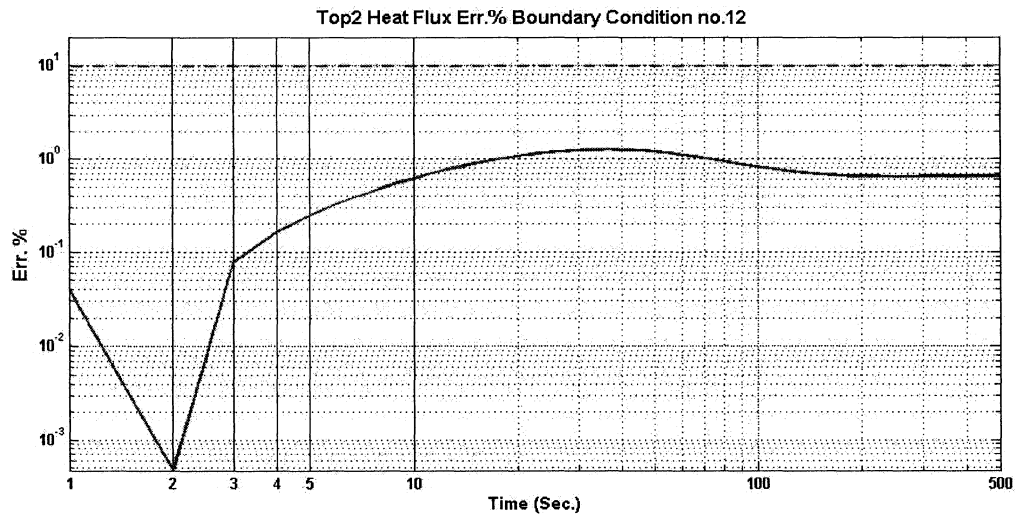


Figure B.1.4: Top2 heat flux relative error for BC no. 12

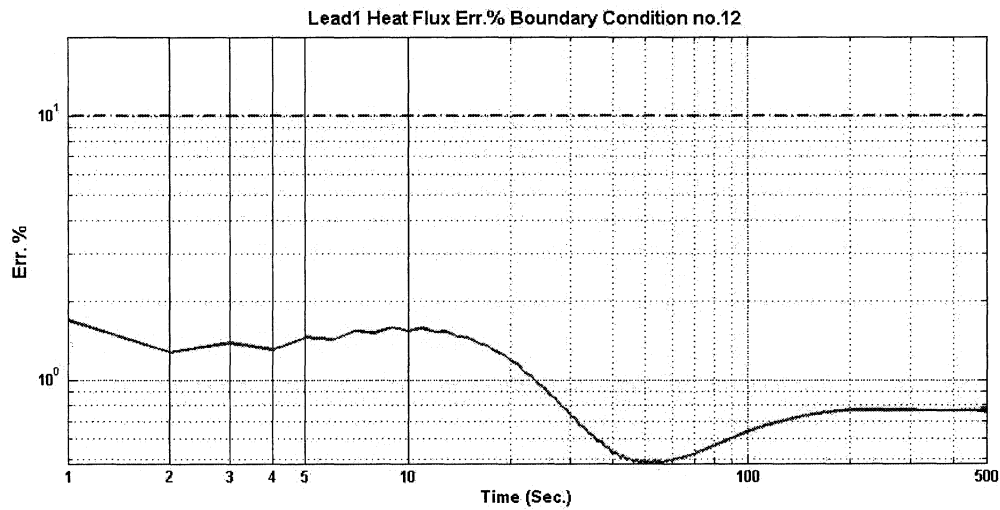


Figure B.1.5: Lead1 heat flux relative error for BC no. 12

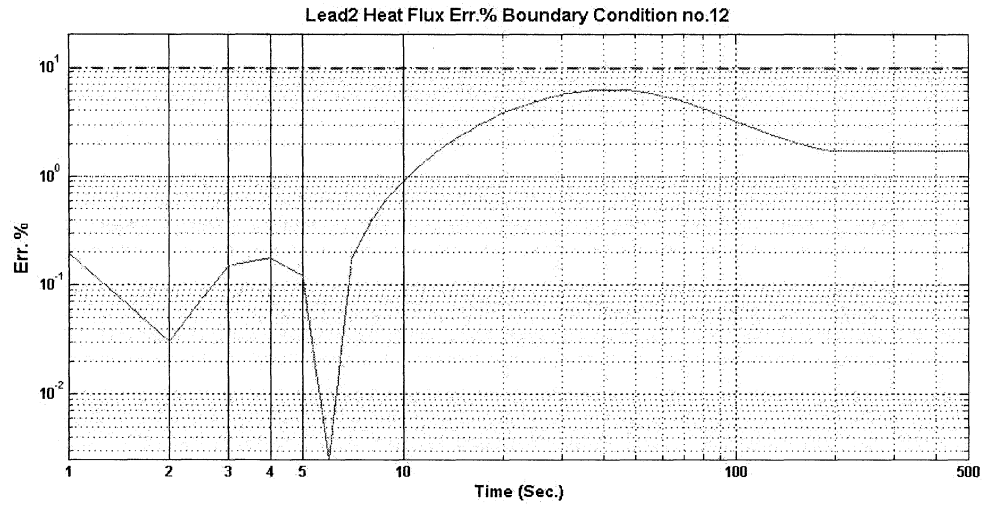


Figure B.1.6: Lead2 heat flux relative error for BC no. 12

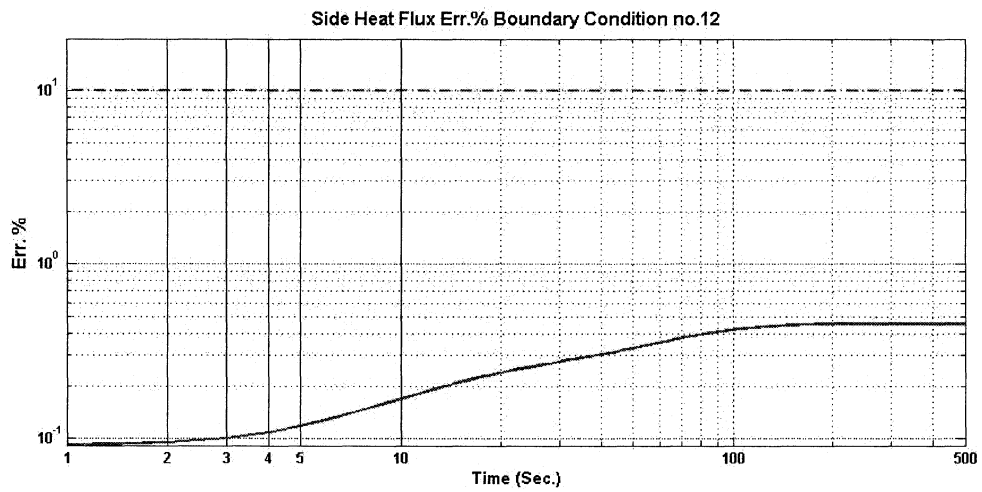


Figure B.1.7: Sidewalls heat flux relative error for BC no. 12

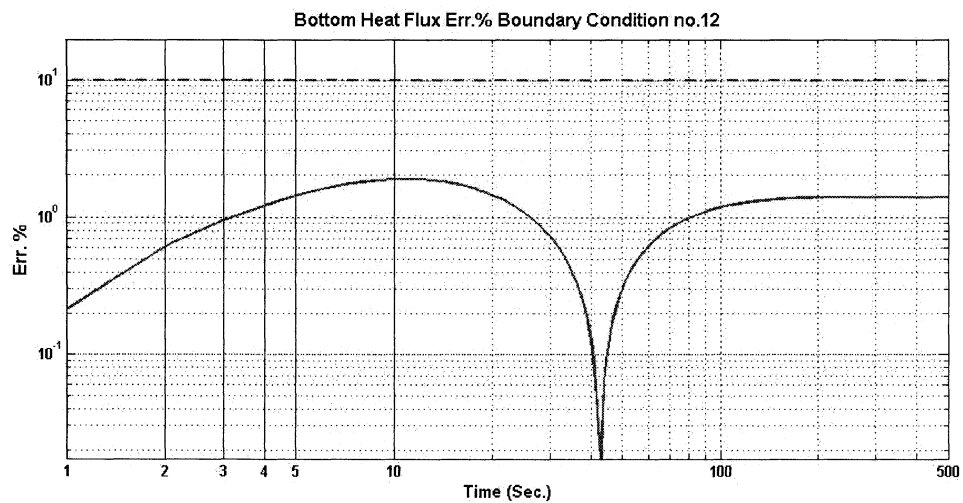


Figure B.1.8: Bottom heat flux relative error for BC no. 12

**B.2 Case study 5 - BC no. 23 - Forced convection boundary condition**

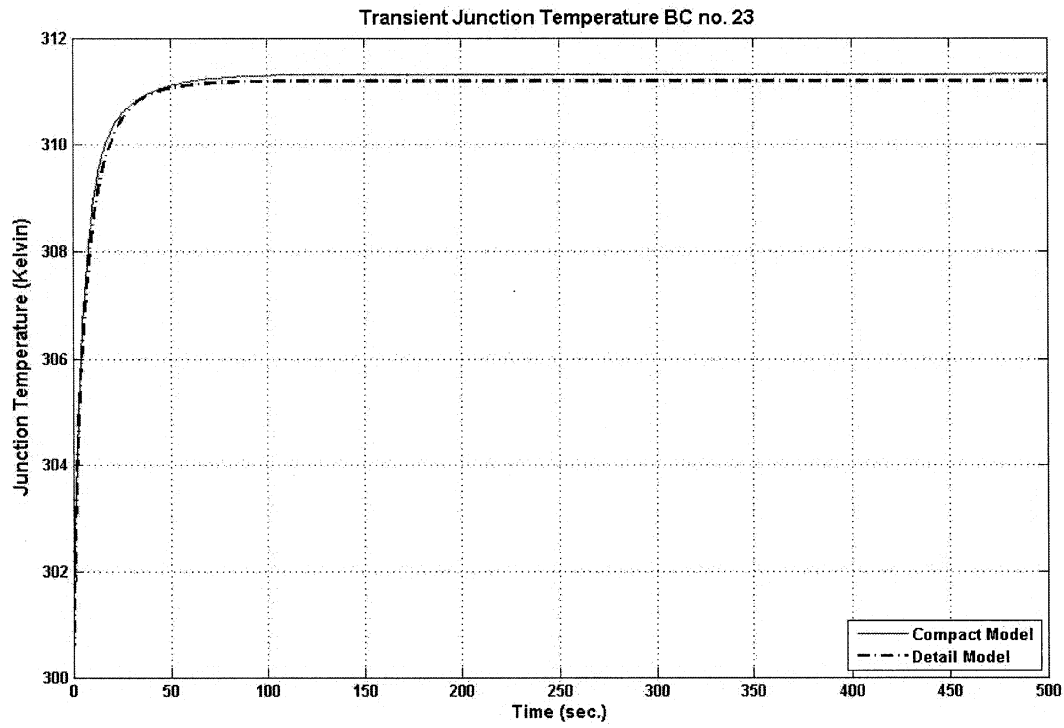


Figure B.2.1: Detailed and Compact model junction temperature for BC no. 23

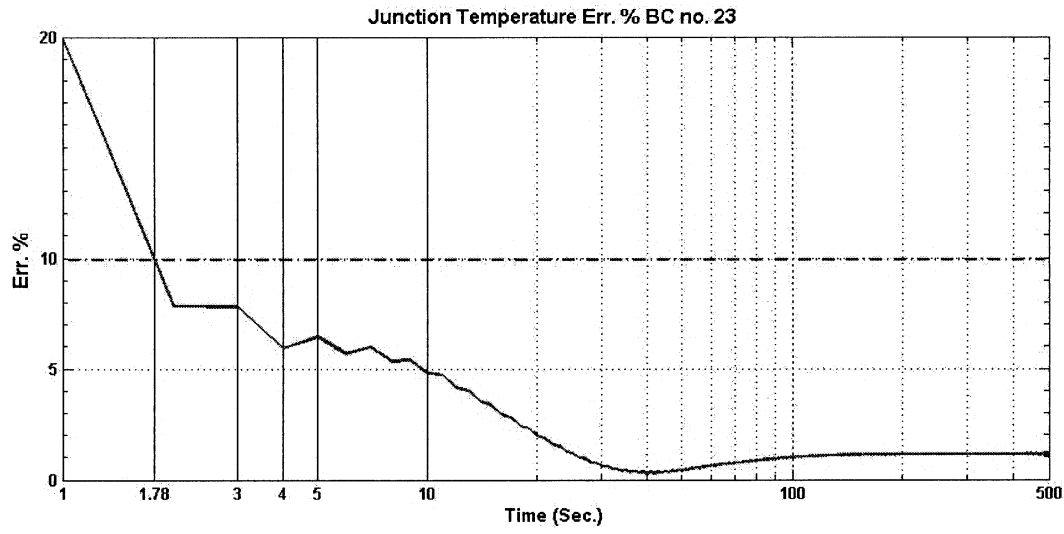


Figure B.2.2: Junction temperature relative error for BC no. 23

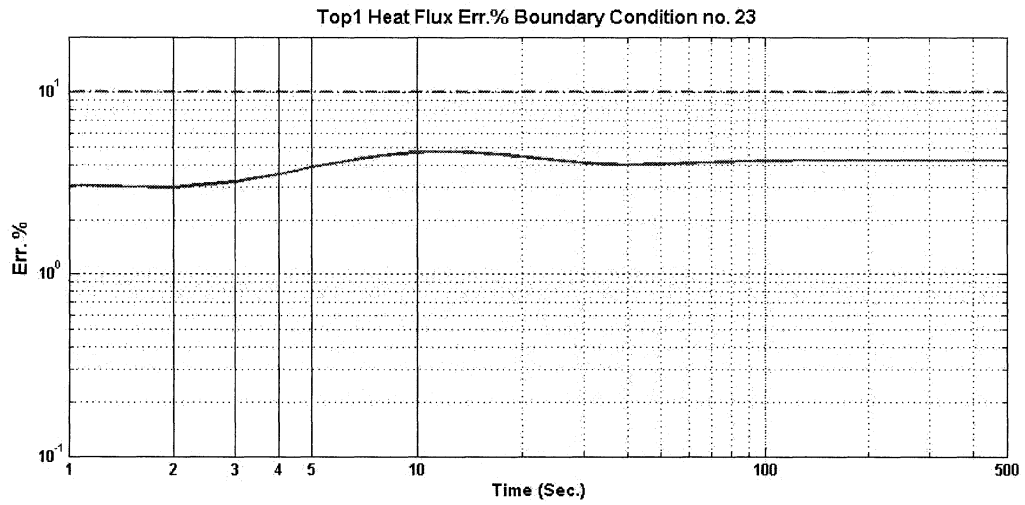


Figure B.2.3: Top1 heat flux relative error for BC no. 23

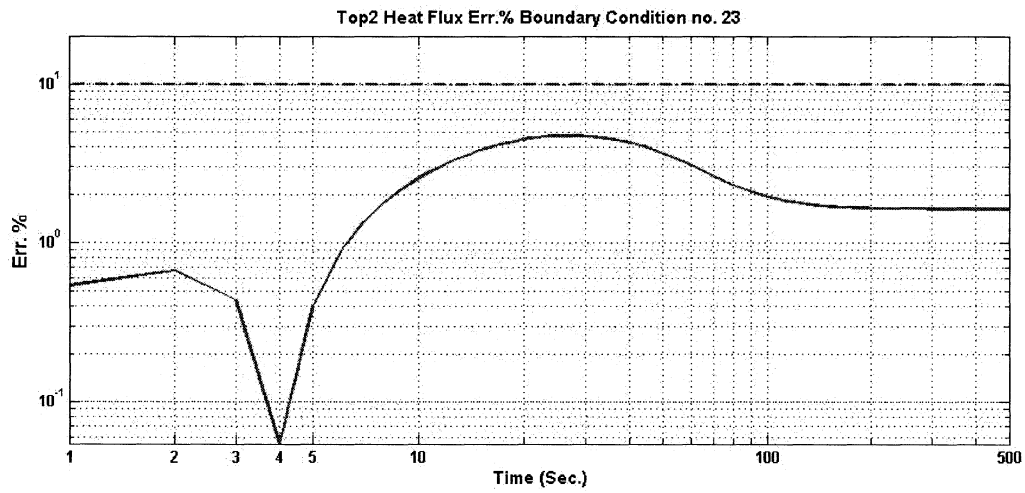


Figure B.2.4: Top2 heat flux relative error for BC no. 23

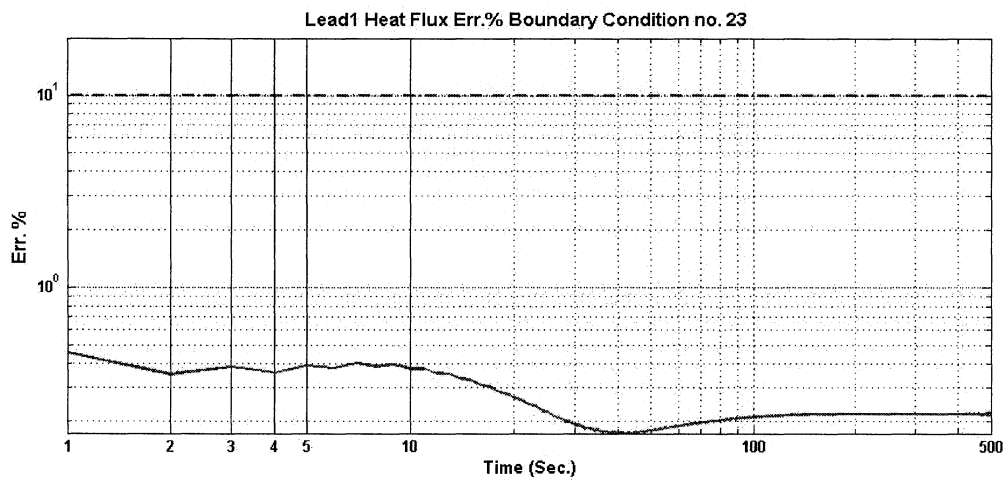


Figure B.2.5: Lead1 heat flux relative error for BC no. 23

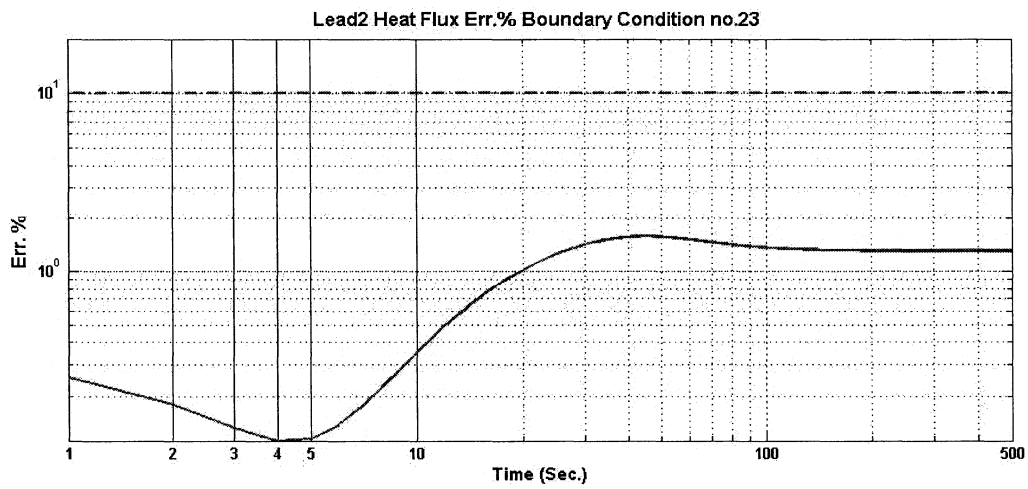


Figure B.2.6: Lead2 heat flux relative error for BC no. 23

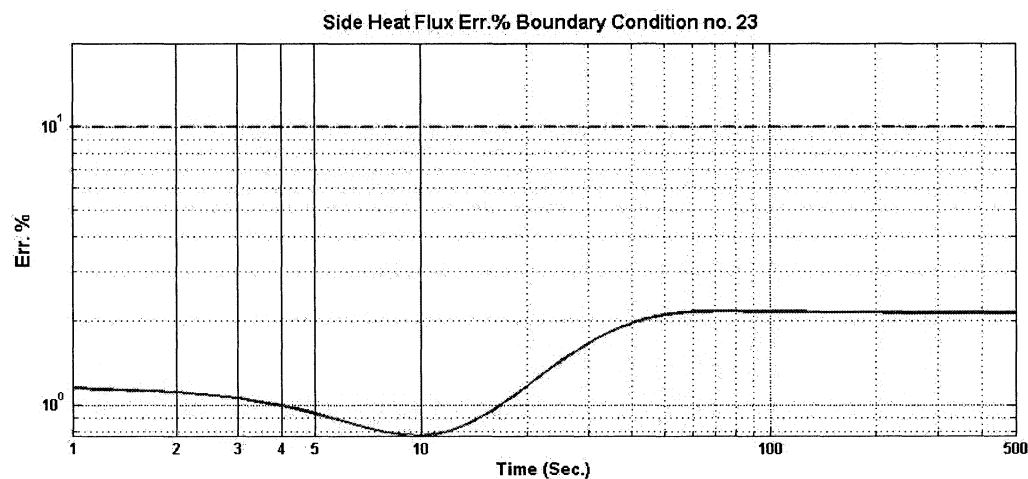


Figure B.2.7: Sidewalls heat flux relative error for BC no. 23

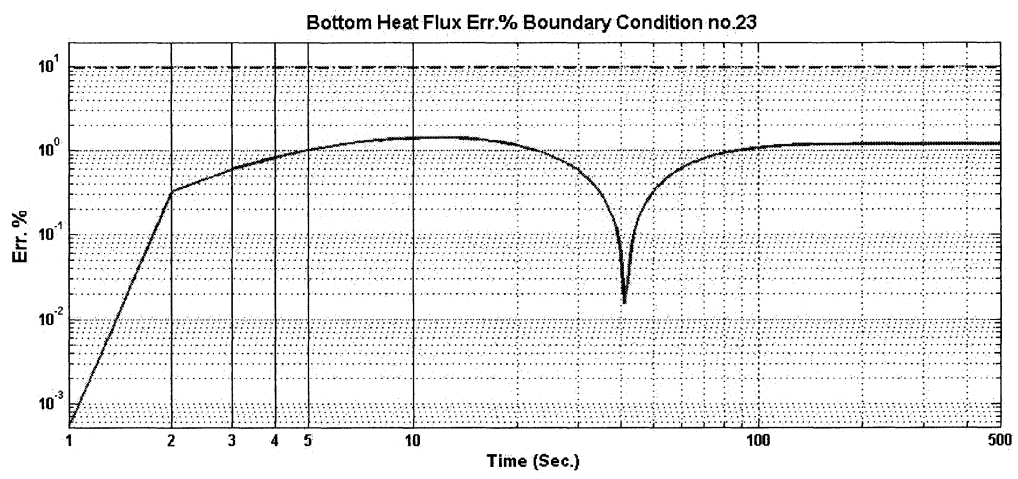


Figure B.2.8: Bottom heat flux relative error for BC no. 23

### B.3 Case study 6 - BC no. 35 - Heat sink and Free convection boundary condition

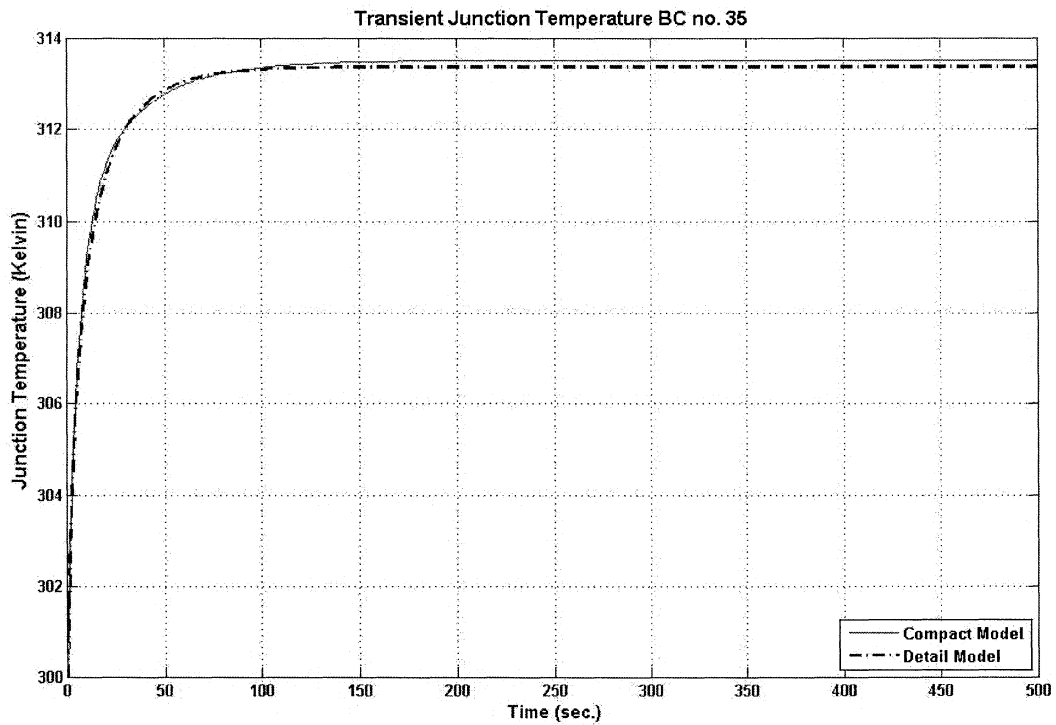


Figure B.3.1: Detailed and Compact model junction temperature for BC no. 35

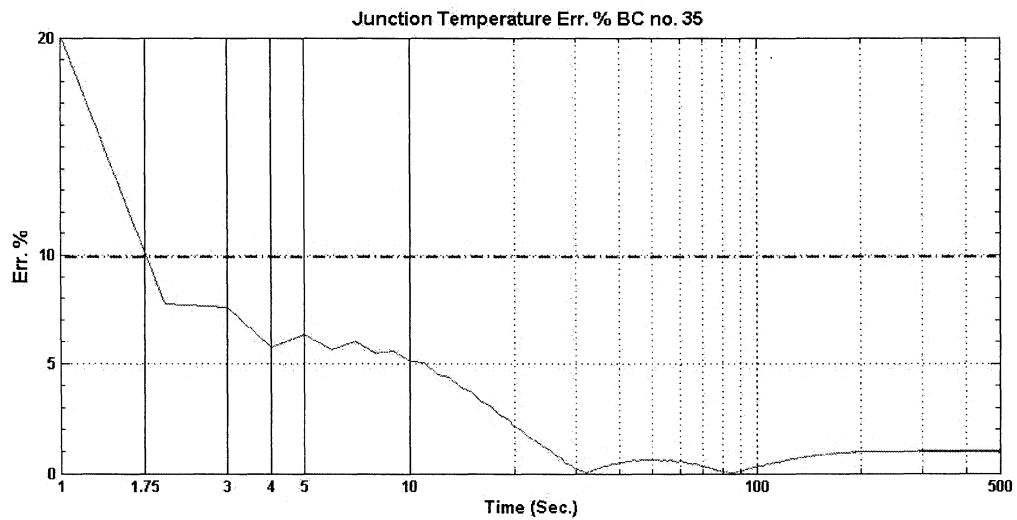


Figure B.3.2: Junction temperature relative error for BC no. 35

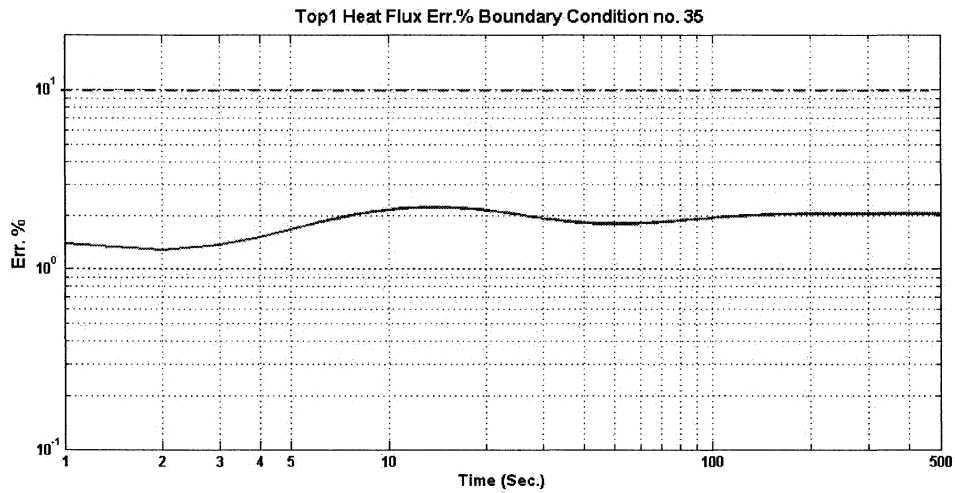


Figure B.3.3: Top1 heat flux relative error for BC no. 35

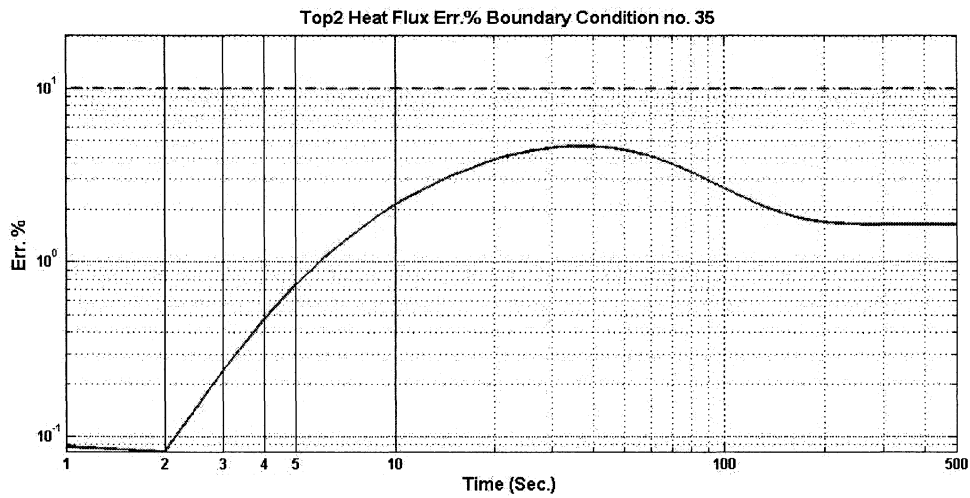


Figure B.3.4: Top2 heat flux relative error for BC no. 35

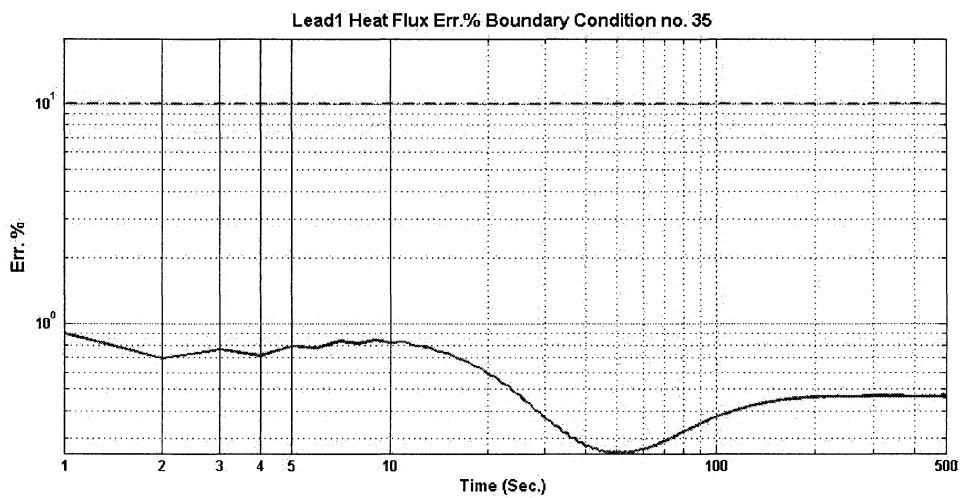


Figure B.3.5: Lead1 heat flux relative error for BC no. 35

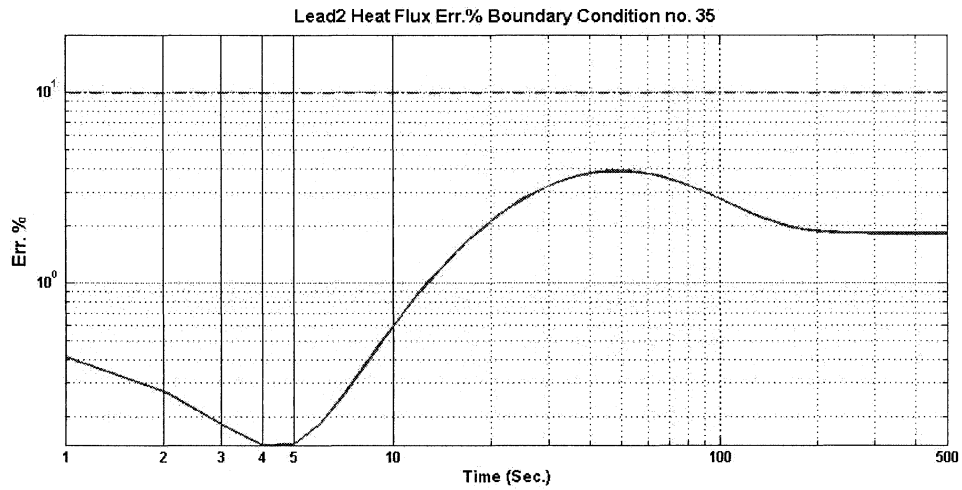


Figure B.3.6: Lead2 heat flux relative error for BC no. 35

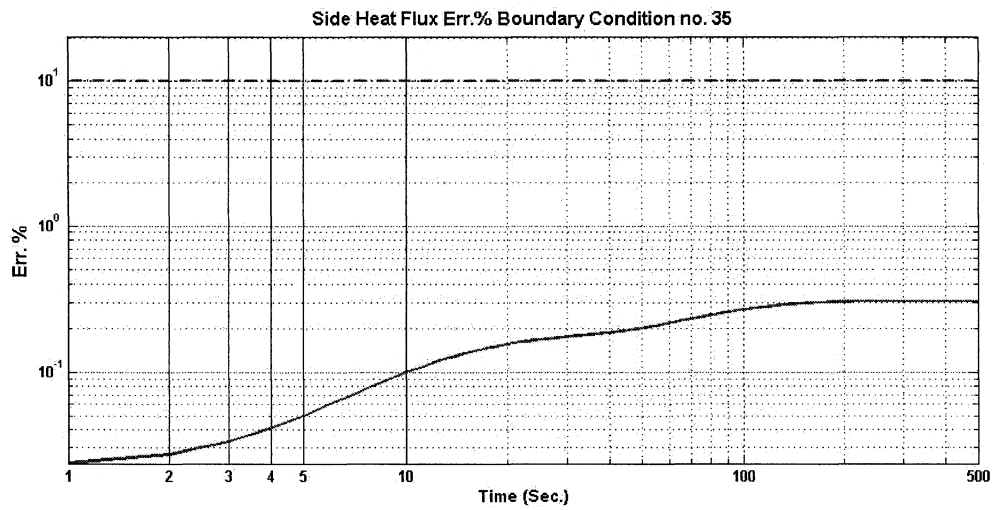


Figure B.3.7: Sidewalls heat flux relative error for BC no. 35

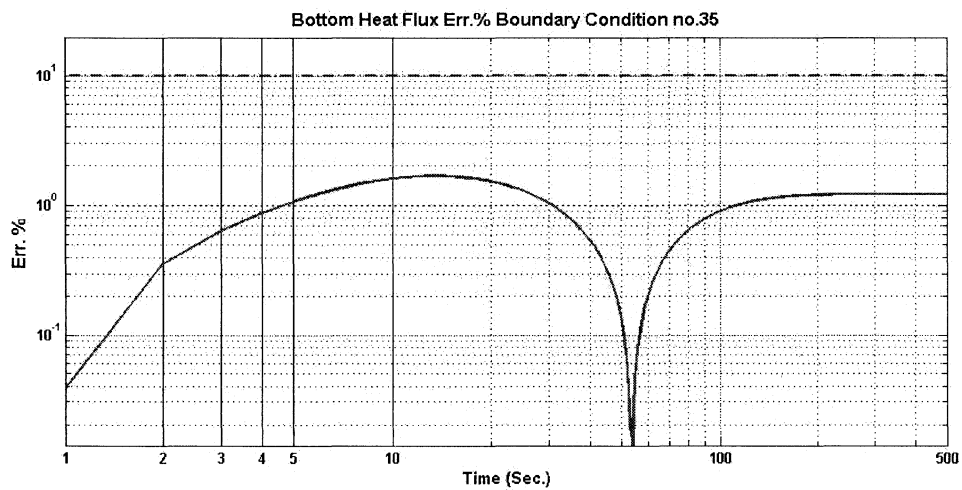


Figure B.3.8: Bottom heat flux relative error for BC no. 35

**B.4 Case study 7 - BC no. 40 - Heat sink and Forced convection boundary condition.**

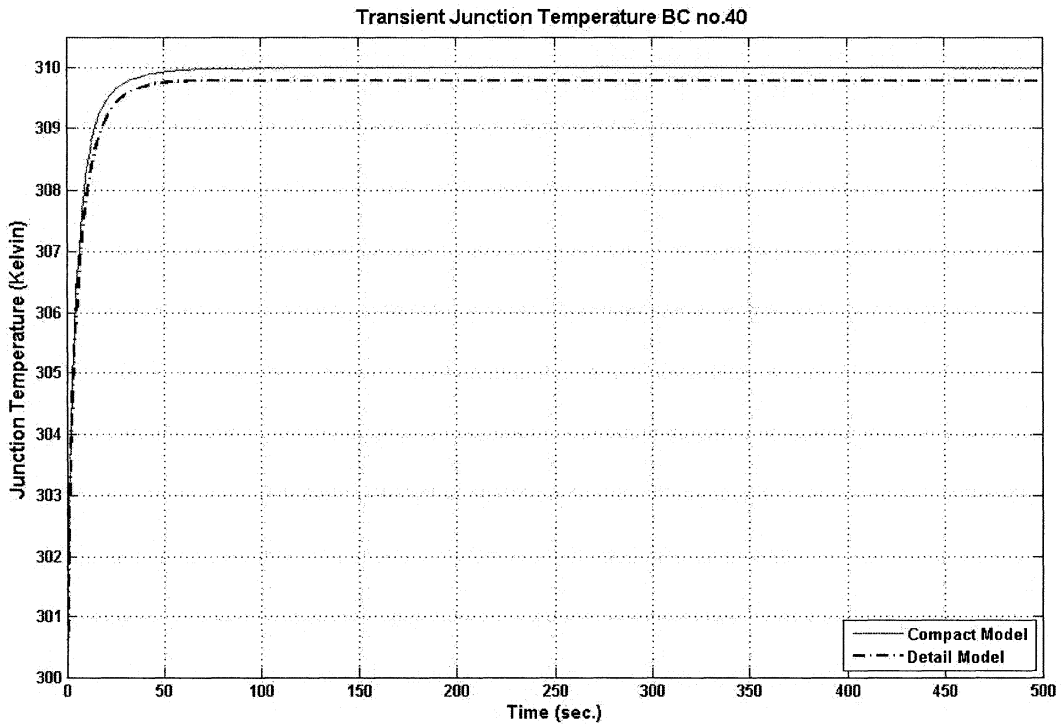


Figure B.4.1: Detailed and Compact model junction temperature for BC no. 40

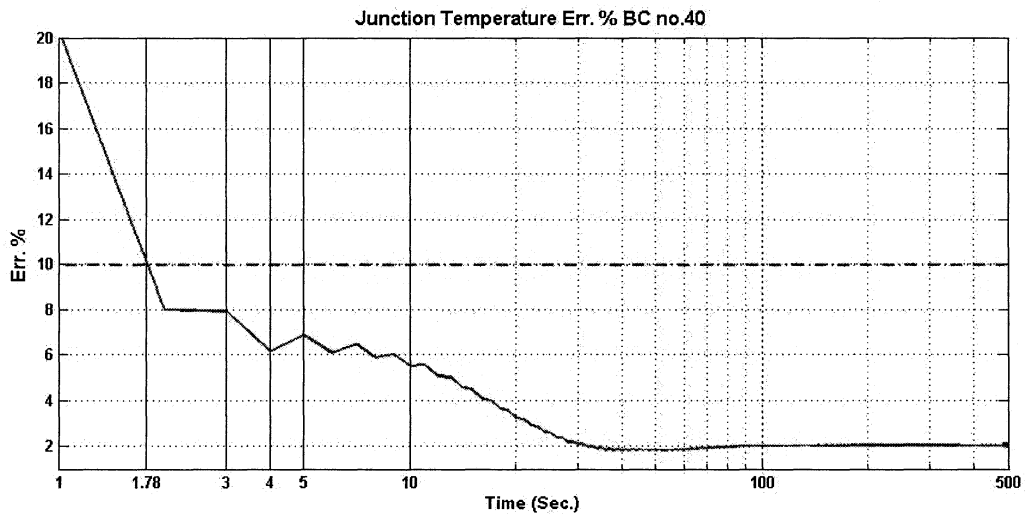


Figure B.4.2: Junction temperature relative error for BC no. 40

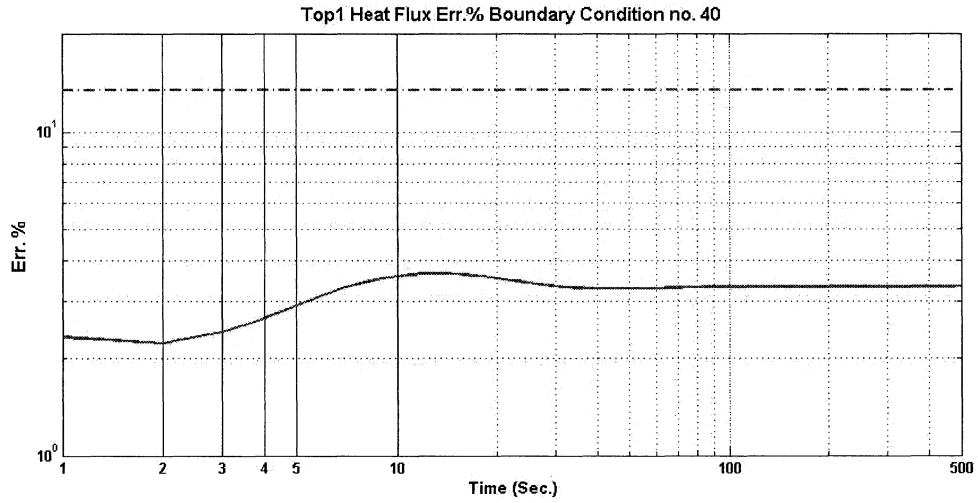


Figure B.4.3: Top1 heat flux relative error for BC no. 40

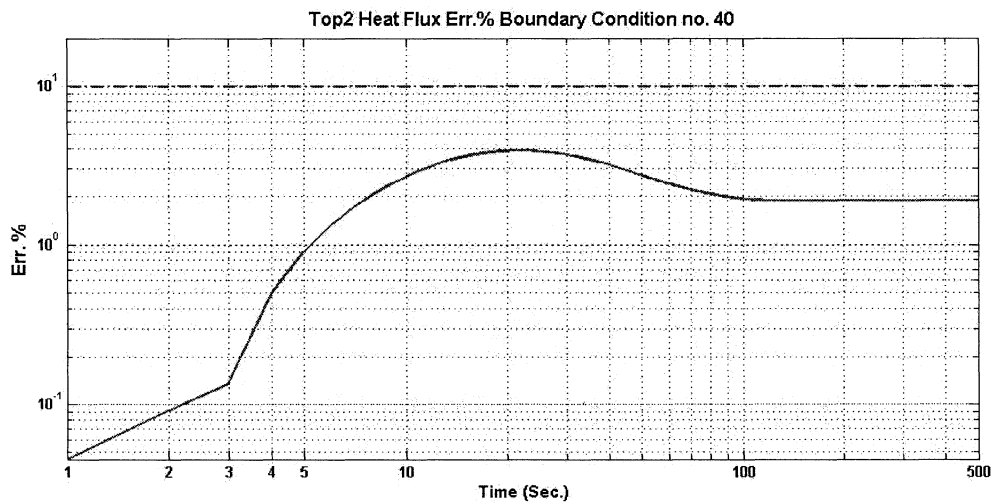


Figure B.4.4: Top2 heat flux relative error for BC no. 40

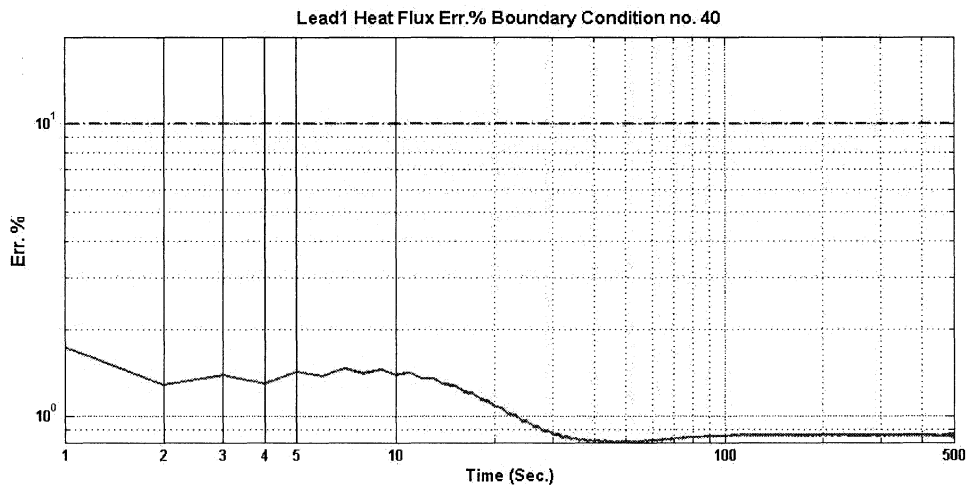


Figure B.4.5: Lead1 heat flux relative error for BC no. 40

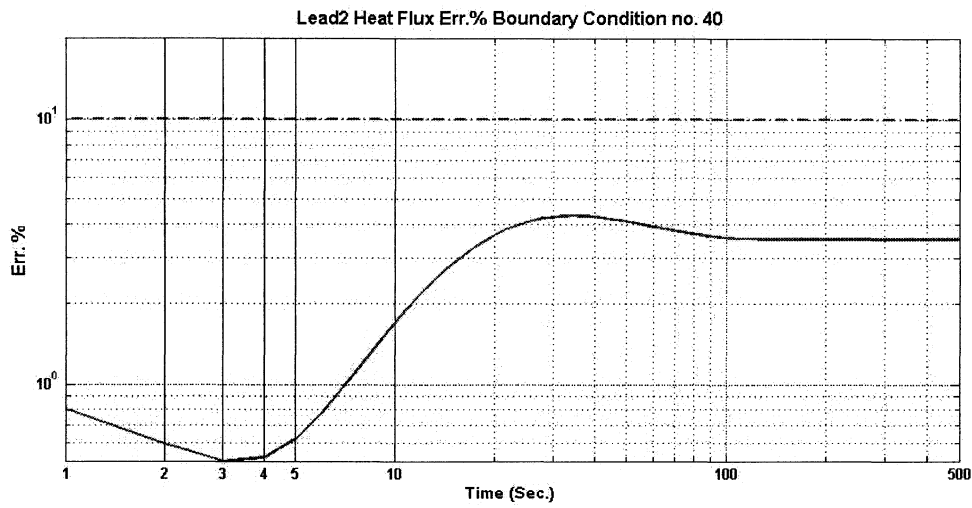


Figure B.4.6: Lead2 heat flux relative error for BC no. 40

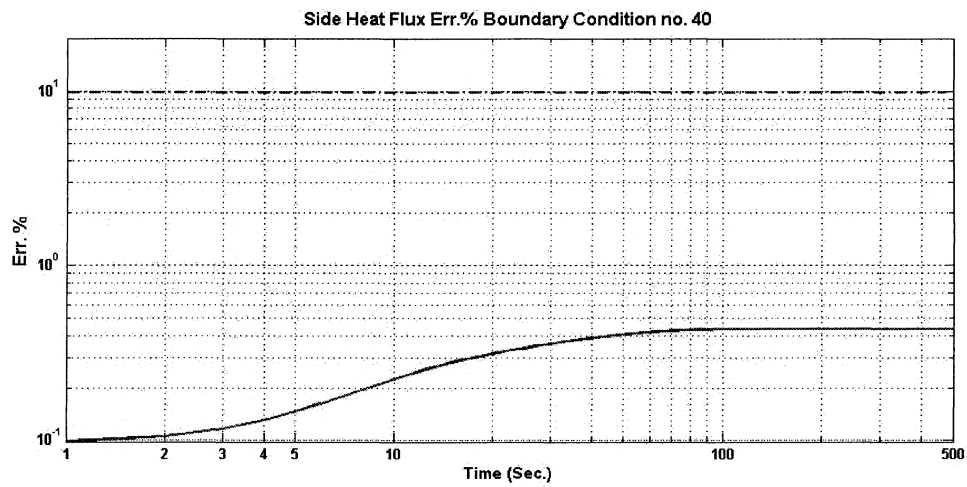


Figure B.4.7: Sidewalls heat flux relative error for BC no. 40

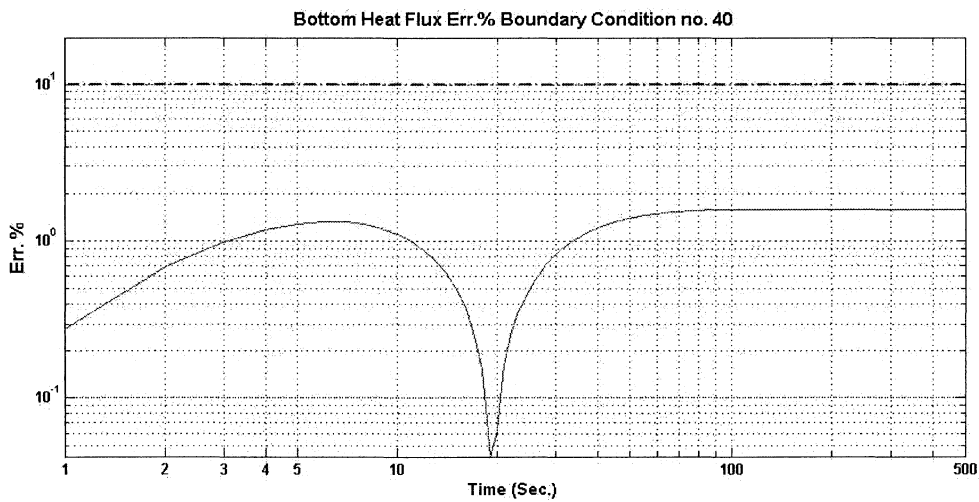


Figure B.4.8: Bottom heat flux relative error for BC no. 40

## B.5 Case study 8 - BC no. 46 - Cold Plate Convection Boundary Condition

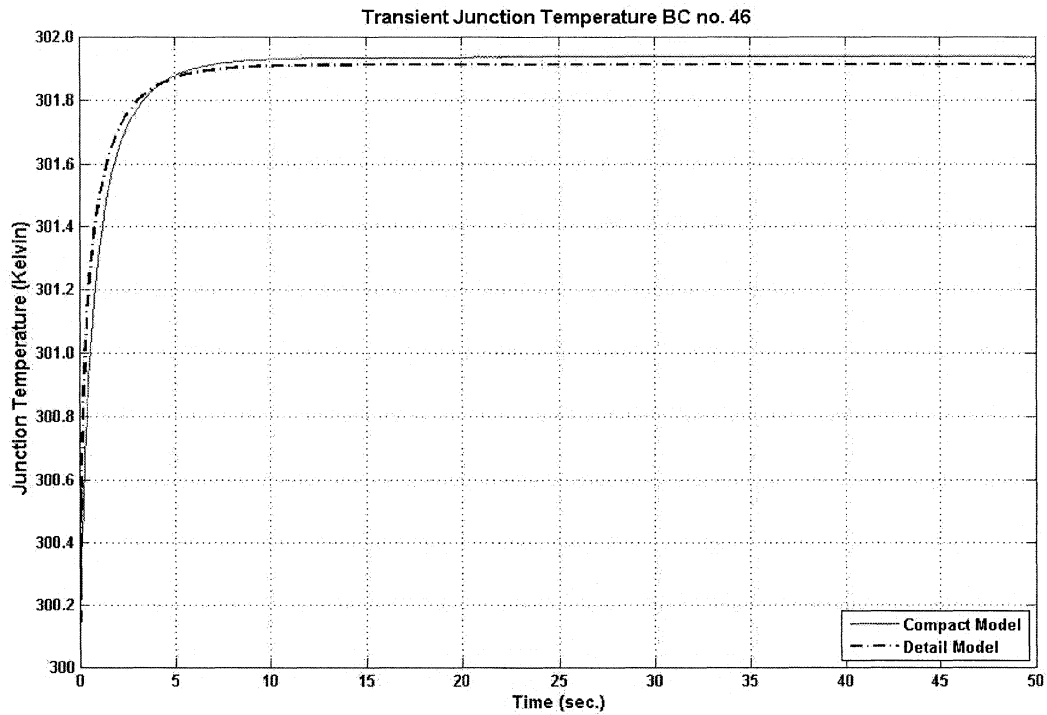


Figure B.5.1: Detailed and Compact model junction temperature for BC no. 46

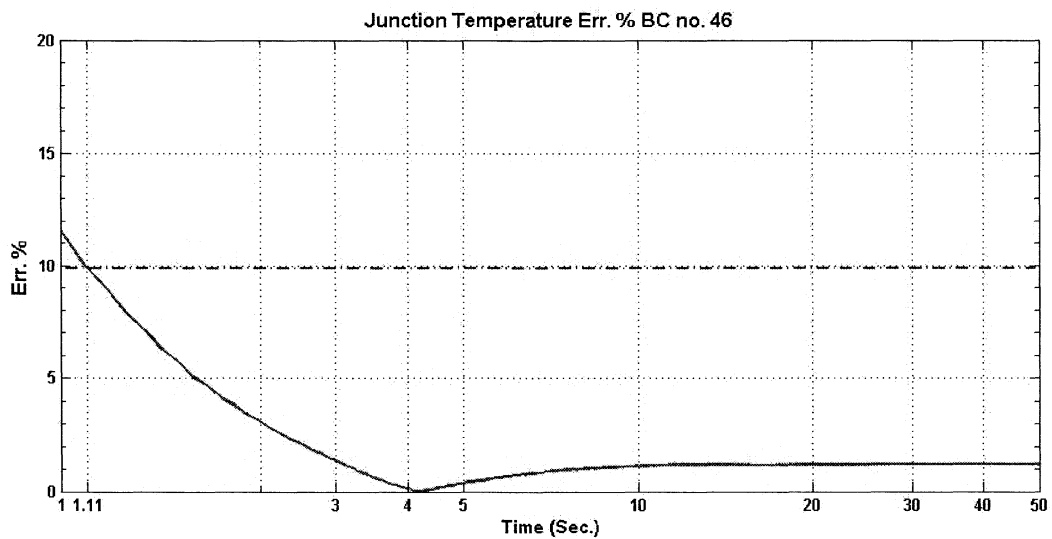


Figure B.5.2: Junction temperature relative error for BC no. 46

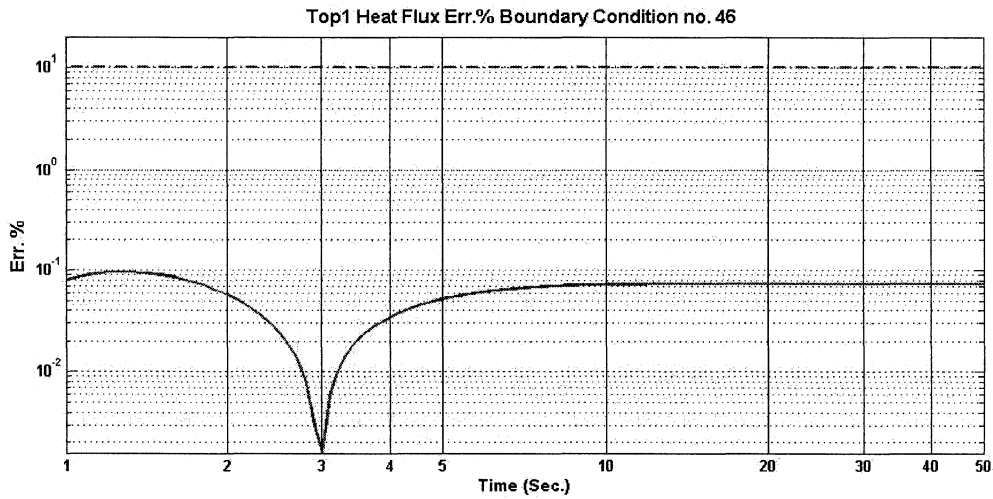


Figure B.5.3: Top1 heat flux relative error for BC no. 46

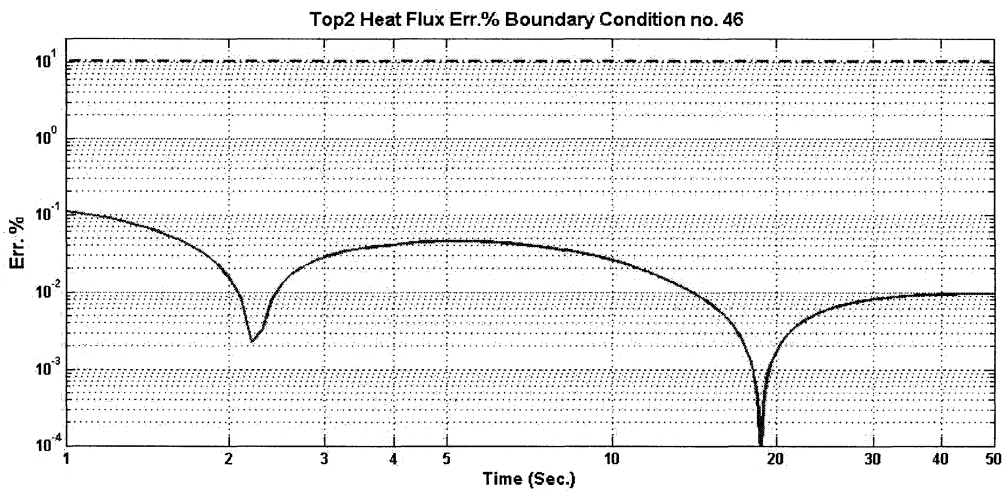


Figure B.5.4: Top2 heat flux relative error for BC no. 46

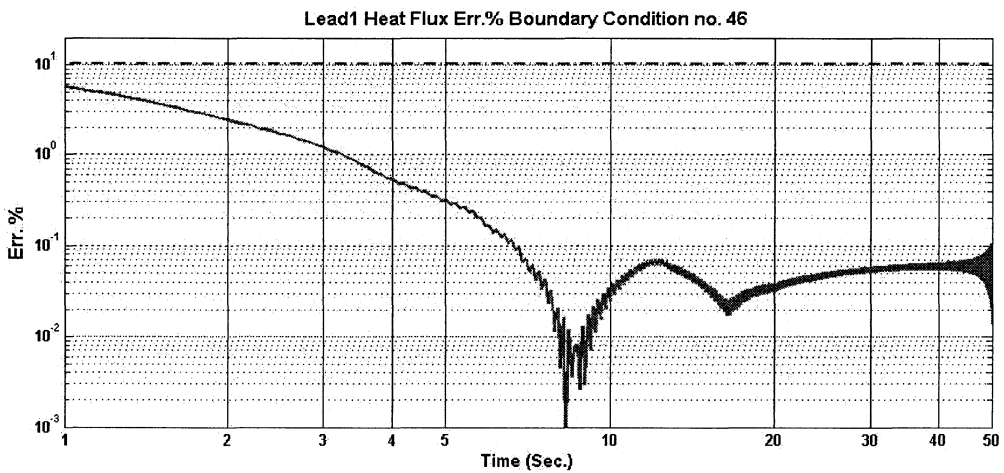


Figure B.5.5: Lead1 heat flux relative error for BC no. 46

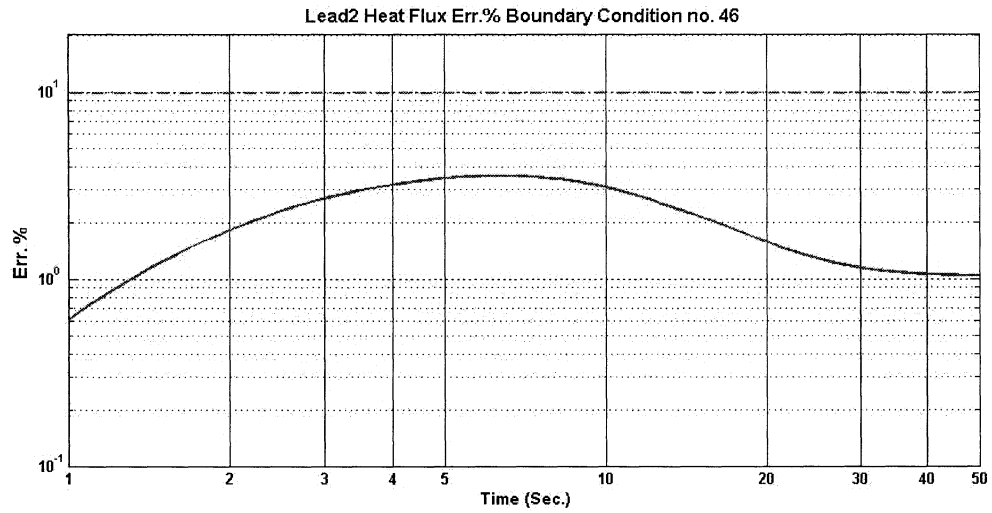


Figure B.5.6: Lead2 heat flux relative error for BC no. 46

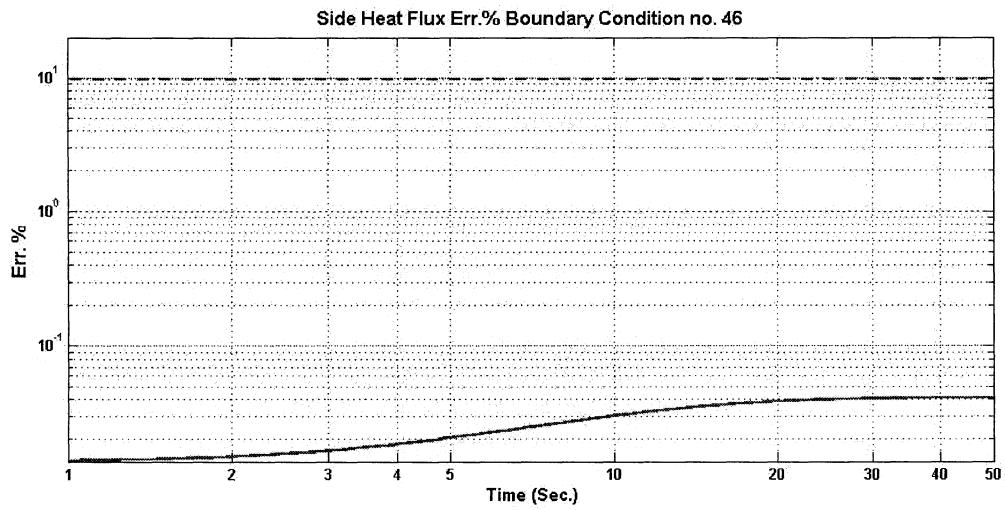


Figure B.5.7: Sidewalls heat flux relative error for BC no. 46

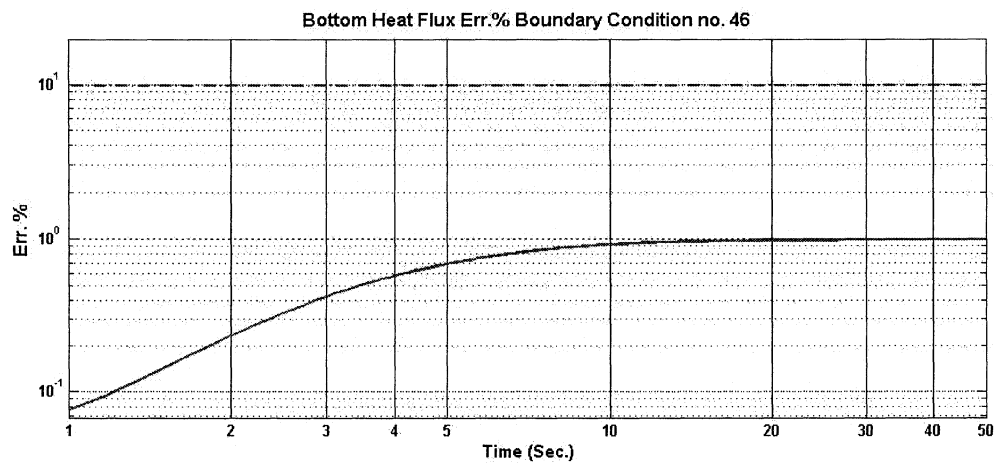


Figure B.5.8: Bottom heat flux relative error for BC no. 46

## B.6 Case study 9 - BC no. 52 - Fluid Bath boundary condition

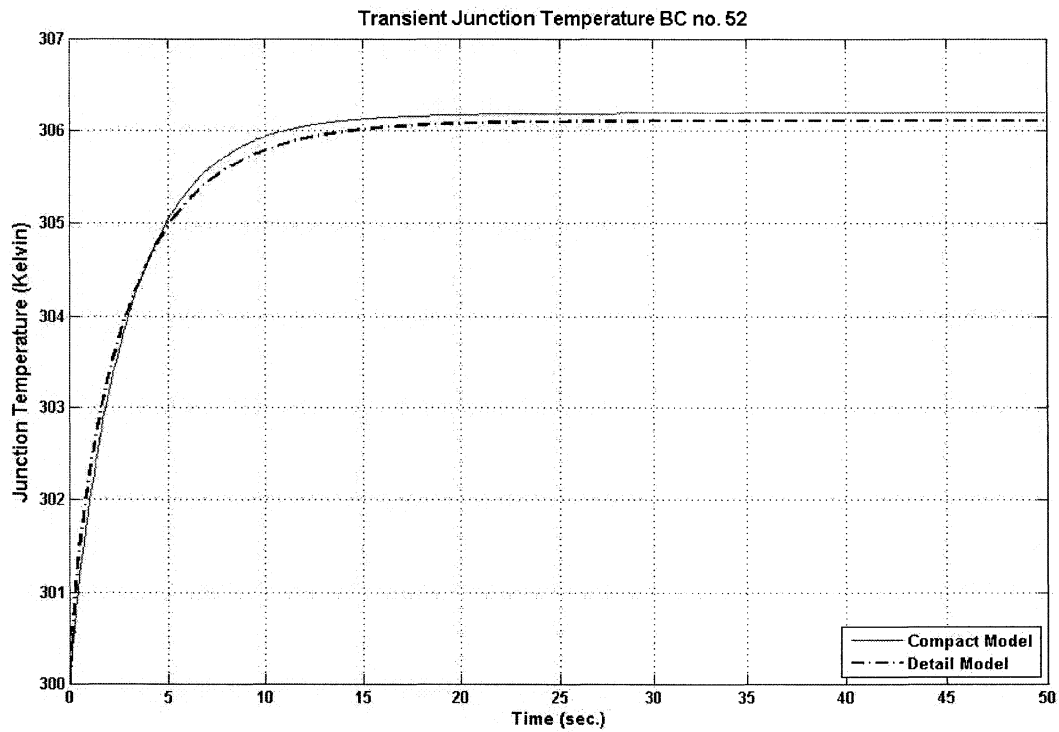


Figure B.6.1: Detailed and Compact model junction temperature for BC no. 52

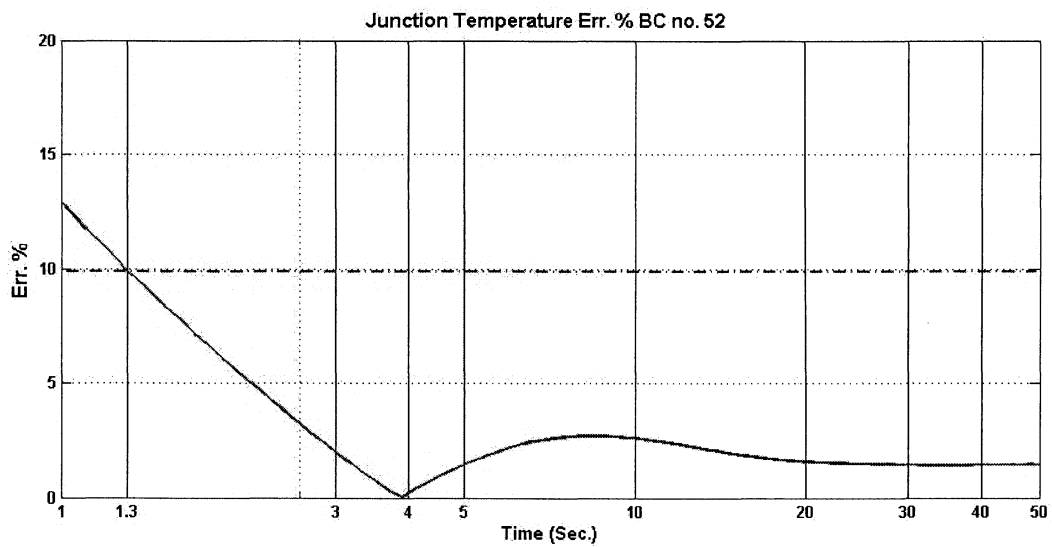


Figure B.6.2: Junction temperature relative error for BC no. 52

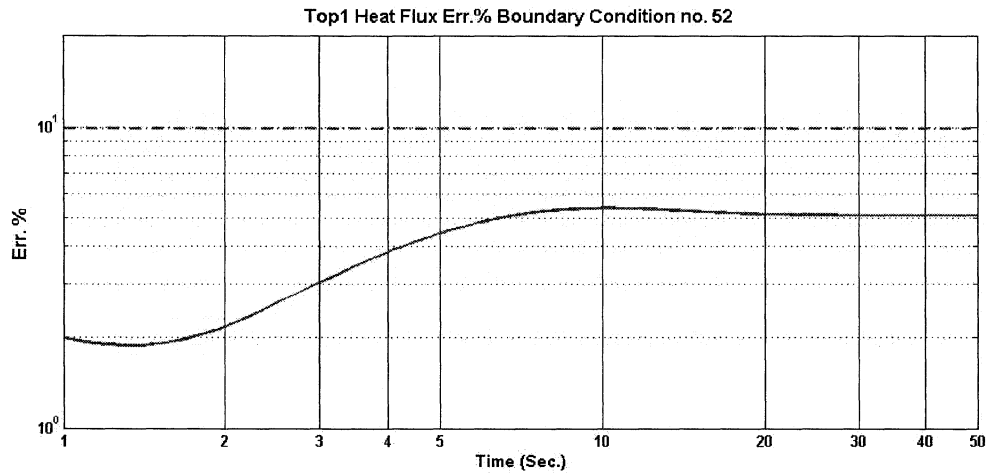


Figure B.6.3: Top1 heat flux relative error for BC no. 52

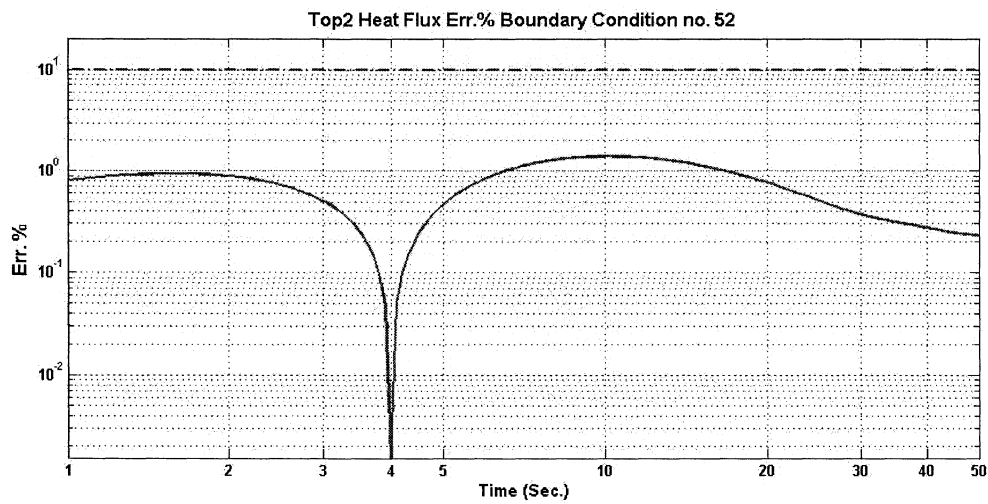


Figure B.6.4: Top2 heat flux relative error for BC no. 52

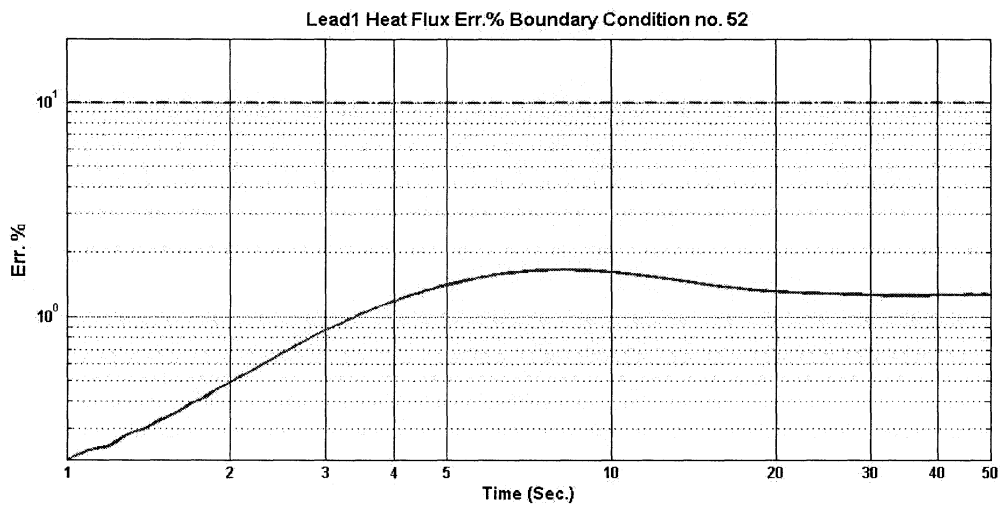


Figure B.6.5: Lead1 heat flux relative error for BC no. 52

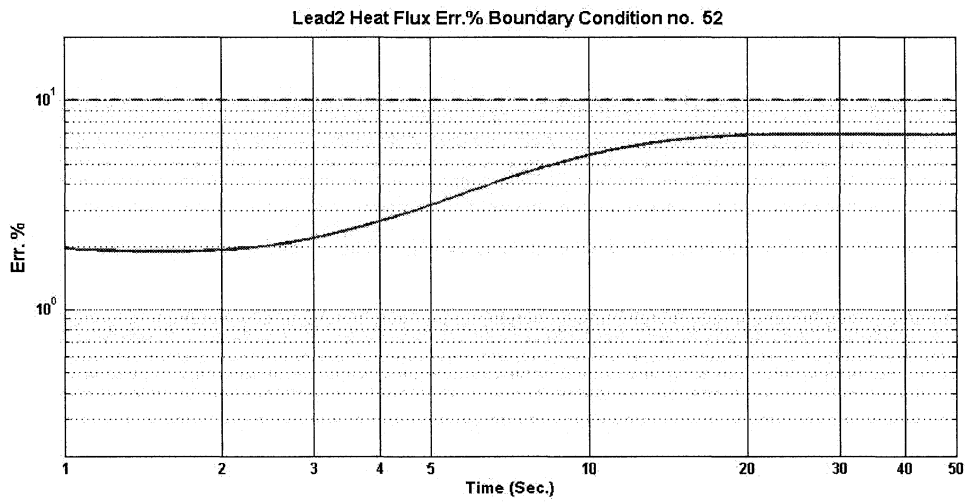


Figure B.6.6: Lead2 heat flux relative error for BC no. 52

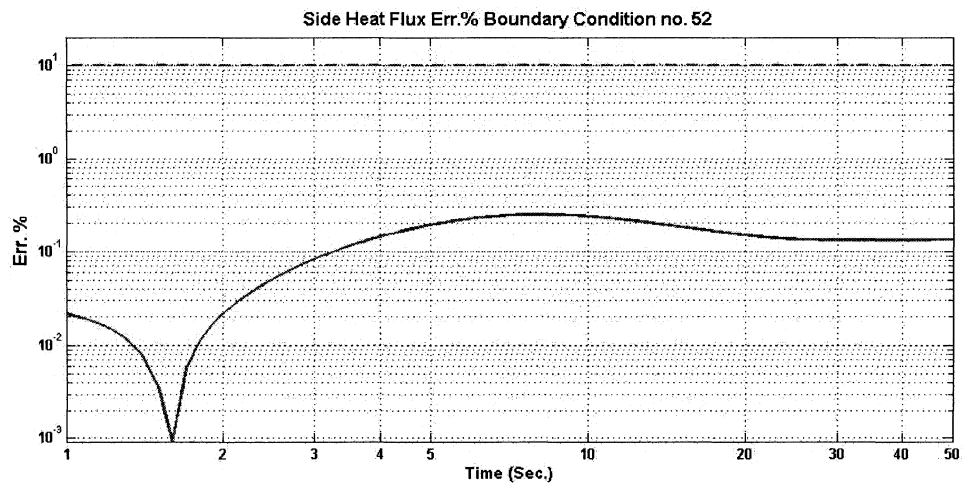


Figure B.6.7: Sidewalls heat flux relative error for BC no. 52

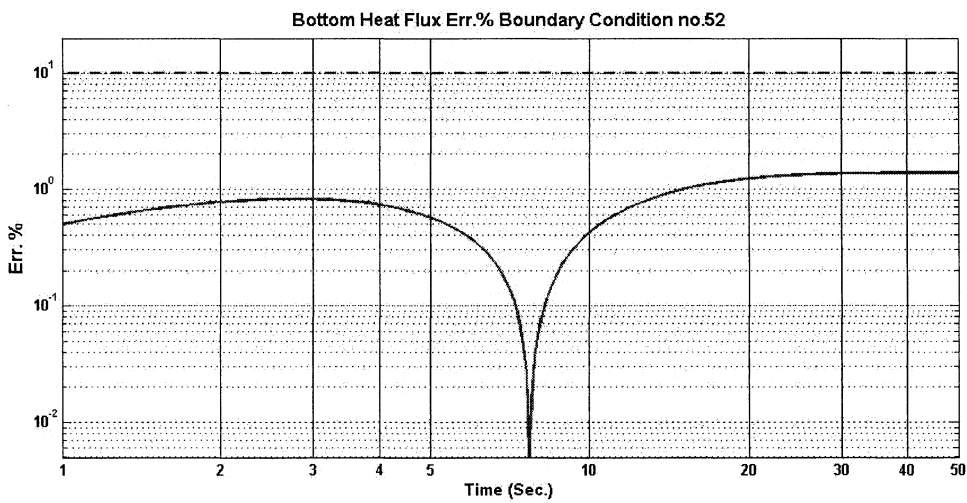


Figure B.6.8: Bottom heat flux relative error for BC no. 52

